

Springer Geography

Sathaporn Monprapussorn

Zhaohui Lin

Asamaporn Sitthi

Parichat Wetchayont *Editors*

Geoinformatics for Sustainable Development in Asian Cities

 Springer

Springer Geography

Advisory Editors

Mitja Brilly, Fac. Civil & Geodetic Engineering, University of Ljubljana, Ljubljana, Slovenia

Richard A. Davis, School of Geosciences, dept. of Geology,
University of South Florida, Tampa, FL, USA

Nancy Hoalst-Pullen, Dept. Geography & Anthropology, Kennesaw State
University, Kennesaw, GA, USA

Michael Leitner, Department of Geography & Anthropology, Louisiana State
University, Baton Rouge, LA, USA

Mark W. Patterson, Dept. Geography & Anthropology, Kennesaw State University,
Kennesaw, GA, USA

Márton Veress, Department of Physical Geography, University of West Hungary,
Szombathely, Hungary

The Springer Geography series seeks to publish a broad portfolio of scientific books, aiming at researchers, students, and everyone interested in geographical research.

The series includes peer-reviewed monographs, edited volumes, textbooks, and conference proceedings. It covers the major topics in geography and geographical sciences including, but not limited to; Economic Geography, Landscape and Urban Planning, Urban Geography, Physical Geography and Environmental Geography.

Springer Geography—now indexed in Scopus

More information about this series at <http://www.springer.com/series/10180>

Sathaporn Monprapussorn · Zhaohui Lin ·
Asamaporn Sitthi · Parichat Wetchayont
Editors

Geoinformatics for Sustainable Development in Asian Cities

 Springer

Editors

Sathaporn Monprapussorn
Faculty of Social Sciences,
Department of Geography
Srinakharinwirot University
Bangkok, Thailand

Asamaporn Sitthi
Faculty of Social Sciences,
Department of Geography
Srinakharinwirot University
Bangkok, Thailand

Zhaohui Lin
Institute of Atmospheric Physics
Chinese Academy of Sciences
Beijing, China

Parichat Wetchayont
Faculty of Social Sciences,
Department of Geography
Srinakharinwirot University
Bangkok, Thailand

ISSN 2194-315X

Springer Geography

ISBN 978-3-030-33899-2

<https://doi.org/10.1007/978-3-030-33900-5>

ISSN 2194-3168 (electronic)

ISBN 978-3-030-33900-5 (eBook)

© Springer Nature Switzerland AG 2020

This work is subject to copyright. All rights are reserved by the Publisher, whether the whole or part of the material is concerned, specifically the rights of translation, reprinting, reuse of illustrations, recitation, broadcasting, reproduction on microfilms or in any other physical way, and transmission or information storage and retrieval, electronic adaptation, computer software, or by similar or dissimilar methodology now known or hereafter developed.

The use of general descriptive names, registered names, trademarks, service marks, etc. in this publication does not imply, even in the absence of a specific statement, that such names are exempt from the relevant protective laws and regulations and therefore free for general use.

The publisher, the authors and the editors are safe to assume that the advice and information in this book are believed to be true and accurate at the date of publication. Neither the publisher nor the authors or the editors give a warranty, expressed or implied, with respect to the material contained herein or for any errors or omissions that may have been made. The publisher remains neutral with regard to jurisdictional claims in published maps and institutional affiliations.

This Springer imprint is published by the registered company Springer Nature Switzerland AG
The registered company address is: Gewerbestrasse 11, 6330 Cham, Switzerland

Preface

Nowadays many global environmental issues have become one of the severe problems that our planet is facing today. The problem has become worsen every day and shown visible effects. Environmental problems from climate change, natural disasters to biodiversity loss, have a great impact on environmental degradation, economic slowdown and human well-being. Given the fundamental geographic underpinning of environmental problems, geography and geoinformatics can be applied in assessing environmental problems and planning for sustainable environmental development which is largely required by scientists, social scientists, policy makers and communities.

Prepared in the context of sustainable development goals (SDGs) initiative, led by the United Nations. This publication will be useful to all those interested in the handling of matters related to climate change, land use, natural disaster and urban growth problems and in applying geography and geoinformatics for spatial problem solving.

This volume contains a revised version of selected papers presented at the 1st International Conference on Geography and Geoinformatics for Sustainable Development (ICGGS), which was held in Bangkok, July 19–20, 2018. It aims to especially focusing on using geospatial knowledges, methods and tools as the significance of natural resources and environment, socioeconomic and societal planning in promoting sustainable development.

July 2018

Sathaporn Monprapussorn
Asamaporn Sitthi
Zhaohui Lin
Parichat Wetchayont



Contents

Apply Deep Learning Techniques on Classification of Single-Band SAR Satellite Images	1
Chairath Sirirattanapol, Noppawan Tamkuan, Masahiko Nagai, and Michio Ito	
Detecting the Potential Roof for Green Rooftop Development Using Geospatial Techniques: A Case Study in North of Bangkok	12
Chomchanok Arunplod	
Land Use and Land Cover Change of Chanthaburi Watershed Following 1999, 2006 and 2013 Floods	21
Chuti Chatewutthiprapa, Srilert Chotpantararat, and Sombat Yumuang	
Identification of Urban Expansion Patterns in Bangkok Metropolitan Region Through Time Series of Landsat Images and Landscape Metrics	32
Chudech Losiri and Masahiko Nagai	
Monitor the Land Use Change and Prediction Using CA-Markov Model in Li Pe Island, Satun Province, Thailand	46
Katawut Waiyasusri, Nayot Kulpanich, Morakot Worachairungreung, and Pornperm Sae-ngow	
Sustainable Cultivation Planning in Ban Phaeo District, Samut Sakhon Province with Goal Programming and Geographic Information System	59
Talisa Niemmanee and Walaiporn Phonphan	
Drought Assessment During Dry Season Derived from LANDSAT Imagery Using Amplitude Analysis in Sa Kaeo, THAILAND	68
Tawatchai Na-U-Dom, Prasarn Intacharoen, Thippawan Thodsan, and Siriprapha Jangkorn	

Determination Critical Rainfall Threshold for the Initiation of Landslides Using Rainfall-Infiltration Model and Infinite Slope Stability Model	75
Thapthai Chaithong	
Comparison of Rice Phenology from MODIS and Ground Image Data in Sakaeo Province, Thailand	85
Wannaphorn Srichupieam, Narut Soontranon, and Sutatip Chavanavesskul	
Application of Geographic Information System to Predict Land Use Change for Maximum Flow Rate Calculation	96
Yutthana Chaona, Teerawate Limkomonvilas, and Sathaporn Monprapussorn	
A Study of Köppen-Geiger Climate Classification Change in Thailand from 1987–2017	109
Nutthakarn Phumkokrux	
Analysis Forest Fire Cause and Different Land Use Within Buffer Zones in Kanchanaburi Province, Thailand	118
Walaiporn Phonphan	
Spatiotemporal Analysis of Urban Agglomeration: A Case Study of Hyderabad City, Telangana State, India	128
Ashok Kumar Lonavath, Karunakar Virugu, V. Sathish Kumar, B. Ravi Naik, and Krishna Naik	
Modelling of Potential Sites for Residential Development at South East Peri-Urban of Kolkata	138
Rukhsana and Md. Hasnine	
Author Index	151



Apply Deep Learning Techniques on Classification of Single-Band SAR Satellite Images

Chairath Sirirattapol¹ , Noppawan Tamkuan² ,
Masahiko Nagai², and Michio Ito³

¹ Remote Sensing and GIS FoS, School of Engineering and Technology, Asian Institute of Technology, P.O. Box 4, Klong Luang 12120, Pathumthani, Thailand
schairath@gmail.com

² Graduate School of Sciences and Technology for Innovation, Yamaguchi University, 2-16-1, Tokiwadai, Ube, Yamaguchi 755-8611, Japan

³ Japan Aerospace Exploration Agency, Chofu, Japan

Abstract. Synthetic Aperture Radar (SAR) images have been widely applied to compensate the optical satellite images. SAR can be performed night and day, as well as be able to penetrate the cloud is one of advantages. It is famously used in disaster applications for gathering the damaged area information. Apart from that, SAR images are also contained with speckle noises, which cause the difficulty of the images for human visualization as well as the one band of SAR image is insufficient, they are additionally required skillful specialists. Therefore, to work on manual classification purpose would face the questionable objects and easy to be misclassified. Nowadays, the deep learning techniques could be capable of solving classification problems due to outperformed accuracy. In this study, we proposed the end-to-end classification framework using single band SAR image, which applied the deep learning to solve the problems. Our framework is divided into three main parts consisting of preparing and the dataset, developing the classification model, and classifying our testing images. We experimented on four classes using ALOS 2 satellite images. Finally, the prediction model reached to 91% accuracy on our test dataset with adding dropout techniques. Expectedly, our framework could be practically adopted in different applications in advance.

Keywords: Deep learning · Convolutional neural networks (CNNs) · VGG16 · Single-band SAR images · Classifications

1 Introduction

Satellite images have influenced to various applications such as agriculture, forestry, weather, ocean, urban management, change detection, even disaster application [1–4]. Many applications apply the benefits from optical satellite images due to hyper-spectral reflectance and easy interpretation. On the other hand, the limitations occurred when they are facing to weather conditions and cloud covered.

Synthetic Aperture Radar (SAR) images are well-known to be compensated utilization. SAR could be performed night and day, as well as to penetrate the cloud is one of advantages of SAR characteristics. The image is represented backscattered values, which high values are shown as bright areas, conversely the dark areas could be represented the flat smooth surfaces like road and water. It is useful for disaster applications to gather the damaged area information [5, 6]. There are many advantages of SAR images but they still need some specialized knowledge to visualize the SAR images. The images are also difficult to human visualization due to the radar characteristics, and speckle noise problems [7] as shown in the Fig. 1. To interpret the single-band SAR, one-band information is insufficient for classification in traditional methods. It has been still facing with difficulties to differentiate and perceive the useful information such as forest area, water area, agriculture area, and housing area compared to optical satellite images. It is required some domain experts to correctly identify the images. The human interpretation could sometimes lead to misclassify the areas due to the radar characteristics. To correctly classify the land cover or land use, are importantly helpful when the disaster occurred such as finding the land-slide, or flooding areas. Also, the SAR images are covered the large area more than 1,000 km, if the classifying processes are done by manually, that would be a problem.

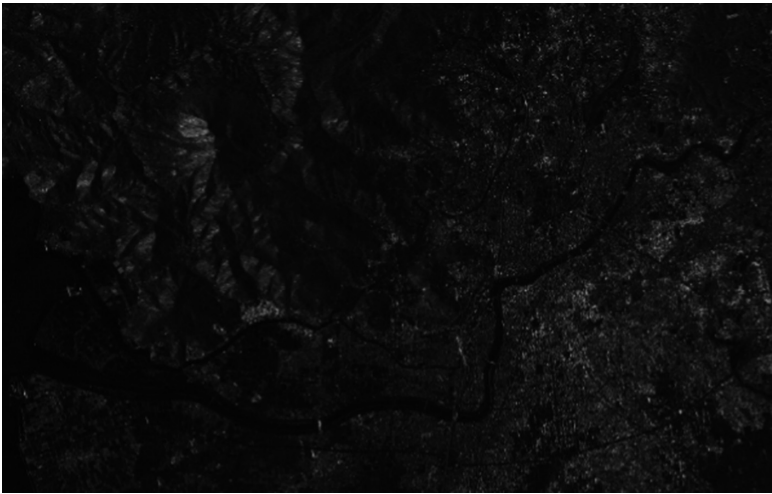


Fig. 1. Example of SAR images (HH band)

Nowadays, deep learning techniques have been playing the import role due to the outperformed accuracy and hardware capability. One of the deep learning techniques called Convolutional neural networks (CNNs), which are practically well-known for classification problems such as face recognition, medical image classification, scene labeling, human pose estimation, text and document analysis [8–11]. In remote sensing field, the deep learning technique also has utilized for satellite images such as land use and land cover applications, cloud detection, and building detection [12–14]. CNNs

have been developed and optimized in various architectures to improve performance such as AlexNet [15], VGG [16], GoogleNet [17], ResNet [18] in order to compete each other in terms of accuracy and speed. The less complex layers mean faster but giving lower accuracy and vice versa. Therefore, we proposed the utilization of deep learning techniques to classify the single-band SAR image, which will be elaborated in step-by-step how to prepare the training dataset and developing the CNN model including of evaluating the model. Also, the four classes land cover classification were experimented as our example by applying the proposed framework.

2 Materials and Methods

Based on our study is designed for classification problems. This experiment is focused on the four class land cover classification, which is comprised of forest, agricultural, water, and housing areas. However, we have tried to develop the end-to-end framework, which we have expected on our framework could be applied with other applications. Additionally, the detail of dataset and methodology are explained in the Sects. 2.1 and 2.2 respectively.

2.1 Dataset

Our dataset were taken from Japan Aerospace Exploration Agency (JAXA), In our experiment, we also have taken HH band of ALOS-2/ PALSAR-2 SM1 mode level 2.1 into account. The study area is located at Kumamoto, the coordinate is shown in the Table 1 and Fig. 2. The scene was observed on 21 May 2015 from the right-side observation of ascending orbit direction, which also has pixel size 2.5 m.

Table 1. Coordinates of the study area.

Bounding box	UTM	Coordinate
Upper left	649260.521, 3634971.020	130d35'41.63"E, 32d50'33.57"N
Lower left	649260.521, 3624144.945	130d35'35.36"E, 32d44'42.13"N
Upper right	664349.718, 3634971.020	130d45'21.84"E, 32d50'25.80"N
Lower right	664349.718, 3624144.945	130d45'14.94"E, 32d44'34.39"N
Center	656805.120, 3629557.983	130d40'28.45"E, 32d47'34.07"N

2.2 Methodology

To create the end-to-end framework since obtaining the SAR image dataset from JAXA until classifying the images, we developed the methodology of our study, which is comprised of main three parts; preparing the dataset, developing and fine-tuning the convolutional neural networks model for classification and then classifying the testing image. The overall detail of the methodology is shown the Fig. 3.

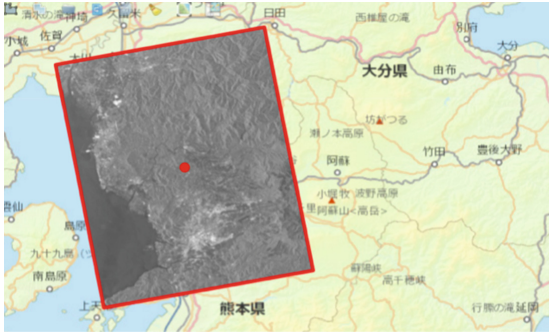


Fig. 2. Observed scene on 21 May 2015

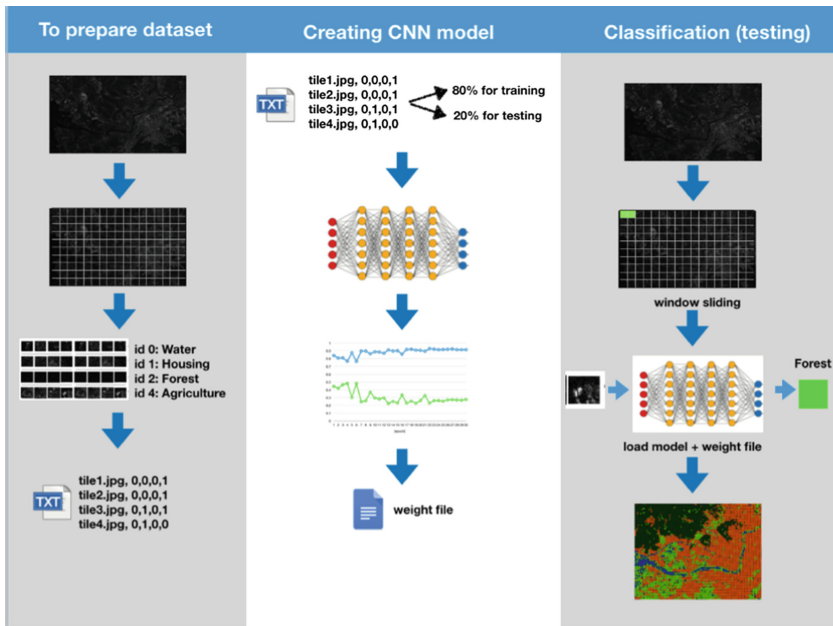


Fig. 3. The framework of the study

Preparing the Dataset

Initially, the HH-band SAR image was taken from ALOS-2. The image was tiled into 25×25 pixels. Those tiled images were used for training and testing the classification model. Each tile could be represented by each area. To assign only the tile images, it is facing unquestionable scenes if lacking of SAR characteristic knowledge such as side looking observation, and geometric effects. Therefore, making the tiled image in order to compare with the optical image are crucially useful. The tiled-grid was also designed in order to easily visualize, compare and validate the tiled images as shown in the Figs. 4 and 5. In this experiment, four classes were selected as forest, agriculture, water

and housing areas, meaning that the tiled images could be represented to each class, each class was assigned the ID using QGIS software providing the information of class ID, and class name. Finally, each tiled information was stored in the text file, which provided image name with one-hot encoder. For example of the forest class is stored as [tile1.jpg, 0, 0, 1, 0], id 3 is represented as forest, the third position will be set as 1 and the rest of them are set as 0. Finally, the tiled images were randomly separated into 80% and 20% as training and testing images in order to be fed into the deep neural network model respectively.

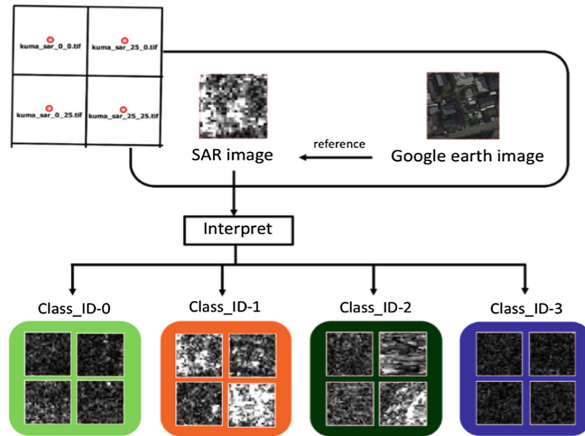


Fig. 4. The process of assignment the tiled images into each class

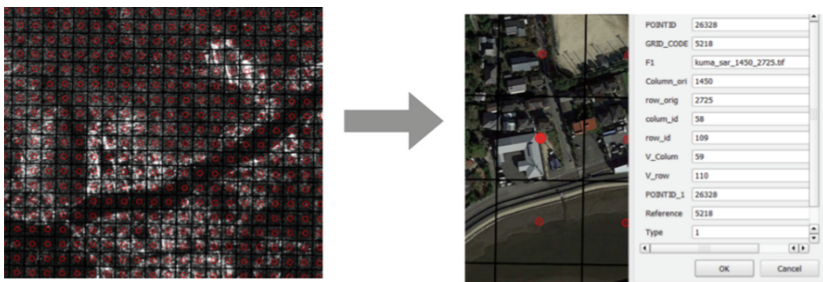


Fig. 5. Tiled-grid was used for understandably assigning the class to each tile.

Creating the Model for SAR Image Classification

In order to develop the deep learning model, Keras framework with Tensorflow backend was taken into account in our study. We applied the benefit of VGG 16 model [16] due to its compact, and outperformance compared to other models, the model was developed for image recognition. The 80% of training dataset is fed to the network by adding dropout technique at 0.4 in order to fine-tune VGG 16 avoid overfitting, the

network is shown in the Fig. 6. We applied SGD optimizer by setting the learning rate at 0.0001, using the categorical cross-entropy loss. The softmax function was added up to top of the layer to classify the output. Also, the training process was set at 30 epochs due to the limitation of CPU performance. Finally, the loss and accuracy were computed after the network was trained.

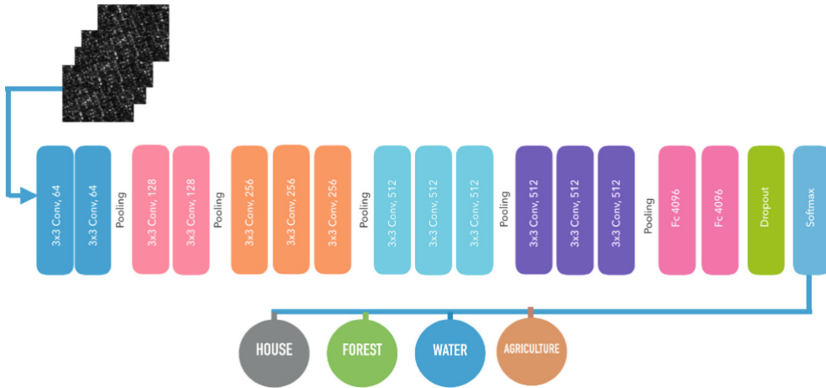


Fig. 6. Fine-tuning VGG16 for Single-band SAR image classification

Classification Image

After the classification model was performed better accuracy, and loss reduced in terms of both training and testing dataset, the process of classifying the whole SAR image was applied. The big SAR image was tiled to 25×25 pixel using window sliding technique by defining window size 25×25 , and slide passing through the whole image from left to right and top to bottom as shown in the Fig. 7. Each tile was sent to the model to classify and the class id was assigned into the tile, repeating this process until covering the whole area.

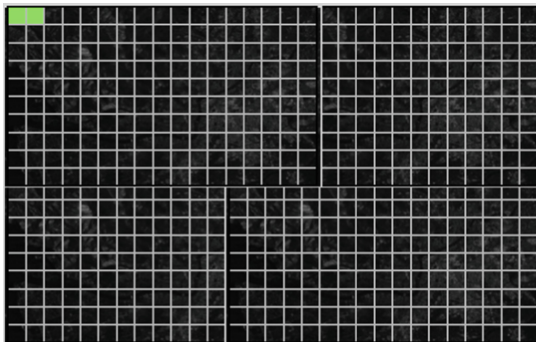


Fig. 7. 25×25 window sliding to the whole image

3 Results

3.1 The Total Number of Dataset

The dataset was divided into 80% and 20% for training and testing set, respectively. The number of each set is shown in the Table 2.

Table 2. Class details and number of training and testing data

Class ID	Class name	No. of training	No. of testing
0	[Water, Wetland]	380	88
1	[Urban, Building, Housing]	545	136
2	[Forest]	385	97
3	[Agriculture, Paddy field, Grassland]	382	98
Total		1,692	419

3.2 Loss and Accuracy of the Classified Model

The loss of training and testing data were decreasing continuously, conversely the accuracy could be rapidly increasing to 99% and 91% for training and testing respectively as shown in the Fig. 8. Moreover, the all testing tiles were predicted, which is shown in the Fig. 9. The blue dot is shown the correct prediction and the red dot is shown wrong classification.

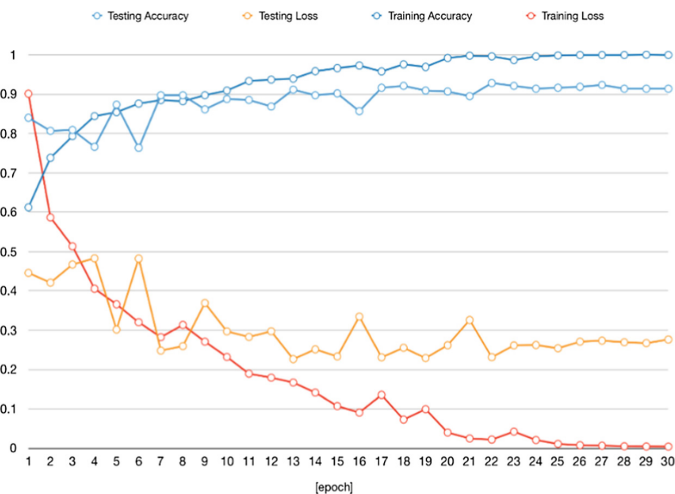


Fig. 8. Loss and accuracy of the model

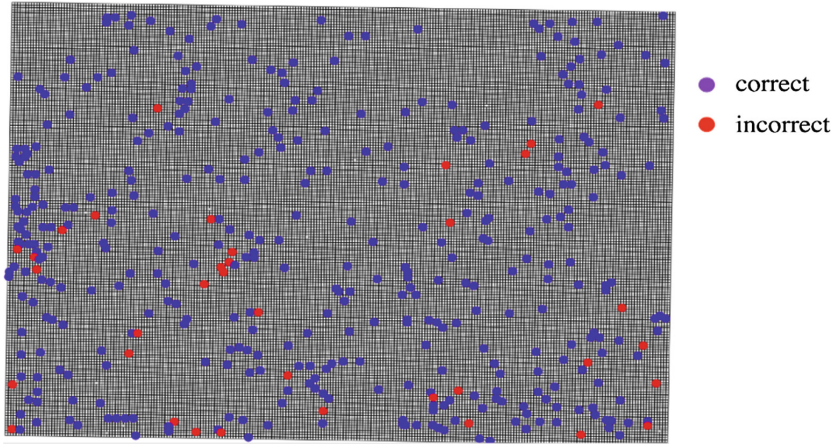


Fig. 9. Results of prediction from the testing dataset

3.3 The Result of Classified SAR Image

To apply the window sliding for the whole image, each tile was classified and given the color to represent each class, the classified image is shown in the Fig. 10. Also, we evaluated our testing tiled image using confusion matrix, which shown in the Table 3, and finally the Kappa coefficient was calculated at 0.884.

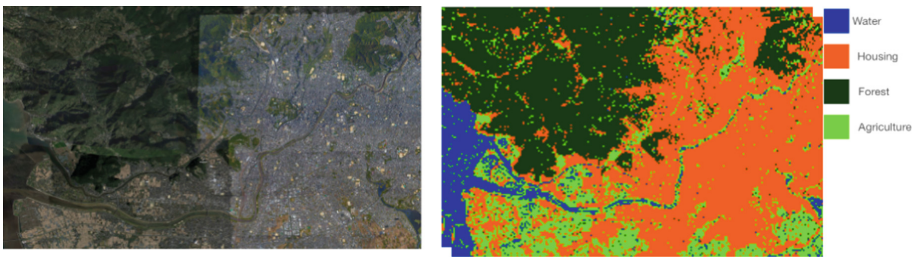


Fig. 10. Result of the classified image compared to optical image (from google)

4 Discussion

The benefits of Deep convolutional neural networks could be well-performed in the SAR classification task. Based on the accuracy of the model could reach to 91% but the losses of training and testing still need to improve due to limited number of training dataset. In the Table 3, there are lot of numbers misclassified from agricultural area and water, because some our dataset could not be strongly classified into one-label class. For example, some agricultural areas are contained with water like planting paddy field, the user assigned these tiles as agricultural class as shown in the Fig. 11. The blue areas were misclassified from agriculture to water, and also some agricultures faced with

misclassified with housing area due to the greenhouse, sometimes the agricultural areas are covered with the protecting roof. For radar characteristics, SAR image generally obtains from side looking observation. SAR data provides surface information by backscattering return to satellite. The image consists of surface characteristic and also geometric effects (layover, shadow and foreshortening). Therefore, it is possible misclassified by radar characteristics. For example, radar shadow in a mountainous area and paddy in the wet-field could be classified as water because of the less backscattering returned to the sensor. To improve our accuracy, the number of training dataset should be more prepared with various temporal data and different areas, also the data augmentation techniques should be implemented appropriately.

Table 3. Confusion matrix reference data (tiles)

		Water	Housing	Forest	Agriculture	Total	Producer's accuracy
Classified data (tiles)	Water	75	1	0	12	88	85%
	Housing	2	134	0	0	136	99%
	Forest	2	3	92	0	97	95%
	Agriculture	16	0	0	82	98	84%
	Total	95	138	92	94	383	
	User's accuracy	79%	97%	100%	87%	Total	419

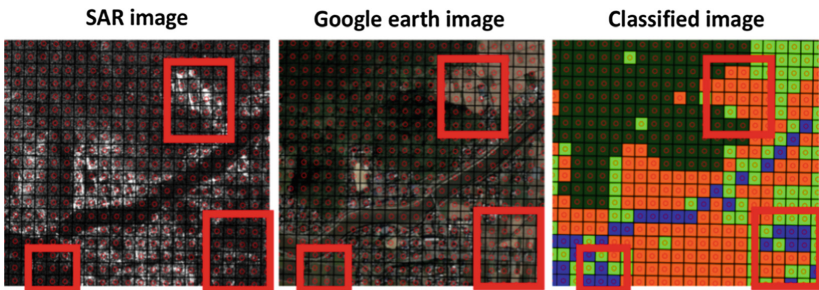


Fig. 11. Misclassified results

In the future, the classification model could be improved in terms of accuracy and time processing, also our framework could be expectedly adapted in various applications such as land slide detection, land use and land cover classification.

5 Conclusions

Single-band SAR images have been facing the problems of understandable visualization due to noise and back-scattering characteristics of radar. Regarding to the out-performed accuracy of deep learning techniques, we proposed the end-to-end framework that could classify the single-band SAR image from preparing the dataset to the evaluation the result. Our model was worked on pre-trained VGG16 model by adding dropout with limited number of training dataset as well as we experimented our framework on four classes classification, which performed 91% accuracy on classification model of our study that could be implemented in other problems in the future.

Acknowledgments. This study is the project on utilization of space technology, under Space Utilization Engineering Laboratory, Yamaguchi university and collaborating with Japan Aerospace Exploration Agency (JAXA) who provided the useful sources such as ALOS2 images, and the best guiding and recommendation to reach this study to achievements.

References

1. Hu, T., Yang, J., Li, X., Gong, P.: Mapping urban land use by using landsat images and open social data. *Remote Sens.* **8**(2) (2016). <http://doi.org/10.3390/rs8020151>
2. Alcantara, C., Kuemmerle, T., Prishchepov, A.V., Radeloff, V.C.: Mapping abandoned agriculture with multi-temporal MODIS satellite data. *Remote Sens. Environ.* **124**, 334–347 (2012). <https://doi.org/10.1016/j.rse.2012.05.019>
3. Sona, N.T., Chen, C.F., Chen, C.R., Chang, L.Y., Minh, V.Q.: Monitoring agricultural drought in the lower mekong basin using MODIS NDVI and land surface temperature data. *Int. J. Appl. Earth Obs. Geoinf.* **18**(1), 417–427 (2012). <https://doi.org/10.1016/j.jag.2012.03.014>
4. Sinha, P., Verma, N.K., Ayele, E.: Urban built-up area extraction and change detection of adama municipal area using time-series landsat images. *Int. J. Adv. Remote Sens. GIS* **5**(1), 1886–1895 (2016). <http://doi.org/10.23953/cloud.ijarsg.67>
5. Matsuoka, M., Yamazaki, F.: Use of satellite SAR intensity imagery for detecting building areas damaged due to earthquakes. *Earthq. Spectra* **20**(3), 975–994 (2004). <https://doi.org/10.1193/1.1774182>
6. Tamkuan, N., Nagai, M.: Fusion of multi-temporal interferometric coherence and optical image data for the 2016 kumamoto earthquake damage assessment. *ISPRS Int. J. Geo-Inf.* **6**(7), 188 (2017)
7. Wang, P., Zhang, H., Patel, V.M.: SAR image despeckling using a convolutional neural network. *IEEE Signal Process. Lett.* **24**(12), 1763–1767 (2017). <https://doi.org/10.1109/LSP.2017.2758203>
8. Sun, Y., Liang, D., Wang, X., Tang, X.: DeepID3: face recognition with very deep neural networks. *CVPR*, pp. 2–6 (2015). <http://arxiv.org/abs/1502.00873>
9. Toshev, A., Szegedy, C.: Deeppose: human pose estimation via deep neural networks. In: *Proceedings of the IEEE Conference on Computer Vision and Pattern Recognition*, pp. 1653–1660 (2014). <http://doi.org/10.1109/CVPR.2014.214>
10. Yuan, Y., Mou, L., Lu, X.: Scene recognition by manifold regularized deep learning architecture. *IEEE Trans. Neural Netw. Learn. Syst.* **26**(10), 2222–2233 (2015). <https://doi.org/10.1109/TNNLS.2014.2359471>

11. Schmidhuber, J.: Deep learning in neural networks: an overview. *Neural Netw.* (2015). <https://doi.org/10.1016/j.neunet.2014.09.003>
12. Kussul, N., Lavreniuk, M., Skakun, S., Shelestov, A.: Deep learning classification of land cover and crop types using remote sensing data. *IEEE Geosci. Remote Sens. Lett.* **14**(5), 778–782 (2017). <https://doi.org/10.1109/LGRS.2017.2681128>
13. Luus, F.P.S., Salmon, B.P., Van Den Bergh, F., Maharaj, B.T.J.: Multiview deep learning for land-use classification. *IEEE Geosci. Remote Sens. Lett.* **12**(12), 2448–2452 (2015). <https://doi.org/10.1109/LGRS.2015.2483680>
14. Cheng, G., Han, J.: A survey on object detection in optical remote sensing images. *ISPRS J. Photogramm. Remote Sens.* (2016). <https://doi.org/10.1016/j.isprsjprs.2016.03.014>
15. Krizhevsky, A., Sutskever, I., Hinton, G.E.: ImageNet classification with deep convolutional neural networks. In: *Advances in Neural Information Processing Systems*, pp. 1–9 (2012). <http://dx.doi.org/10.1016/j.protcy.2014.09.007>
16. Simonyan, K., Zisserman, A.: Very deep convolutional networks for large-scale image recognition. In: *International Conference on Learning Representations (ICRL)*, pp. 1–14 (2015). <http://doi.org/10.1016/j.infsof.2008.09.005>
17. Szegedy, C., Liu, W., Jia, Y., Sermanet, P., Reed, S., Anguelov, D., Erhan, D., Vanhoucke, V., Rabinovich, A.: Going deeper with convolutions. In: *Proceedings of the IEEE Computer Society Conference on Computer Vision and Pattern Recognition*, vol. 07-12-June-2015, pp. 1–9 (2015). <http://doi.org/10.1109/CVPR.2015.7298594>
18. He, K., Zhang, X., Ren, S., Sun, J.: Deep residual learning for image recognition. In: *2016 IEEE Conference on Computer Vision and Pattern Recognition (CVPR)*, pp. 770–778 (2016). <http://doi.org/10.1109/CVPR.2016.90>
19. <http://cs231n.github.io/linear-classify/>
20. <https://keras.io>



Detecting the Potential Roof for Green Rooftop Development Using Geospatial Techniques: A Case Study in North of Bangkok

Chomchanok Arunplod^(✉)

Geography Department, Faculty of Social Sciences,
Srinakarinwirot University, Bangkok, Thailand
chomchanok@g.swu.ac.th

Abstract. Bangkok, a capital city of Thailand, is a life destination of people not only be a capital city but also the center of business, education and tourism. Then Bangkok is one of the fascinating places to visit and live, resulting in over-capacity. The highly demand of land allocation which shifts from agriculture or other spaces to shelter function. The green space in urban area is dramatically decreasing since last decade. In 2015, a green space in Bangkok appeared less than 20% of the total area, especially in north of Bangkok due to urban expansion. In contrast, the demand of green space is increasing year by year. Government authorities and communities are endeavoring to get a green space. The main find out of this research is to identify the potential area for green space developing on rooftop in a northeast area of Bangkok. Best Management Practices (BMPs) for urban green space development process by using Geographic Information System (GIS)-based model is applied for site suitability analysis. The criteria for potential green space on rooftop are defined in term of physical and economic aspects. The preliminary result of suitable green-rooftop development are identified and compared with the land-price. Finally, the green rooftop areas were identified based on economic factor as a main driver for decision making for urban planner and communities.

Keywords: Green rooftop · Best management practice · Geographic information system (GIS) · Bangkok

1 Introduction

Bangkok is like almost every Southeast Asian metropolis, the population has nearly tripled from 1960 to 2010 and since 2000 the city recorded average growth of 2.5%, per year. Urban expansion was the major reason behind the issue [1]. Bangkok is the center of all; administrations, economy and industries. Moreover Bangkok knows as one of the fascinating cities in Thailand for visiting, living and working. The population of Bangkok is stroking increasing in this decade, cross the city's capacity [2]. Most of city dominated by air-conditioned complexes environment and crowded [3]. There are small numbers of green areas in Bangkok likes other major cities in Asian, unable to fulfill the demand of people. Since Bangkok Metropolitan Administrative (BMA) has enacted the master plan for Bangkok area, neither slowing down the growth

rate. In other words, it fascinates people to move into the Bangkok year by year. An extended boundary needs a transportation to carry on the commuters then the primary transportation mode of Bangkok is road-based transportation. The covered road-networks and first-car policy in 2010 resulted in sharp increases in private car return in more air pollution added in Bangkok [4]. The static endorses the push & pull conditions of Bangkok growth including transportation networks, are getting to become an increasingly more important factor in the future urban densification [5].

Urban-Heat-Island (UHI) issue in Bangkok is raised by several stakeholders in 2012. Unfortunately, the urban extent of Bangkok is continued to increase at an average rate of 4.8% since 2002 [5, 6]. Demand for built-up areas is rising and urban areas tend to be widely sprawled out from inner of Bangkok to nearby provinces. Physical effects are clearly defining like congestion, equity in public services, pollution etc. Major effect of urban expansion is the increased in average temperature.

The heat prevents water vapor from cooling and condensing to produce rainfall. Water vapor collects and allies with energy from downtown Bangkok, which moves up to meet cool, moist bodies of air in the north of Bangkok, called Rangsit-PathumThani area [7]. Moreover, the concert construction, also called grey construction, directly changes the character of urban, especially runoff consumption. When rain falls on our roofs, streets, and parking lots in cities and their suburbs, the water cannot soak into the ground as it should. The fast and strong runoff, called stormwater, is a main of water pollution in urban areas. Because stormwater carries trash, bacteria, heavy metals, and other pollutants from the urban landscape, are damaging habitat, property, and infrastructures [8].

According to ongoing global trend of sustainable development and impacts of urban expansion, it is increasing awareness and perception of urban green concept. A green concept is introducing as the new way to sustain our urban environment, get rid of the pollution and heat problems in urban area. Hence, modern urban has recently turned their attention into environment-friendly constructions or urban agriculture [9]. Green roofs are one specific types of green concept [10]. The green roof constructions are concerning surface area of rooftop. An increasing of green awareness and perception of urban effects lead the widespread of green roof in Europe [11, 12]. Several scientific literatures have mentioned about the benefits of green rooftop application and one of the vast recognized benefits was the capacity for thermal decreasing [10, 13]. The scientists report a significant green roof that it is able to decrease of surface and air temperature comparing with conventional roofs [14–16].

The keys to success are ability of monitoring urban environment situation and strengthen urbanites of green perception. Literatures disclose that a geospatial technique provides significant contributions in green concept more than a decade, ranging from an overlay technique to complex criteria of site suitability selection. Tuntaopas [7] used image classification techniques to detected land use change of green area in the east of Bangkok, Nongchok district by using satellite images; 10-year in range. Results stated that a compound agriculture was rapidly changed to built-up area. The study confirmed the useful to apply Geoinformatics techniques for monitoring and detecting green area. Additionally, success stories on an urban green area monitoring using geoinformatics techniques has been evidenced. Wong and Lau [17] published the potential green roof retrofit in the densely old urban district of Mongkok in Hong

Kong. Two variables were analyzed: exposure to sunlight and roof space which manually extracted from Google View images. They found that many of the rooftops have the potential for green roof retrofit due to building conditions. As same as Tian and Jim [18] who have studied the factors that affect the spatial pattern of sky garden in Hong Kong using orthophoto maps, building's footprint and zoning plans information. The buildings were classified according their characters at district level. Both of two researches aim to study current green rooftops and podiums rather than to identify the new area for green rooftops.

Best Management Practices (BMPs) is proposed to provide more practically development in green concept. BMPs was developed by United States Environmental Protection Agency (EPA), a main function is site selection for different types of low impact development (LID) [19] according to the defined site suitability criteria, such as land use, soil, height information etc.

In this study, we determine the potential area for green rooftop development in the North of Bangkok where urban expansion is increasing. Multi spatial datasets are collected and prepared for GIS-based analysis. The analysis based on BMPs model which is plug-in in ArcGIS software to selects a suitable site for green roof development. However, to motivate people turn their conventional rooftop into green roof needs more than physical factor alone. This study also focused on socio-economic factor. The results were then overlay with the land price, the average income layers to explain a possibility of development the green-rooftop both in common and policy levels. Consequently, the green roofs are related to the characteristics, spatial and economic extent of different environment.

2 Materials and Methods

2.1 Study Area and Available Spatial Data

Bangkok has a registered population of 5,696,409 according to the 2015, the ten districts where the population have more than 100,000 mostly located in the north part of Bangkok [5]. The blooming of population results from promoting public transport policy by extending sky train networks construction projects (red & green lines), the connecting new CBD-to-motorway. For the past five years, a rapid change in land use reflects by the increase in construction activities. Area of study site is shown in Fig. 1. The major land use type is residential, government, commercial and tiny industrial respectively. The lower of study site is connected with an old city area, high density resident with old construction models. The upper zone is newly construction area consisting of transportation networks.

This study has utilized different spatial data sources in GIS environment (ArcMap version 10.2, ESRI). The spatial data collected from various government official sources as the following;

1. A digital elevation model (DEM) from aerial photo with 5 meters resolution and a height accuracy 1 m (RTSD, 2016)
2. A vector based land use map based on Bangkok's planning laws. The map was generated from aerial photo at scale of 1:4000 (BMA, 2016)

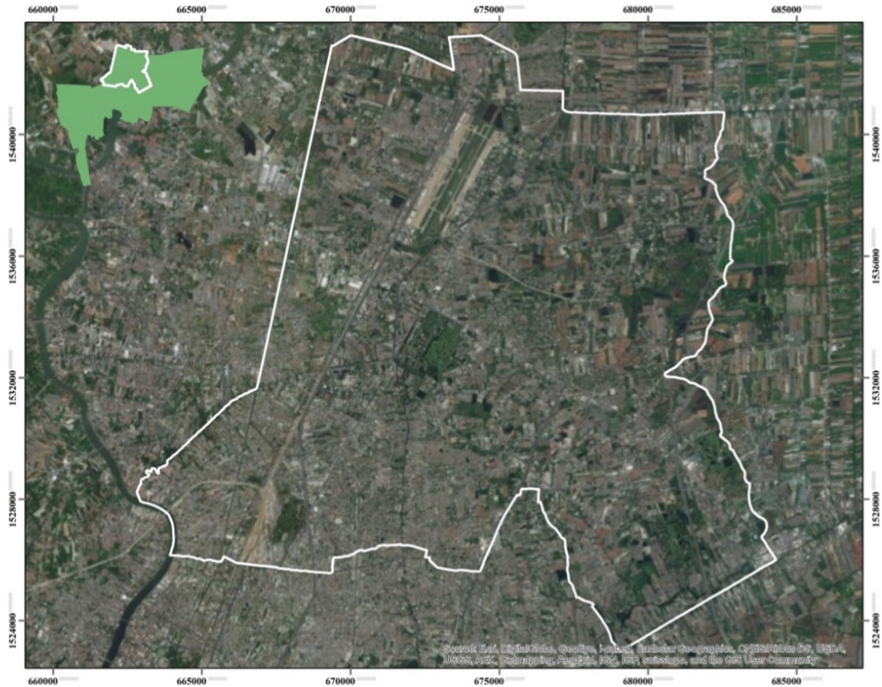


Fig. 1. Map of north area of Bangkok (white boundary) (map source: google earth data through ArcGIS software)

3. Utilities life line of study area based on 2015 which were provided as polyline vector data of roads and major river network. (BMA, 2016)
4. Soil map which provides a soil character of the study area in polygon format. (BMA, 2016)
5. Groundwater map. (DGR, 2016)

2.2 Data Preparation

All spatial data layers (Table 1) were prepared by a ready-format of ArcMap-BMPs. This section briefly explains the preparation process through various layers.

Noises in elevation layer were filled by using Raster management tool in GIS software to represent contiguous surface (Fig. 2). Stream network defined as river and irrigation network provides location of water run-off area and direction (Fig. 3). Drainage area of urban run-off water is derived by road network.

Land use data collected from BMA is classified into 12 types of land use. According to definition of ArcMap-BMPs, land use was recoding as number 1–10 and transformed into raster format with the same pixel size of DEM (Fig. 4).

Urban land use data is digitized through GIS software and was generated from land use data to identify public or private area for land ownership. An initial land use data is

Table 1. The input layer of ArcMap-BMPs tool.

Input	Explanation	Format
DEM	To calculate the drainage slope and drainage areas	Raster
Soil	To provides the percent impervious layer	Vector
Stream	To define a buffer area, can be placed outside the buffer to minimize the impact on streams	Vector
Road	To identify suitable location according in a specific road buffer	Vector
Land use	To eliminate the unsuitable areas from analysis	Raster
Urban land use	To contain the boundaries for the buildings and the impervious area	Vector
Groundwater	To locates the infiltration capacity	Vector
Land ownership	To identify the public or private land	Vector

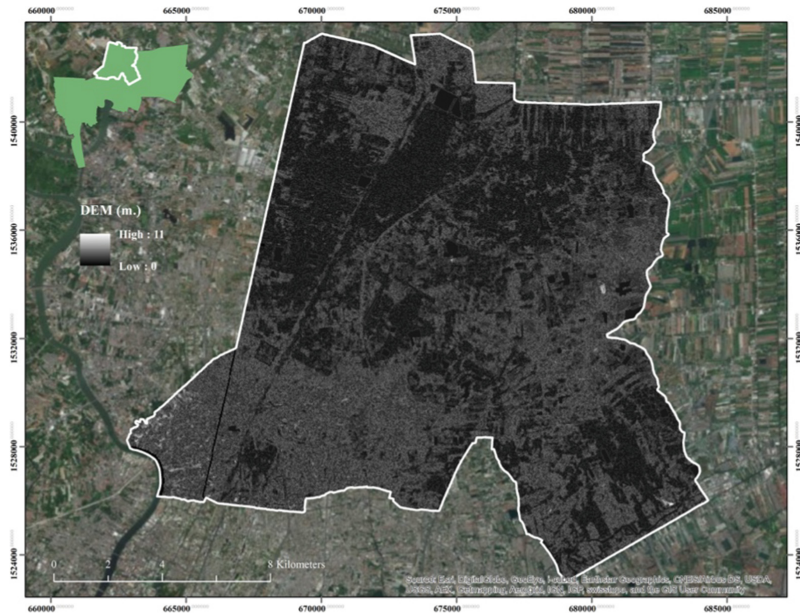


Fig. 2. Digital Elevation Model (DEM) of study site, the dark represents the low and the light represents the high.

recorded by using two categories; a government and public services category are recording as public whereas residential, commercial and industrial area are recorded as a private area (Fig. 5).

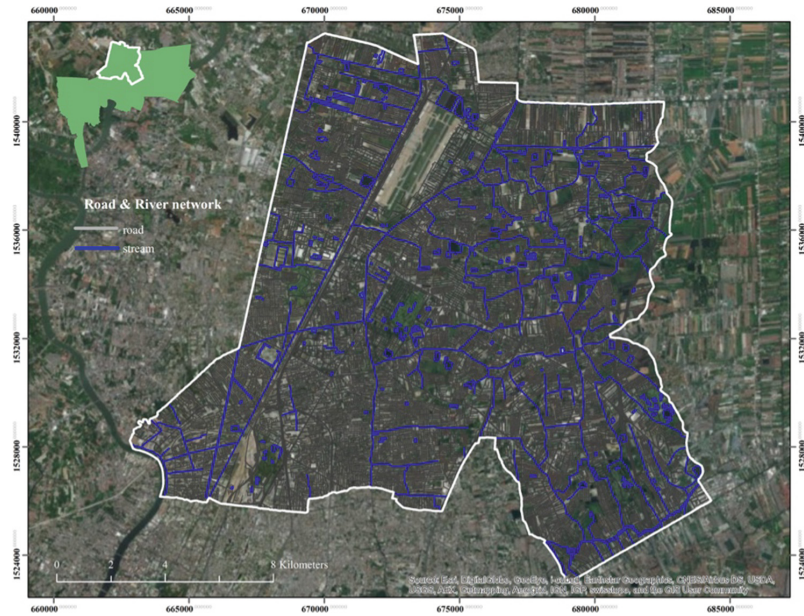


Fig. 3. Stream and road networks are the initial data to generated the impact area on streams.

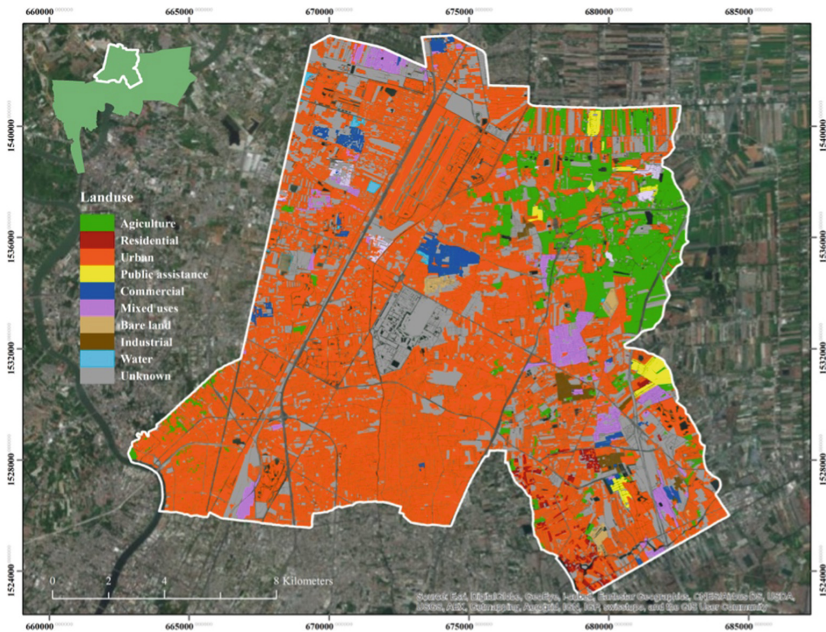


Fig. 4. Land use map from BMA, an initial data to generated the other layers



Fig. 5. Public and private land ownership in a study area

3 The Green Rooftop in Expanded Urban

All required layers were obtained scores based on suitability level for green rooftop development. In consequence, an initial result is the locations of potential green rooftop which only consider the physical factors according to Arc-BMPs model. Aforementioned, this study concerns not only physical factor but economic factors need to be taken into account also. A land price map and an average income map were overlay with the identified green rooftops to suggest the potential of green rooftop installation in practical way (Fig. 6). The result demonstrated the potential area to develop green rooftop. The most proper buildings is identified as public buildings like hospital, government offices and airport because the size and the shape of these rooftop are large and flat. Moreover, the public buildings can be funding support by government which easy to rooftop renovation and promoting the green infrastructure concept. Another alternative buildings are flatted-rooftop of private buildings with pretty high average income. The shape of rooftop is suitable to develop to be green rooftop but decision has to be made by owner of buildings. Finally, the low potential of green rooftop development is the private buildings with sloped-rooftop.

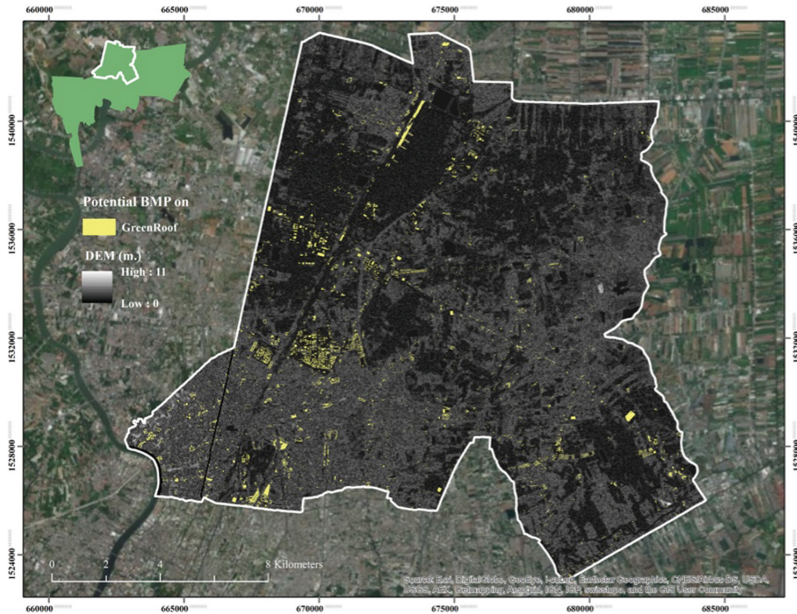


Fig. 6. The suitable buildings for green rooftop development based on their physical and economic factors.

4 Concluding Remarks

The motivation of this study is to address and map the area for green rooftop development. A GIS-based model was selected to analysis, all model requirement maps prepared. The output shows the potential area based on physical criteria. To encourage people on green concept, green rooftop do needs to consider socio-economic criteria. Even the green concept is wide spreading in Thailand but the installment cost of green rooftop system is still expensive. This study applied the land price and average income layers to analyze a possibility of development the green-rooftop. Furthermore, the age of building should be considering in analysis; it relates to ability of structure-weighting. The type of plant has to be specified in various literatures for urban area. The green rooftop is proven to be useful in several countries [20, 21], reducing the global warming and energy consumption in household level. This attempts cannot be success without promoting to increase the green rooftop development in urban area for a sustain urban environment.

References

1. Urbanalyse. <https://urbanalyse.com/research/growing-bangkok/>
2. Shlomo, A., Jason, P., Daniel, L.C., Blei, A.M.: Making Room for a Planet of Cities. Lincoln Institute of Land Policy, USA (2011). https://www.researchgate.net/publication/267418628_Making_Room_for_a_Planet_of_Cities_Ma-ing_Room_for_a_Planet_of_Cities

3. NationNEWS. <http://www.nationmultimedia.com/business/Green-roof-the-environment-friendly-urban-access-t-30236625.html>
4. Clean Air Initiative, Archive.org. Developing Integrated Emission Strategies for Existing Land-transport (2012). https://web.archive.org/web/20130603110642/http://cleanairinitiative.org/portal/system/files/articles-72628_Ch3.pdf
5. Table of Population and household statistics by districts in 2015. BMA Data center <http://203.155.220.230/bmainfo/esp/>. Accessed 4 May 2018
6. Atlas of Urban Expansion. <http://atlasofurbanexpansion.org/cities/view/Bangkok>
7. Tuntaopas, S.: Application for green area change detection in Nongchok District, Bangkok. Master thesis of Environmental Management. National Institute of Development Administration (NIDA), Bangkok (2008)
8. Environmental Protection Agency (EPA). <https://www.epa.gov/green-infrastructure/what-green-infrastructure>
9. Modern urban has recently turn their attention into life with green environment like environment-friendly constructions or urban agriculture [Berger thesis 2013]
10. Sutton, R.K.: Introduction to green roof ecosystem. In: *Green Roof Ecosystems*, pp. 1–25. Springer, Heidelberg (2015)
11. Larsen, L.: Urban climate and adaptation strategies. *Front. Ecol. Environ.* **13**(9), 486–492 (2015)
12. Berardi, U., GhaffarianHoseini, A., GhaffarianHoseini, A.: State-of-the-art analysis of the environmental benefits of green roofs. *Appl. Energy* **115**, 411–428 (2014)
13. Sun, T., Grimmond, C.S.B., Ni, G.-H.: How to green roofs mitigate urban thermal stress under heat waves? *J. Geophys. Res.: Atmos.* **121**, 5320–5335 (2016)
14. Teemusk, A., Mander, Ü.: Temperature regime of planted roofs compared with conventional roofing systems. *Ecol. Eng.* **36**, 91–95 (2010)
15. VanWoert, N.D., Rowe, D.B., Andresen, J.A., Rugh, C.L., Fernandez, R.T., Xiao, L.: Green roof stormwater retention: effects of roof surface, slope, and media depth. *J. Environ. Qual.* **34**(3), 1036–1044 (2005)
16. Heusinger, J., Weber, S.: Surface energy balance of an extensive green roof as quantified by full year eddy-covariance measurements. *Sci. Total Environ.* **577**, 220–230 (2017)
17. Wong, K.W., Lau, L.S.-K.: From the ‘urban heat island’ to the green island? A preliminary investigation into the potential of retrofitting green roofs in Mongkok district of Hong Kong. *Habitat Int.* **39**, 25–35 (2013). <https://doi.org/10.1016/j.habitatint.2012.10.005>
18. Tian, Y., Jim, C.Y.: Factors influencing the spatial pattern of sky gardens in the compact city of Hong Kong. *Landscape Urban Plan.* (2011). <https://doi.org/10.1016/j.landurbplan.2011.02.035>
19. Environmental Protection Agency (EPA). <https://www.epa.gov/water-research/best-management-practices-bmps-siting-tool>
20. Cook-Patton, S.C., Bauerle, T.L.: Potential benefits of plant diversity on vegetated roofs: a literature review. *J. Environ.* **106**, 85–92 (2012)
21. Grunwald, L., Heusinger, J., Weber, S.: A GIS-based mapping methodology of urban green roof ecosystem services applied to a Central European city. *Urban Forest. Urban Greening* **22**, 54–63 (2017). <https://doi.org/10.1016/j.ufug.2017.01.001>



Land Use and Land Cover Change of Chanthaburi Watershed Following 1999, 2006 and 2013 Floods

Chuti Chatewutthiprapa^(✉), Srilert Chotpantararat,
and Sombat Yumuang

Department of Geology, Faculty of Sciences, Chulalongkorn University,
254 Phayathai Road, Pathumwan, Bangkok 10330, Thailand
cuchaleck@gmail.com

Abstract. The application of remote sensing (RS) and Geographic Information System (GIS) have become an effective tool, which is labor, cost and time effective to assess and widely used in detecting, monitoring environmental change on the earth surface. Moreover, it can be used to study a pattern of land use and land cover (LULC) in the past, present and future. For this study, Landsat imageries were used as a data to deal with the assessment of land use and land cover changes (LULCC) before and after 3 flooded periods in 1999, 2006 and 2013. The images were used to create a false color composite and classified by supervised classification process, it can be identified as 9 LULC types, which consist of paddy field, field crop, para rubber, orchard, aquaculture, forest, mangrove, urban and built-up area, including water body. According to the result of this study, LULC types which mainly cover in the watershed are forest and orchard. After that, LULC were reclassified into 4 main classes for change detection, comprising of agricultural, forest, urban and built-up, and water bodies. The results showed LULC transformation mainly occur among agricultural land into the urban built-up area in the period 1999, 2006, and 2013. As a result, this study found that the socioeconomics factor plays an important role in LULC in Chanthaburi watershed. The results of this study can be used as data for making decision and planning LULC management, also in disaster response planning and flood risk management.

Keywords: Land use and land cover change (LULCC) · Flood ·
Geoinformatics · Chantaburi

1 Introduction

Watershed is an area which catches the water from precipitation and then drained by a river and its tributaries. It is a resource region where the ecosystem is closely interconnected around a basic resource – water, soil, vegetation etc. The watershed or river basin is therefore an ideal management unit and it is the place where we live and play. Everyone relies on water and other natural resources for living. Every activity in watershed is connected to each other so if some part was disturbed or encroached, it will affect to another part of watershed area [1]. So, the watershed is the logical unit for

coordinated land-use planning and management and effective and sustainable resource and environmental management [2].

Chanthaburi Province is in the eastern part of Thailand. There are many watersheds locate in this area. One of famous watersheds is Chanthaburi watershed, where located in East-coast gulf of Thailand and Chanthaburi River serve as a main stream. A river flows from the mountain area in upstream of the watershed to floodplain in downstream, then drain into the Gulf of Thailand. This area is influenced by Northeast Monsoon, especially Southwest Monsoon, which blows for 5 months from May to October [3], increases humidity in the rainy season and it plays an important role in distributing rainfall in watershed area.

The important issues of this watershed is a heavy rainfall that lead to flash flood and riverine flood. It usually happens in every year, and causes damages to properties, infrastructures, agricultural areas and transport routes.

For the last 15 years, there was 3 significant floods in 1999, 2006 and 2013 in Chanthaburi watershed which caused loss and damage than previous flood events [4]. Moreover, LULC in Chanthaburi watershed have been changed enormously by many activities [5], the flood may be one of the reason behind LULC change, especially in a downstream area. The study of LULC change after flooding might reveal its pattern and lead to effective land use planning in the future.

The Geo-Informatics, which consist of remote sensing (RS) and Geographic Information System (GIS) techniques are art and science to obtain the reliable information about physical object on the earth surface through the process of recording, measuring and interpreting imagery and digital representations of energy pattern which can retrieve information by non-contact sensor system [6]. GeopInformatics were applied to investigate and detect LULC change over Chanthaburi basin after the flooding events in the past 15 years.

This research aims to determine LULCC after flooding in 1999, 2006 and 2013. So, the satellite image data is very important to study and understand the event in the past. LANDSAT satellite image is an easy accessible data and widely used in many researches. There are 6 satellite images from 3 Landsat satellite systems were used in this study, namely LANDSAT 5 Thematic Mapper (TM) (30 m resolution RGB band) Landsat 7 Enhanced Thematic Mapper Plus (ETM+) and Landsat 8 Operational Land Imager (OLI) (30 m resolution RGB band). The combination of LULCC and RS provide a useful information for LULC management.

2 Materials and Methods

2.1 Study Area

Chanthaburi watershed which situate in Chanthaburi province, cover 5 districts area, namely Muang Chanthaburi, Khao Khitchakut, Makhnam, Tha Mai and Laem Sing. The total area of this watershed is about 1600 km². The extend of the coordinates of the study area are approximately defined as 820000 E, 1380000 N in the northwestern edge and 860000 E, 1455000 N in the southeastern edge in Universal Transverse Mercator projection with 48 North zones in WGS 1984 ellipsoid. This study area

covers path 128 row 51 of LANDSAT satellite. The hinterland of the watershed is a mountainous area, with the Chanthaburi mountain ranges. Its elevation ranges from 0 to 1675 m above average mean sea level (Fig. 1).

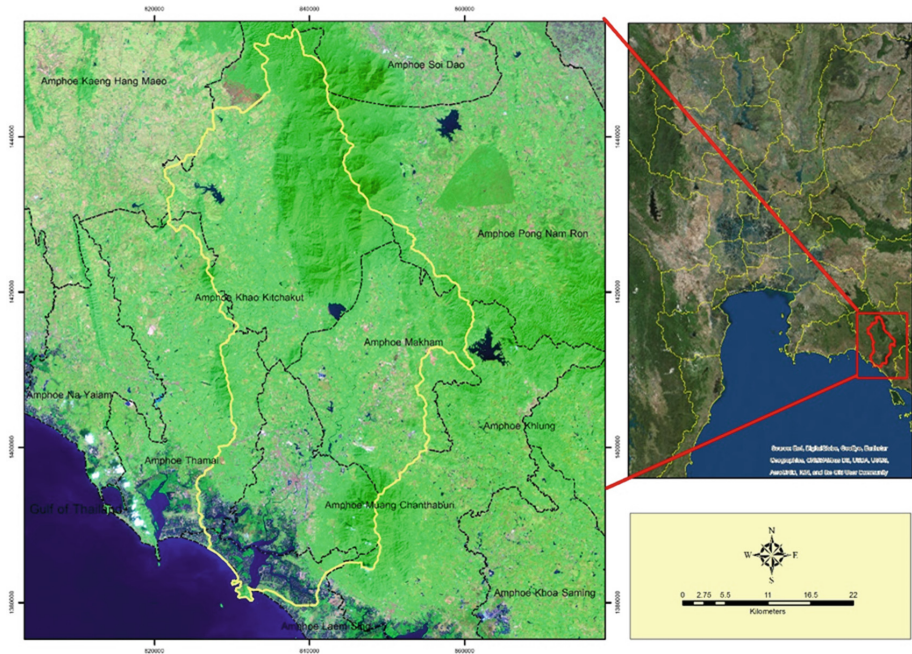


Fig. 1. Landsat imagery of the Chanthaburi watershed (study area)

2.2 Materials

Satellite Image

In this study, 6 Landsat satellite images were used for LULC classification. The multi-temporal Landsat is used for detecting LULC, offering information in the current and past of earth's surface, tracking vegetation, agricultural, urban and built-up, and hydrology. So, it is a valuable tool in qualitative and quantitative LULCC. They were downloaded from United States Geological Survey (USGS) website, which the acquisition date is decided based on the time of before and after flood period in years 1999, 2006 and 2013 and minimum or no cloud coverage (Table 1).

There are 9 categories of LULC for this study based on the secondary data from Land development department of Thailand and the classification system from USGS, consists of paddy field, field crop, para rubber, orchard, aquaculture, forest, mangrove forest, water bodies and urban and built-up area (Table 2). Then ERDAS 2014 and ArcGIS 10.2.2 software was utilized for image processing and mapping layout respectively.

Table 1. The remote sensing data attributes and accessing period for this study.

Image type	Path/Row	Band (R:G:B) ^a	Acquisition date	Original		
				Format	Resolution	Source ^b
Landsat-5 TM	128/51	5:4:3	1999-02-02	TIFF	30 m	USGS
Landsat-7 ETM+	128/51	5:4:3	1999-12-27	TIFF	30 m	USGS
Landsat-5 TM	128/51	5:4:3	2005-02-18	TIFF	30 m	USGS
Landsat-5 TM	128/51	5:4:3	2006-11-04	TIFF	30 m	USGS
Landsat-5 TM	128/51	5:4:3	2011-01-18	TIFF	30 m	USGS
Landsat-8 OLI/TIRS	128/51	7:5:3	2014-01-26	TIFF	30 m	USGS

^aR:G:B red:green:blue

^bUSGS United States Geological Survey

Table 2. Classes delineated on the basis of supervised classification

LU CODE	
Level 1	Level 2
A Agricultural land	A01 Paddy field
	A02 Field crop
	A03 Para rubber1
	A04 Orchard
	A05 Aquacultural land
F Forest land	F01 Forest
	F02 Mangrove forest
U Urban and built-up area	U00 Urban and built-up area
W Water bodies	W00 Water bodies

2.3 Methodology

Image Processing

The LULC classification were derived by image processing. unsupervised and supervised classification approach, which integrated with successive Geographic Information System (GIS) to classify the imageries of Landsat 5 TM, 7 ETM+ and 8 OLI to LULC classes. In determining the spectral classes Iterative Self-Organizing Data Analysis (ISODATA) clustering was performed and the satellite images were classified into LULC maps using the Maximum likelihood classification algorithm [7], an area of interest (AOI) file were selected to represent each LULC class and converted into the correct class using fill algorithm in Erdas Imagine version 2014 software [8]. In this

study, there is an approach to validate the classification results; namely accuracy and Kappa coefficient [9]. Overall accuracy was carried out by using the point from ground truth data and visual interpretation, all of the data will be compared by statistical method using error matrix. In other words, Kappa will be used to measure the accuracy in classification [10] (Fig. 2).

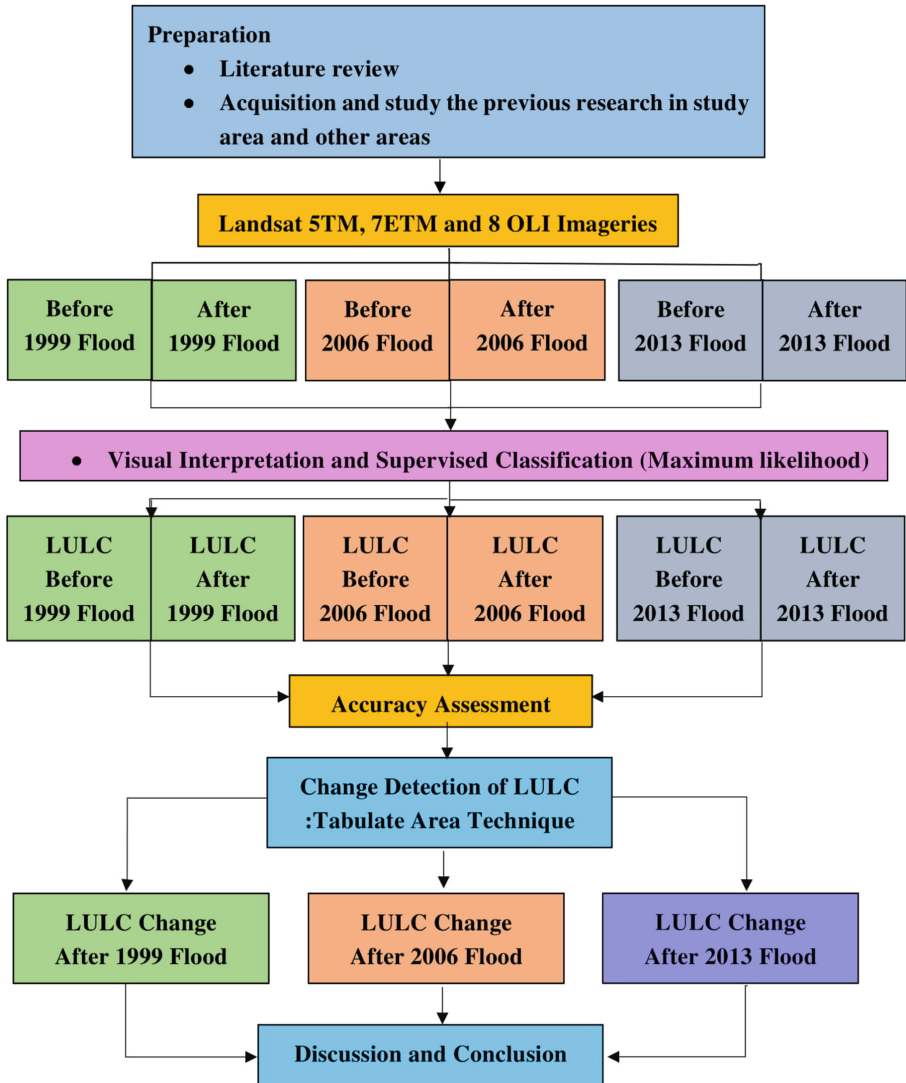


Fig. 2. Schematic diagrams illustrating the research methodology system.

Change Detection

Change detection technique was calculated using cross-tabulated areas between two datasets. This approach used the Tabulate Areas tool in ArcGIS to produce a cross-tabulation table. This was used to compare and calculate coincident areas. As an example, using Tabulate Area, one could calculate the area of each land use category in each zoning district. The first input was a land use raster, and the second was zoning [11].

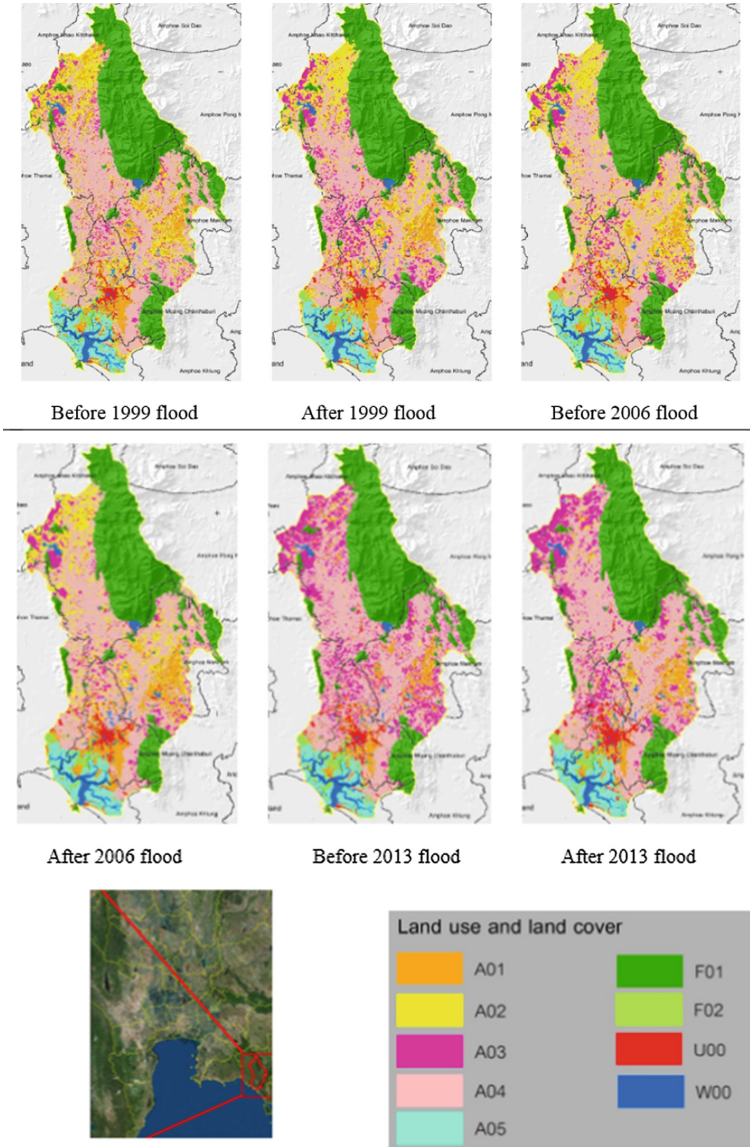


Fig. 3. LULC classification of Chanthaburi watershed

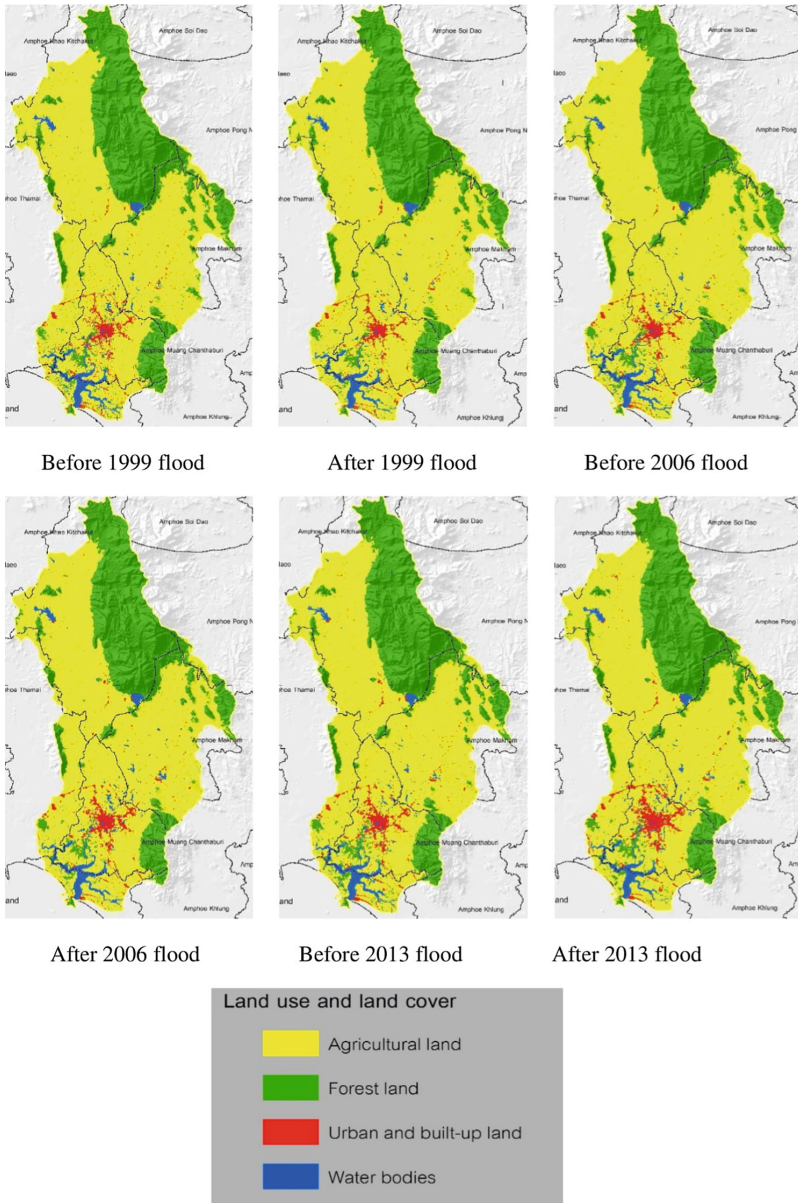


Fig. 4. Land use and land cover classification (Level 1) of Chanthaburi watershed

3.2 Land Use and Land Cover Change

The agricultural land in Chanthaburi watershed has increased by 10.77 km² and 0.11 km² after 1999 and 2006 flood respectively. On the other hand, after 2013 flood agricultural land tends to be slightly decreased by 7.88 km² which turns to be urban and built-up area.

The forest land of the study area mainly includes mangrove forest and forest on the mountainous area. It has witnessed a decrease in forest land from 1999, 2006 and 2013 which decrease in the land area of 7.58 km², 3.74 km², and 0.89 km², respectively.

The information revealed by classification result, urban and built-up area have increased by 0.45 km² in 1999 flood, 1.85 km² in 2006 flood and 9.22 km² in 2013

Table 4. Changes in area of different LULC types in Chanthaburi watershed during 1999, 2006 and 2013 floods as area in km²

Land use and land cover	Area (Square kilometers)		
	LULC change 1999 flood	LULC change 2006 flood	LULC change 2013 flood
Agricultural land	10.77	0.11	-7.88
Forest land	-7.58	-3.74	-0.89
Urban and built-up land	0.45	1.85	9.22
Water bodies	-3.64	1.78	-0.45
Total	22.44	7.48	18.44

Table 5. Cross tabulation matrix between each pair of land use and land cover as area in km²

	After 1999 flood	Agricultural land	Forest land	Urban and built-up land	Water bodies
Before 1999 flood	Agricultural land	993.82	9.12	10.01	3.58
	Forest land	16.87	481.27	0.31	0.74
	Urban and built-up land	0.0	0.33	22.41	0.31
	Water bodies	7.63	0.46	0.64	37.18
Before 2006 flood	After 2006 flood	Agricultural land	Forest land	Urban and built-up land	Water bodies
	Agricultural land	1003.17	14.25	9.94	8.20
	Forest land	16.81	469.29	0.20	0.61
	Urban and built-up land	0.25	0.03	25.75	0.38
Before 2013 flood	After 2013 flood	Agricultural land	Forest land	Urban and built-up land	Water bodies
	Agricultural land	999.10	10.86	16.58	6.23
	Forest land	10.74	479.63	0.26	0.46
	Urban and built-up land	0.64	0.15	29.87	0.49
	Water bodies	6.53	0.36	0.64	36.20

flood. As shown in Table 4, water bodies have decreased by 3.64 km² in 1999 flood, then increased by 1.78 km² in 2006 flood and decreased again by 0.45 km² in 2013 flood (Table 5).

4 Discussion

Urban expansion has contribute to a decrease in agricultural land by 7.88 km², especially in area of Muang Chanthaburi. There are many types of a crop plantation in the agricultural class consists of paddy field, field crop, para rubber, orchard and aquaculture, orchard and para rubber has continuously increasing due to economic forces and agricultural production expansion whereas, field crop has decreased and has shifted to a perennial plantation.

The forest land has witnessed a decrease from 1999, 2006 and 2013. Forest land was replaced by agricultural land which encroached the forest in the mountainous area around the watershed. Moreover, the information reveals that urban and built-up area has intensely increased from 1999–2013 due to the increasing of new housing, including road construction and improvement.

5 Conclusions

The LULC classification of Chanthaburi watershed before and after 1999, 2006 and 2013 floods were obtained by the employment of Geoinformatics approach to explore a change in land use. The main goal of this study is classified LULC pattern in the watershed and its changes after major floodings in 1999, 2006 and 2013. Results reveal that the major type of LULC in Chanthaburi watershed is agricultural land comprising of various plantation; orchard, para rubber, paddy field, field crop, and aquaculture, followed by forest land, water bodies and urban and built-up area. The analysis of LULCC reveals that the agricultural land has increased after 1999 and 2006 flood and decreased after 2013 flood, most of the field crop turned to be orchard because of rising in market demand. The forest land has also continued to decrease which has been transformed to agricultural land in the mountainous area. The urban and built-up area has increased due to a new building, construction of infrastructure. Flooding in Chanthaburi watershed doesn't play a great role in LULCC. In the other hand, economics and social conditions are the important aspect in changing land use. This study can be used as a basis for the other watershed studies which lead to proper watershed management and sustainability in LULC planning in the future using GIS analysis and remote sensing techniques.

Acknowledgement. This research was partially funded by the Ratchadapisek Sompoch Endowment Fund (2017), Chulalongkorn University (760003-CC).

References

1. Ma, Y.: GIS application in watershed management. *Nat. Sci.* **2**(2), 1–7 (2004)
2. UN Economic Commission for Asia and the Pacific -Bangkok: Guidelines and Manual on Land Use Planning and Practice in Watershed Management and Disaster Reduction. United Nations Economic and Social Commission for Asia and the Pacific (ESCAP), Bangkok (1997)
3. Climatological Center - Thai Meteorological Department. Climate of Chanthaburi (2014). <http://climate.tmd.go.th>. Accessed 08 July 2018
4. Royal Irrigation Department. Flood mitigation of Muanf Chanthaburi (Khlomg Bhakti Rambhai) (2012). <http://www.rid.go.th/royalproject>. Accessed 01 Oct 2016
5. Soyong, P., Janchidfa, K., Phengphit, N., Chayhard, S., Perera, R.: The effects of land use change and climate change on water resources in the eastern region of Thailand. *Int. J. Agric. Technol.* **12**, 1697–1724 (2016)
6. Jensen, J.R.: Remote sensing of the environment: An earth resource perspective. Pearson Education, India (2009)
7. Islam, K., Jashimuddin, M., Nath, B., Nath, R.K.: Land use classification and change detection by using multi-temporal remotely sensed imagery: the case of Chunati wildlife sanctuary, Bangladesh. *Egypt. J. Remote Sens. Space Sci.* **2018**(21), 37–47 (2018)
8. Nautiyal, S., Kaechele, H., Tikhile, P., Subbanna, S., Baksi, S.: Study on land use dynamics: appropriate methods for change estimation in social science research. *Earth Syst. Environ.* **1**(2), 27 (2017)
9. Lillesand, T.M., Kiefer, R.W., Chipman, J.W.: Remote Sensing and Image Interpretation. Wiley, New Jersey (2015)
10. Butt, A., Shabbir, R., Ahmad, S.S., Aziz, N.: Land use change mapping and analysis using remote sensing and GIS: a case study of simly watershed, Islamabad, Pakistan. *Egypt. J. Remote Sens. Space Sci.* **18**(2), 251–259 (2015)
11. Liu, Y., Huang, X., Yang, H., Zhong, T.: Environmental effects of land use/cover change caused by urbanization and policies in Southwest China Karst area – a case study of Guiyang. *Habitat Int.* **44**, 339–348 (2014)
12. Mosammam, H.M., Nia, J.T., Khani, H., Teymouri, A., Kazemi, M.: Monitoring land use change and measuring urban sprawl based on its spatial forms: the case of Qom city. *Egypt. J. Remote Sens. Space Sci.* **20**(1), 103–116 (2017)
13. Waiyasusri, K., Yumuang, S., Chotpantararat, S.: Monitoring and predicting land use changes in the Huai Thap Salao Watershed area, Uthathani Province, Thailand, using the CLUE-s model. *Environ. Earth Sci.* **75**, 1–16 (2016)



Identification of Urban Expansion Patterns in Bangkok Metropolitan Region Through Time Series of Landsat Images and Landscape Metrics

Chudech Losiri¹✉ and Masahiko Nagai²

¹ Department of Geography, Faculty of Social Sciences,
Srinakharinwirot University, Sukhumvit 23, Bangkok 10110, Thailand
chudech@g.swu.ac.th

² Graduate School of Sciences and Technology for Innovation,
Yamaguchi University, 2-16-1, Tokiwadai, Ube, Yamaguchi 755-8611, Japan

Abstract. Urban expansion has different patterns which affect land development and police planning. Increasing in the number of the population puts force to expand the built-up areas in the Bangkok Metropolitan Region (BMR) predominantly in vicinities of Bangkok, which causes several problems in terms of physical and social aspects. Therefore, understanding the pattern of the urban expansion is a key challenge to allocate enough infrastructure and respond to the land demand for inhabited people in this area. The classification of the pattern of urban expansion analyzed from Landsat5-TM images in 1988, 1993, 1998, 2003, 2008, 2011, and 2014 respectively. The urban area, built-up construction, was mainly extracted by supervised classification and was analyzed patterns using spatial landscape metrics. The result could be found that the origin of the urban area of the BMR was established in the east of the Chao Phraya River with a clustered or radial settlement. Each province of the BMR is extended from the urban area itself, from the center of the city, and is also connected together via the main road as a linear settlement. Finally, a dispersed settlement could be discovered in the areas which are far away from the road network like an urban sprawl.

Keywords: Urban expansion · Patterns · Landsat · Landscape metrics · Bangkok Metropolitan Region

1 Introduction

Urban growth is an interesting phenomenon on the Earth surface which spotlights to a number of people related in the field of urban planning, geography, and geoinformatics. It is an increase of urban features physically resulted from increasing in the number of population living and working the city [1]. There are many processes of change involved in such as economic, demographic, politic, culture, social, technology, and environment. The effects of the urban growth can be yielded on the urban system, land use, building environment and townscape, social ecology, and urbanism [2]. To understand the urban

growth, several research scholars have addressed through studies of urban expansion patterns because they can measure directly directions and areas of the urban.

The most important aspect of monitoring the urban growth patterns is demonstrated by lots of numbers of works from the long history [3–5]. For instance, earlier, several research scholars used models such as concentric, sector, and multiple nuclei models to understand the pattern of the city [6]. However, those methods are based on the basic knowledge of economic theory which is quite difficult to comprehend in the real world currently. Moreover, some studies used population density and housing price to explore the urban expansion like von Thünen who developed the spatial-explicit model from the land use to analyze a spatial structure of the city [7].

Due to the advanced technology of satellites from the remote sensing system, the satellite images can provide significant data of the land use and land cover change and their impacts at various spatial scales [8]. In addition, the satellite image can support users to observe and map the urban area for a recent year [9]. The characteristics of the remote sensing data including temporal, spatial, spectral resolutions are useful to remark the spatial-temporal of the urban growth and expansion [10]. The pattern of the urban expansion is an interesting and challenging topic for spatial planners to identify a type [11]. The urban expansion pattern also gives the information to allocate enough infrastructure to respond the demand of people in this area.

To detect the pattern of the urban expansion, many studies are focusing on using images obtained from the remote sensing data. Visual interpretation becomes one of the well-known methods which geographers and spatial planners always use to identify the pattern according to the settlement theory such as cluster, linear, and dispersion. However, other studies suggest that a quantitative method should be applied [12]. Landscape metrics are quantitative approach usually adopted to study in the landscape ecology which reflect the consequence of ecological processes in a specific site [11]. Moreover, many researches have confirmed that they are highly potential schemes to analyze urban expansion patterns [12].

In this study, Bangkok Metropolitan Region (BMR), a big agglomerated-urbanized area of Thailand, consisting of six provinces; Bangkok Metropolis, Nonthaburi, Samut Prakan, Pathum Thani, Samut Sakhon, and Nakhon Pathom, was analyzed the pattern of the urban expansion through the time series of Landsat image from 1988 to 2014 using landscape matrices from FRAGSTATS. The outcome of this study can be delivered to the spatial planning unit or the relevant organizations to improve and understand the urban growth situation in this area.

2 Landscape Metrics and Their Applications in Urban Area

2.1 Landscape Metrics

Landscape metrics are one of the spatial metrics which is used to measure quantitatively to assess spatial characteristics of forms and structures. They have been applied since the 1980s in the field of landscape ecology to identify the pattern and shape of vegetation [12]. The environment protection and resource conservation are two main consideration in the field of landscape ecology focusing on undeveloped natural areas

and on the spatial implications of ecological processes in landscapes. These metrics are used to determine the effect of system interaction in a varied landscape from the structure change, numerical comparison of landscapes, and the recognition and monitoring the landscape change [13]. Therefore, landscape metrics have traditionally been used to quantify several aspects of landscape configuration and composition, focusing primarily on types of land cover rather than land use [12].

2.2 Applications of Landscape Metrics in Urban Area

Landscape metrics have been increasingly considered to apply to the urban pattern study. Several studies used the adapted landscape metrics called spatial metrics to identify the urban spatial characteristics [11, 12, 14, 15]. Other studied also linked them with economic processes to see the change in land use patterns and also integrated with urban growth models [14].

Clifton et al. [16] explained that the spatial landscape metric, which is adapted from the landscape ecology, use the data gathered from aerial photography and satellite remote sensing. The metrics use patches which are polygons with similar characteristics for a specific property of the landscape as a basic unit for analysis. In order to determine a spatial pattern of the urban expansion, there are four categories of the metrics which are always applied for quantifying. The detail of each metric can be elaborately explained in detail as follows [12].

- (1) Shape irregularity consists of metrics which assess the physical form of an urban settlement. The general form can be divided into a regular or even shape and a complex shape with a ragged edge. These metrics can be characterized as a single patch (fractal dimension or shape index) or a complex landscape level (landscape shape index, edged density or area-weighted mean patch (AWMP) fractal dimension). In general, the metrics usually implemented to detect the shape irregularity are area-weighted mean patch (AWMP) fractal dimension, edge density, area-weighted mean (AWM) shape index and landscape shape index.
- (2) Fragmentation metrics are used to measure the extent of the urban settlement or patches which are close to each other (aggregated) or dispersed (fragmented). These metrics are used at the landscape level. A fragmented landscape is normally characterized by a higher number of patches, with a smaller average size located further away from each other. The metrics mostly used to measure fragmentation are mean patch size, the number of patches, patch density and contagion index.
- (3) Diversity metrics pay attention to the urban landscape composition rather than to its shape. The famous metrics are Shannon's diversity and evenness indexes, which measure the distribution of different patch types (such as land use types) throughout the urban area. Patch size standard deviation measures whether the size of the patches varies considerably across the urban area. It may be considered a diversity measure, although it focuses on spatial configuration.
- (4) Other metrics include the largest patch index, measuring the relative importance of the largest patch (which may be useful to study, for instance, the importance of the urban center), and the compactness index, which uses concept of compactness based on both fragmentation and shape irregularity.

3 Data and Methodology

In order to analyze the pattern of urban expansion of BMR, this study implemented several processes. The first one was mapping the built-up area to identify the extended urban zone of BMR from the time series of satellite images. The second was a selection of the spatial landscape metrics. The third was the identification of the urban expansion pattern. Each process can be detailed as follows and the overall operation of the methodology is shown in Fig. 1.

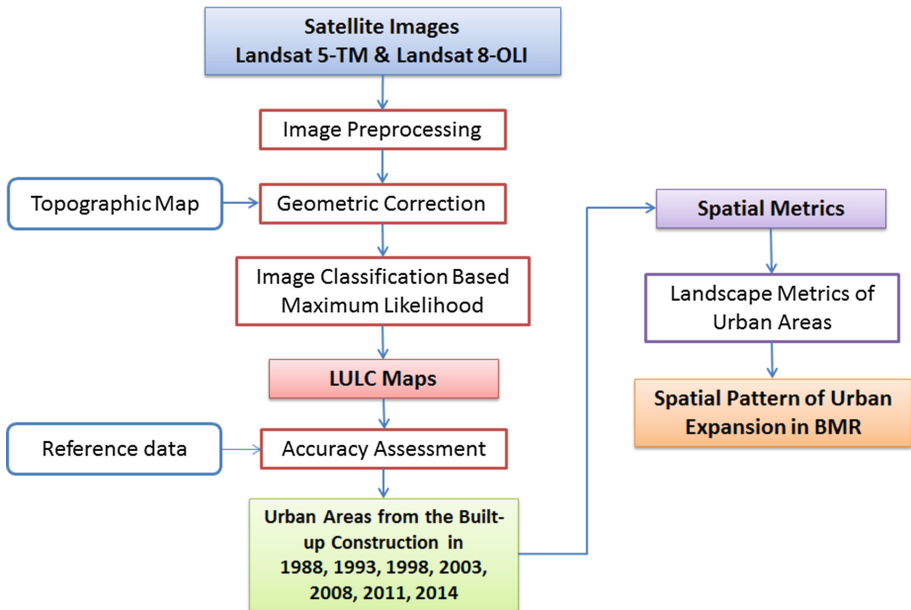


Fig. 1. Overall operation of the methodology

3.1 Urban Land Use Maps for the Bangkok Metropolitan Region

Mapping the urban area of the BMR is the most important process of this objective. The time series of the Landsat data, acquired from the U.S. Geological Survey (USGS) via the USGS Global Visualization Viewer site, were utilized in this study. The six periods of satellite images were generated using the Landsat 5-TM images in November of 1988, 1993, 1998, 2003, 2008, and 2011 and by Landsat 8-OLI image for 2014 of path/row 129/50 and 129/51. After the mosaic process, a couple of the images in the same year applied a geometric correction and re-projection into a common UTM zone 47 North. The first 2014 Landsat image was geo-reference using topographic map from the Royal Thai Survey Department (RTSD). Then the other images were corrected through an image-to-image rectification method based on the corrected 2014 image. The total root mean square error (RMSE) of each image was assessed to confirm

the geometric error, which was less than one pixel. Furthermore, the Landsat images were classified into land use maps by maximum likelihood method. Additionally, the accuracy assessment was implemented to confirm the quality of the classified maps through the overall accuracy. Finally, the built-up area from the classification results were extracted to generate urban land use maps in each specific year.

3.2 Set of Spatial Landscape Metrics

For the quantification of the urban expansion patterns, a set of spatial landscape metrics was selected. As mention earlier about the influence of landscape metric, several metrics were selected based on the purpose of this research. This study selected seven metrics from the basic information that proposed by O'Neill et al. [17], McGarigal et al. [18], and Rempel et al. [19]. The list of and detail of each metrics are shown in Table 1.

Table 1. Selected metrics for the analysis of urban expansion pattern.

Metrics	Description	Units	Range
Total Class Area (CA)	The total area of all urban patches. Changes can be identified over time with CA	Hectares	CA > 0, no limit
Number of patches (Nump)	The number of urban patches in the landscapes	None	NP ≥ 1, no limit
Mean Patch Size (MPS)	The calculation of the average mean surface of patches	Hectares	MPS > 0, no limit
Edge density (ED)	The sum of the lengths of all edges segments involving the urban patch type, divided by the total landscape area	Meter/m ²	ED ≥ 0, no limit
Mean shape Index (MSI)	The measurement of the ratio between the perimeter of a patch and the perimeter of the simplest patch in the same area	None	MSI ≥ 1, no limit
Area weighted mean shape index (AWMSI)	Area weighted mean value of the fractal dimension values of all urban patches, the fractal dimension of a patch equals two times the logarithm of patch perimeter divided by the logarithm of patch area; the perimeter is adjusted the raster bias in perimeter	None	AWMSI ≥ 1, no limit
Mean Nearest Neighbor (MNN)	The measurement of the average distance between urban patches of the same patch type	None	MNN ≥ 0, no limit

Source: Megahed, Cabral, Silva, and Caetano [20]

3.3 Identification of Urban Expansion Pattern

The identification of the urban expansion pattern had been done through the analysis of FRAGSTATS using Patch Analyst 5.0 built in ArcGIS software [19]. In this study, the urban maps over 26 years (1988 to 2014) were utilized to calculate spatial metrics. The procedure for interpretation of each metric is displayed in Table 2.

Table 2. The urban spatial process analysis from the spatial metrics

Metric	Interpretation	Urban expansion process
Total Class Area (CA)	Changes can be identified over time with CA	–
Number of patches (NUMP)	If NUMP value increases, it is understood fragmentation increases in the field	Aggregation
Mean Patch Size (MPS)	Inverse tend to the NUMP	Aggregation
Edge density (ED)	High ED: ragged ED decreases when urban areas fuse together and boundaries dissolve and increase with new nuclei	Compaction
Mean shape Index (MSI)	MSI is equal to 1 when all patches are circular, and it increases with increasing patch shape irregularity	Compaction
Area weighted mean shape index (AWMSI)	The average shape index of patches of the correspondent type, weighted by patch area, so that large patches weigh more than small one	Compaction
Mean Nearest Neighbor (MNN)	If MNN increases, it reflects greater isolation	Dispersion/Isolation

Moreover, the urban spatial process, resulted from the spatial metrics, was analyzed to determine the state of the urban expansion (Table 2). The spatial urban expansion process can be divided into three processes such as:

- (1) Aggregation corresponds to the clustering of patches from the patches size. The decreasing in the total number of patch (NUMP) can increase in the mean patch size (MPS). The aggregation process was analyzed by mean of integrating the evolution of the NUMP and MSP.
- (2) Compaction involves in the formation of rounded patches such as a circular shape that make them more compact. The inversion of the compaction is an elongation (or linear shape) which the patch shape becomes more elongated. By this process, the edge density (ED), mean shape index (MSI), and area weighted mean shape index (AWMSI) were calculated to indicate the compaction. The lower values from three metrics indicate the high compaction. On the other hand, the higher metric values indicate elongated shape.

- (3) Dispersion or isolation involves increasing of the distance which separates patches from the same land use class. It can be measured by a mean nearest neighbor (MNN). The high value from the metric shows a greater isolation which indicates greater dispersion as well.

4 Result and Discussion

4.1 Mapping the Urban Land Use of BMR

After the maximum likelihood classification process, the urban land use maps from the Landsat images were created for seven time periods from 1988 to 2014. It can be seen obviously from the Fig. 2 that the origin of the urban expansion was located in the center of Bangkok Metropolis and then expanded according to the national plan policy of the country and development of transportation networks. This area is also known as the biggest urban agglomeration of Thailand. In addition, the total urban area was increased dramatically from about 600 km² in 1988 to 3,060 km² in 2014 (Fig. 3(a)). However, there was a slightly decrease in the number of the urban area in two periods (e.g. 2003–2008 and 2011–2014) (Fig. 3(b)).

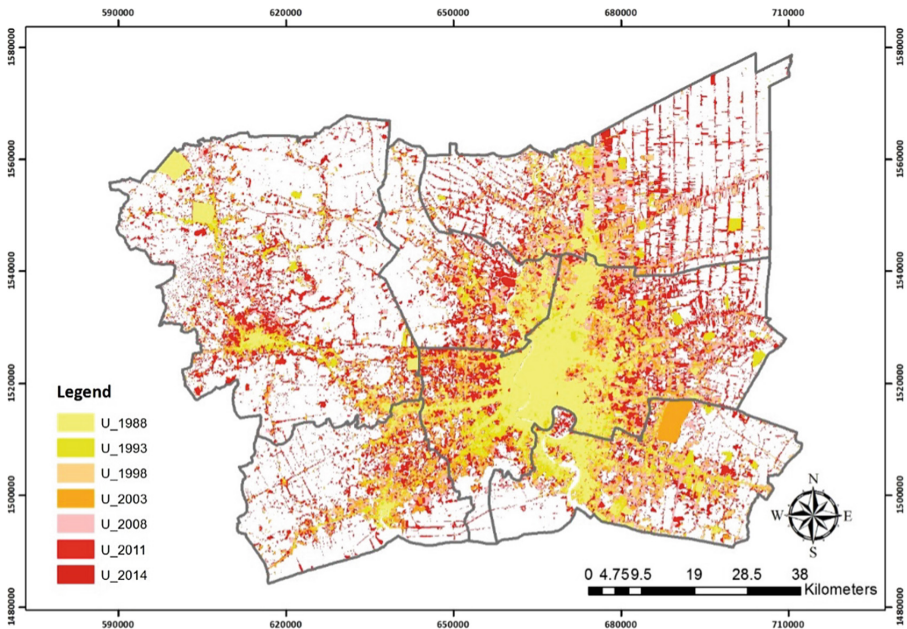


Fig. 2. Urban land use map of BMR in 1988, 1993, 1998, 2003, 2008, 2011, and 2014

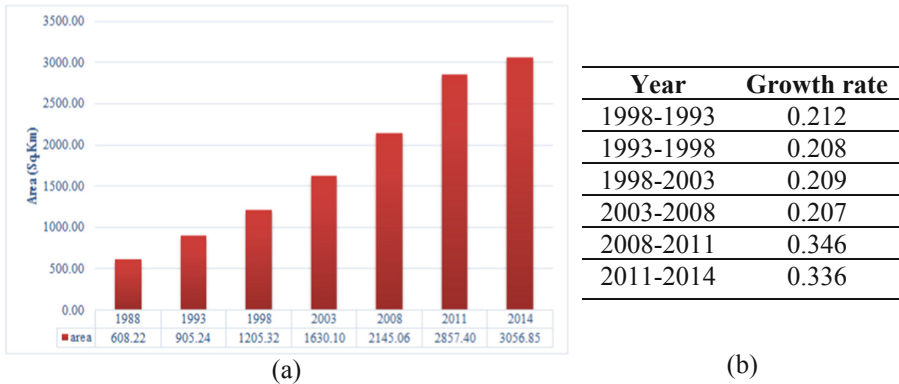


Fig. 3. (a) The total number of the urban area (b) the growth rate of the urban land use.

4.2 Urban Expansion Pattern

To analyze the pattern of the urban expansion in BMR, this study applied seven spatial landscape metrics, CA, NUMP, MPS, ED MSI, AWMSI, and MNN, to evaluate the urban spatial process and pattern at the patch level. The result from the analysis of this section can be divided into two scales. The first is analyzing the pattern as a whole of BMR. The second is analyzing the pattern as individual provinces. The result of each analysis is given in detail as follows.

Bangkok Metropolitan Region (BMR). The CA metric indicated that there was an increase in the number of the urban area throughout the period of study. The NUMP dramatically increased from 1988 to 2003. However, the values slightly decreased in 2008 and continued increased again in 2011 and slightly decreased in 2014. On the other hand, the all values of the MPS showed the reversed trend of the NUMP. It suggests that BMR slightly decreased in the aggregation. In the aspect of compaction, the ED and AWMSI values showed increasing numbers. It means the urban area expanded year by year with a complex shape. The result from the MSI metric displayed a value greater than 1. It also confirmed that the urban shape was irregular. Moreover, the value of MNN indicated a downward trend which implied the BMR facing a low dispersion (Fig. 4).

Bangkok Metropolis. The CA metric indicated that there was an increase in the number of the urban area throughout the period of study like the BMR. The NUMP dramatically increased from 1988 to 2003, fell down in 2008, and remained stable until 2014. On the other hand, the all values of the MPS metric showed the inversion trend of the NUMP. It suggested that in the later state BMR had more aggregation of the urban area. In the aspect of compaction, the ED and AWMSI values showed a fluctuation. It seems that the urban area increased regularly; however, the shape of the urban of Bangkok Metropolis was not stable (mixed between compact and elongated). The MSI metric showed a value greater than 1. It also confirmed that the urban shape was irregular. Moreover, the value of MNN indicated a downward trend which indicated a low dispersion (Fig. 5).

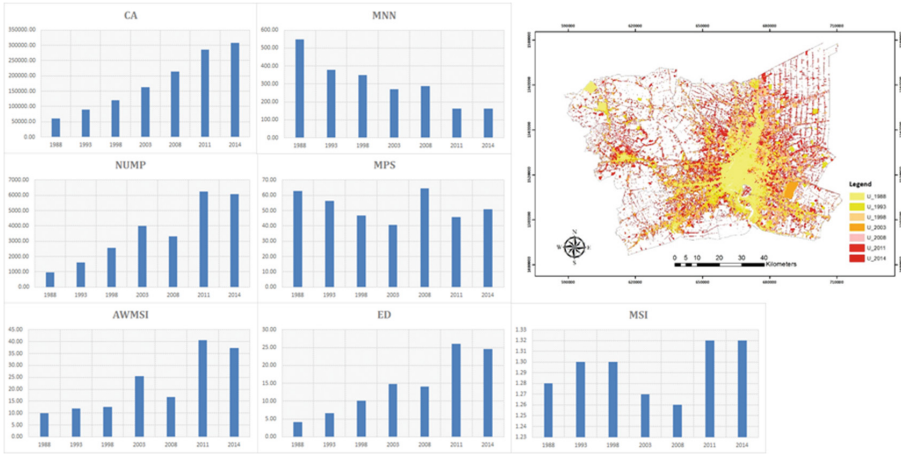


Fig. 4. Trend of the spatial landscape metric of BMR

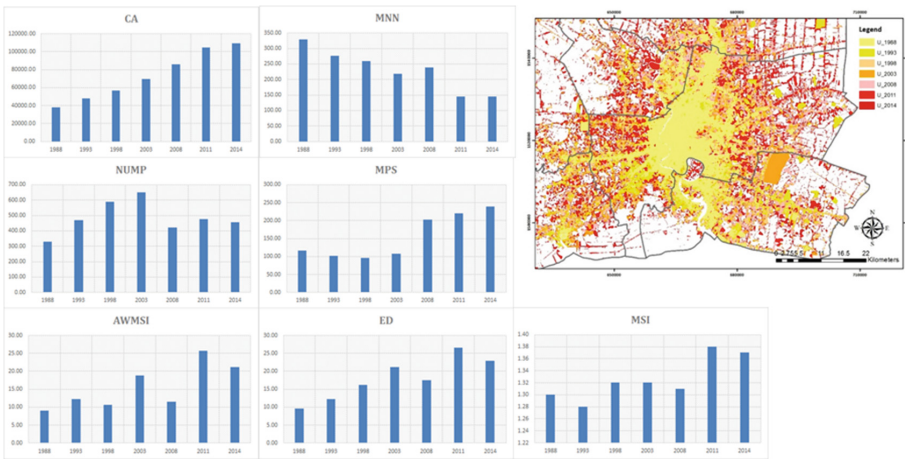


Fig. 5. Trend of the spatial landscape metric of Bangkok Metropolis

Nakhon Pathom. The CA metrics showed an urban expansion of Nakhon Pathom from about 5,000 to 50,000 m² in 26 years. The NUMP dramatically increased from 1988 to 2008 and continued to soar to 2,500 in 2014. By contrast, the MPS illustrated the inverted value from the NUMP. It suggest that this province was slightly fragmented. For the compaction, the ED increased from 2 to about 25. Moreover, there was a fluctuated increase in the AWMSI. Both metrics implied that the urban zone always increased with the complex shape especially in 2011 and 2014. All MSI values were greater than 1. Therefore, the urban shape was also irregular. In terms of dispersion, the MNN was on the decline, which means this province had a low dispersion because the urban expansion trend of Nakhon Pathom was close to the urban core (Fig. 6).

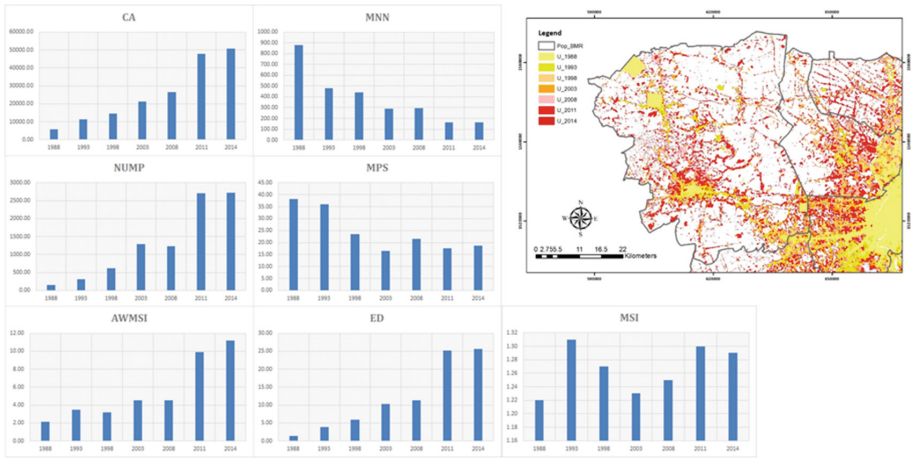


Fig. 6. Trend of the spatial landscape metric of Nakhon Pathom.

Nonthaburi. The trend of the CA showed the same situation as two aforementioned provinces, which dramatically increased from 1988 to 2014. The NUMP indicated that the urban area had increased since 1988 to hit the highest at around 500 in 2003 and declined to about 400 in 2014. Moreover, the MSP also confirmed it was aggregated in the first year of study and then declined to the lowest at 2003 and continued increase to above 70 in 2014. Both NUMP and MSP metrics implied that Nonthaburi had more aggregation especially in the southern-west of the province. In case of compaction, the ED and AWMSI illustrated the increasing number throughout the study period. It implied that there was a high compaction in this area. In addition, the shape of the compaction was irregular as the MSI metric yielded a value greater than 1. From the analysis of MNN, there was an isolation of the urban area in the first-two times. However, the isolation radically decreased into below 200 at 2014. The urban expansion trend of Nonthaburi showed a low dispersion (Fig. 7).

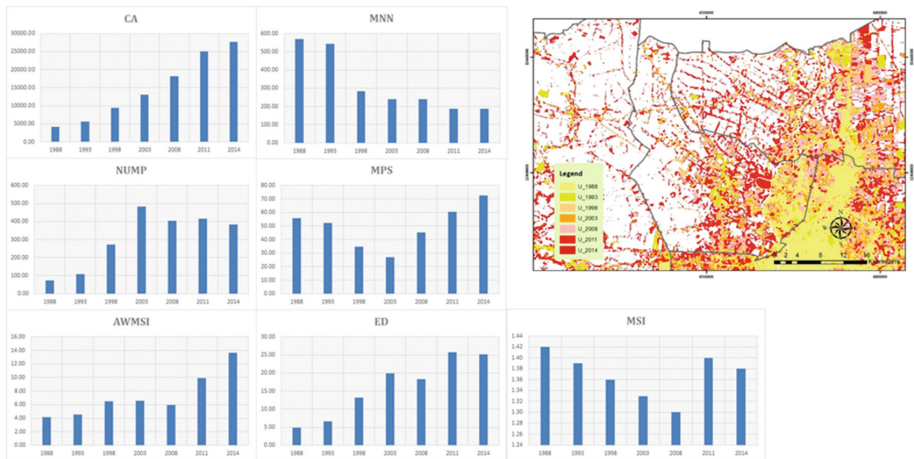


Fig. 7. Trend of the spatial landscape metric of Nonthaburi

Pathum Thani. The urban area of Pathum Thani had expanded continuously as comprehended from the result of the CA metric. The NUMP and MPS illustrated the same situation as the BMR. It implied that the urban expansion of this province slightly decreased in an aggregation. To analyze the compaction, the ED and AWMSI metric was investigated. The results showed the little increase in values of both metrics from 1988 to 2008. Nevertheless, the values from the ED and AWMSI metrics had particularly increased in 2011 and 2014. It means that the urban area expanded in the complex form with a ragged edge and an elongation which showed as the same result evidently from the MSI metric. From 1998 to 2014, the MNN dramatically decreased which reflected that the expansion pattern of this provinces was low dispersion (Fig. 8).

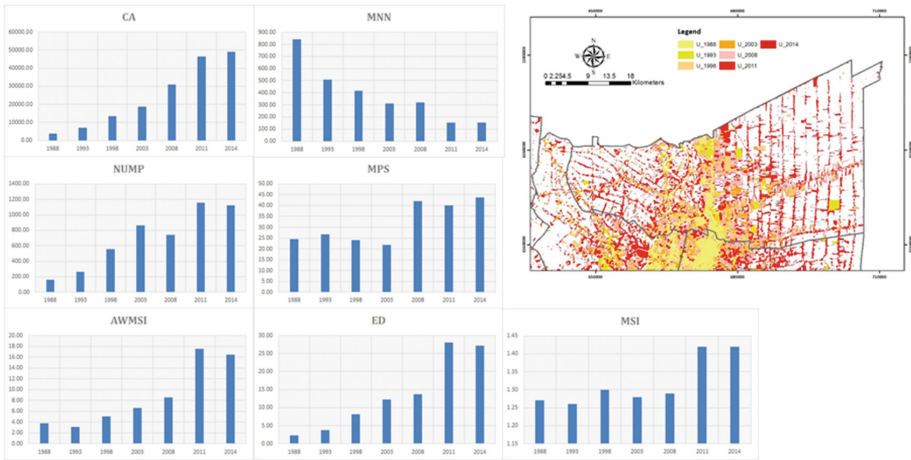


Fig. 8. Trend of the spatial landscape metric of Pathum Thani

Samut Pakan. The urban area was expanded overtime particularly in the adjacent area of Bangkok Metropolis as see from the CA and the map (Fig. 9). The NUMP trend was upward and reached the highest value in 2011. The MPS was fluctuated and then climbed into about 44 in 2014. It could be implied that the urban expansion was an aggregated process. In the compaction aspect, the values of ED and AWMSI rose gradually and climbed sharply in 2011 and dropped slightly in 2014. Moreover, the value of MSI in each year was greater than 1. All of these pointed out that the urban shape of the Samut Prakan was a complex form. The result from the MNN analysis showed a decreased trend and then leveled off. It implied Samut Pakan had a low dispersion (Fig. 9).

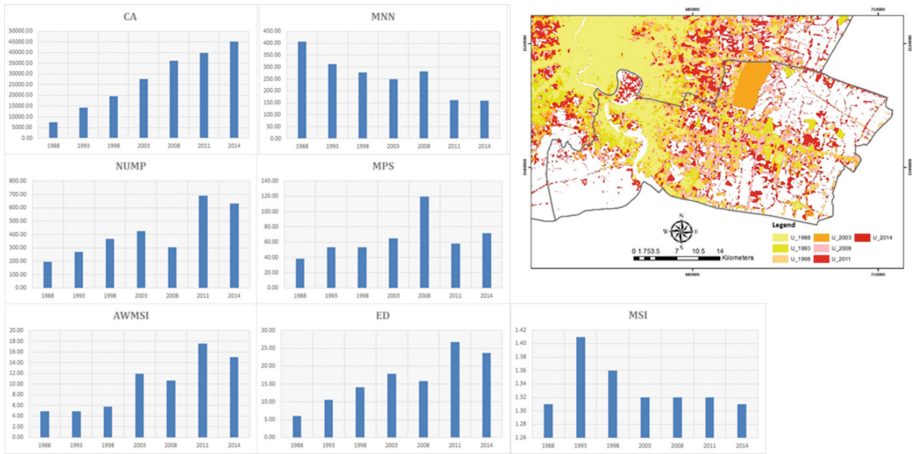


Fig. 9. Trend of the spatial landscape metric of Samut Pakan

Samut Sakorn. The CA value in each year of this province increased noticeably due to the urbanization in the western part of Bangkok Metropolis. The NUMP trend was upward and reached the highest values with 935 in 2011. The MPS was fluctuated and then climbed into about 23 in 2014. It could be implied that the urban expansion was an aggregated process. In the compaction analysis, the ED and AWMSI metrics illustrated the increasing number throughout the study period. It implied that there was a high compaction in this area. The shape of the urban expansion was irregular as the MSI produced the value greater than 1. The MNN of Samut Sakorn province dramatically decreased and reflected that the urban expansion in this province showed a low dispersion (Fig. 10).

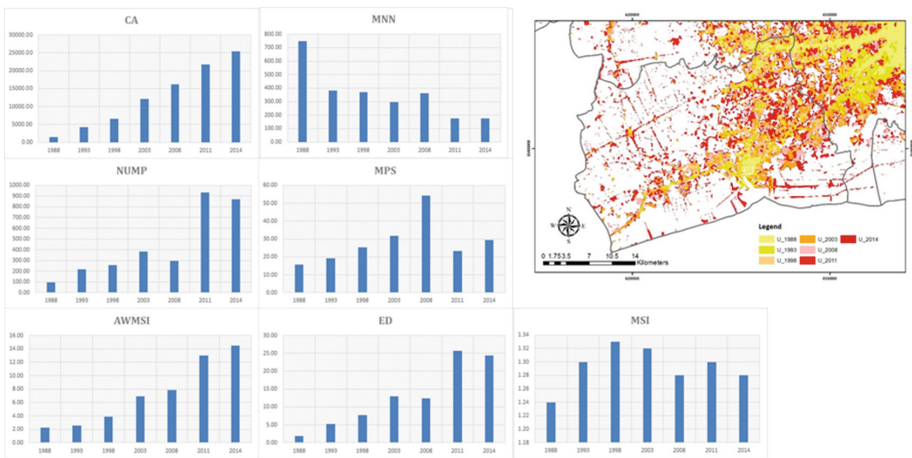


Fig. 10. Trend of the spatial landscape metric of Samut Sakorn

5 Conclusion

In brief, the pattern of the urban expansion in BMR was analyzed through the time series of remote sensing data from Landsat 5 and 8 images between 1988 and 2014. The scientific methodology of the spatial landscape metrics was utilized to see the pattern elaborately by using the patch analysis. Three urban spatial processes were used to analyze the pattern of the urban expansion. The NUMP and MSP metrics were used to identify the aggregated pattern. Moreover, this study investigated the compaction by using ED, MSI, and AWMSI metrics. Furthermore, the dispersion or isolation pattern was examined through the MNN metric. The acquired results illustrate the usefulness of the spatial landscape metrics to classify the spatial pattern of the urban. According to the analysis, it could be found out that the aggregation of the BMR had decreased. On the other hand, the urban areas of the adjacent provinces were an expansion from the center of the city where it did not settle next to Bangkok Metropolis. When diagnosing in detail, however, it could be found that Bangkok Metropolis, Nonthaburi, and Pathum Thani revealed the inverted pattern from the BMR. All urban areas of three provinces were established as a big agglomeration of the region. In case of the compaction, the shape of the urban expansion of the BMR was complex due to the urban areas were expanded apart from the city center via the main transportation network such as main road and other prospective mass transportation. For the dispersion pattern, the result from the analysis confirmed that the BMR had decreased dispersion. All of the urban areas of each province, presently, has expanded itself beyond the political boundary.

From this study, the combination of remote sensing data and spatial metrics yields accurate results and were a good indicator in order to understand the urban expansion pattern. The analyzed results can provide significant suggestions to the urban planners who work on the spatial arrangement of the urban area and infrastructure of the BMR. Moreover, the expansion pattern can be used to control the unplanned settlement such as the urban sprawl which becomes a momentous problem in several countries.

References

1. Aithal, B.H., Ramachandra, T.V.: Visualization of urban growth pattern in Chennai using geoinformatics and spatial metrics. *J. Indian Soc. Remote Sens.* **44**, 617–633 (2016)
2. Knox, P.L., McCarthy, L.: *Urbanization: An Introduction to Urban Geography*, 3rd edn. Pearson, Boston (2012)
3. Wu, J., Jenerette, G.D., Buyantuyev, A., Redman, C.L.: Quantifying spatiotemporal patterns of urbanization: the case of the two fastest growing metropolitan regions in the united states. *Ecol. Complex.* **8**, 1–8 (2011)
4. Wu, J.: Urban ecology and sustainability: the state-of-the-science and future directions. *Landsc. Urban Plann.* **125**, 209–221 (2014)
5. Liu, Z., He, C., Wu, J.: General spatiotemporal patterns of urbanization: an examination of 16 world cities. *Sustainability* **8**, 41 (2016)
6. Lin, Y.: *Modelling Urban Development with Geographical Information Systems and Cellular Automata*. CRC Press, New York (2009)
7. Chang, C.: *Understanding spatial and temporal patterns of urban expansion in Western China during the post-reform era*, Master thesis. University of Wisconsin-Madison (2013)

8. Johnson, M.P.: Environmental impacts of urban sprawl: a survey of the literature and proposed research agenda. *Environ. Plann. A* **33**, 717–735 (2001)
9. Poyil, R.P., Misra, A.K.: Urban agglomeration impact analysis using remote sensing and GIS techniques in Malegaon city, India. *Int. J. Sustain.* **4**, 136–144 (2015)
10. Jensen, J.: *Introductory Digital Image Processing: a Remote Sensing Perspective*, 4th edn. Pearson, Glenview (2015)
11. Aguilera, F., Valenzuela, L.M., Botequilha-Leitão, A.: Landscape metrics in the analysis of urban land use patterns: a case study in a Spanish metropolitan area. *Landscape Urban Plann.* **99**(3–4), 226–238 (2011)
12. Reis, J.P., Silva, E.A., Pinho, P.: Spatial metrics to study urban patterns in growing and shrinking cities. *Urban Geogr.* **37**, 2 (2016)
13. Bhatta, B.: *Analysis of Urban Growth and Sprawl from Remote Sensing Data*. Springer, New York (2010)
14. Herold, M., Liu, X., Clarke, K.C.: Spatial metrics and image texture for mapping urban land use. *Am. Soc. Photogrammetry Remote Sens.* **9**, 99–1001 (2003)
15. Schwarz, N., Haase, D., Seppelt, R.: Omnipresent sprawl? a review of urban simulation models with respect to urban shrinkage. *Environ. Plan.* **37**(2), 265–283 (2010)
16. Clifton, K., Ewing, R., Knaap, G.J., Song, Y.: Quantitative analysis of urban form: a multidisciplinary review. *J. Urbanism* **1**, 17–45 (2008)
17. O'Neill, R.V., Krummel, J.R., Gardner, R.H., Sugihara, G., Jackson, B.L., DeAngelis, D.L., Milne, B.T., Turner, M.G., Zygmunt, B., Christensen, S.W., Dale, V.H., Graham, R.L.: Indices of landscape pattern. *Landsc. Ecol.* **1**, 153–162 (1988)
18. McGarigal, K., Cushman, S.A., Neel, M.C., Ene, E.: FRAGSTATS: Spatial pattern analysis program for categorical maps. Computer software program produced by the authors at the University of Massachusetts, Amherst (2002). www.umass.edu/landeco/research/fragstats/fragstats.html. Accessed 15 Mar 2010
19. Rempel, R.S., Kaukinen, D., Carr, A.P.: Patch analyst and patch grid. Ontario Ministry of Natural Resources. Centre for Northern Forest Ecosystem Research, Thunder Bay, Ontario (2012)
20. Megahed, Y., Cabral, P., Silva, J., Caetano, M.: Land cover mapping analysis and urban growth modelling using remote sensing techniques in Greater Cairo Region—Egypt. *ISPRS Int. J. Geo. Inf.* **4**, 1750–1769 (2015)



Monitor the Land Use Change and Prediction Using CA-Markov Model in Li Pe Island, Satun Province, Thailand

Katawut Waiyasuri^(✉), Nayot Kulpanich,
Morakot Worachairungreung, and Pornperm Sae-ngow

Geography and Geo-Informatics Program, Faculty of Humanities and Social
Sciences, Suan Suandha Rajabhat University, 1 U-Thong Nok Road, Dusit,
Bangkok 10300, Thailand

{katawut.wa, nayot.ku, morakot.wo,
pornperm.sa}@ssru.ac.th

Abstract. Li Pe island is situated on the border of the Tarutao National Marine Park which is one of beautiful seaside tourist attractions. Current tourism in Li Pe island has been greatly developed leap forward due to biological diversity and beautiful seaside nature based attractions. The purpose of this study to generate the land use multi-temporal information during 1990–2014 and to then apply the CA-Markov model to simulate the past land use patterns and to predict future land use patterns over the next two decades (2028). The results revealed change detection for the land use classification in 1990–2017. It could be seen that resorts, villages, commercial and services area have increased by 0.36 km², 0.22 km², 0.06 km² respectively whereas the size of forest and cultivated land have declined by 0.98 km² and 0.22 km², respectively. The 2028 land use map shows the predicted trend of resort and village area expansion to western part of the island along Sunset beach, while land use in eastern part near Sunrise beach area has been changed to tourism business and commercial activities.

Keywords: Li Pe Island · Land use change · CA-Markov model

1 Introduction

Land use is an indicator of human's activities and utilization of natural resources and environment in the area [1, 2]. Changing of the land use means changing of geographical patterns which is correlative with changing of period and development of economy and society [3, 4]. These changes influence on social, cultural and economic characteristic, including ecology in the area. Thus, land use is a significant factor to analyze both environment and economy [5]. Li Pe island is one of beautiful seaside tourist attractions. Current tourism situation in Li Pe island has been greatly leap forward due to biological diversity and beautiful seaside nature based attractions, such as the white and fine sand beach, coral reef, aquatic flora and fauna in deep blue sea water, which led Li Pe island attracted by Thai and foreign entrepreneurs [6]. Then, the land was widely sold from local people to business owners in various ways. The causes mentioned above brought about several problems as well, namely, the instability of

local people to live because the authority of the land has been transferred to entrepreneurs, the land for spiritual ceremony such as graveyard has been used to build resorts and there is nowhere to place the corpse now [7]. While 300 fishermen do not have the way out to go for fishing or even to park fishing vessels because the seashore has all been owned by the entrepreneurs. Now, the exit to the sea is only the walkway built in the middle of the island [8]. There is no entrance to school and public health center because entrepreneurs bought the land and built up the wall around. For environmental aspect, there are also severe problems, for example, all natural 5 waterways have been possessed and covered up to build entertainment spots, without drainage system [9]. This causes underground water smelly and polluted. The several entertainment spots in the area also lack sanitation as well as waste management system. Eventually, in the near future, Li Pe island could turn to be a massive garbage dump. As mentioned above, it is necessary to study and investigate the patterns of the land use and land cover change. This study aimed to study land cover and land use multi-temporal information between 1990 and 2014 and then to apply the CA-Markov model to simulate a future land use patterns over the next decades (2028).

The study area is within the Li Pe island which is situated in Satun Province of southern Thailand on western coast, close to the Malaysian border, with the study area coordinates of 531000 E, 716000 N on the south western edge and 535000 E, 718000 N on north eastern edge in the Universal Transverse Mercator (UTM) projection for the 47 N zone in WGS 1984 ellipsoid. The Total study area is approximately 2.082 km², covering path 129, and row 55 of Landsat-8 OLI/TIRS. The elevation ranges from 0 to 99 meters above average mean sea level as shown in Fig. 1.

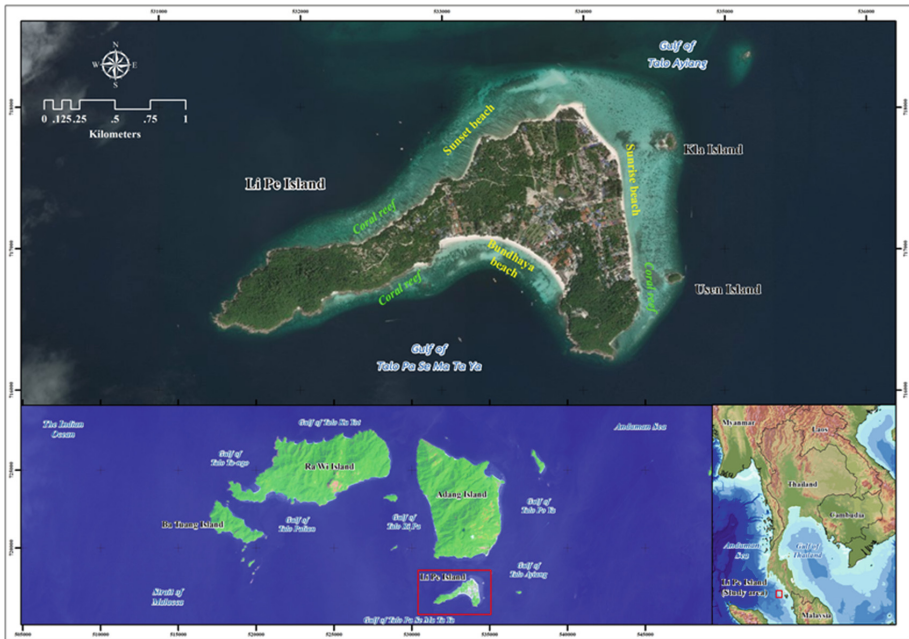


Fig. 1. Sentinel-2A satellite image of the Li Pe island area (study area).

Li Pe island is situated on the border of the Tarutao National Marine Park which is one of beautiful seaside tourist attractions. It is situated on the south of the two largest islands that are Adang and Ko Rawi island, and about 50 km from the island of Tarutao island. It was originally settled by a group of sea gypsies (Chao Leh in Thai), originally from Malaysia, known as the Urak Lawoi people [10].

2 Method

In this study, the satellite image data used to comprise the Landsat-5TM for 1990 and Landsat-8OLI/TIRS for 2014. These data were used for analysis of the land use changes and as inputs in the trend extrapolation to calculate the likely land use demands and trends in the future. The attributes and access periods for the data used in this study are summarized in Table 1.

Table 1. Data sources used in this study.

Image type	Path/Row	Band (R:G:B) ^a	Acquisition date	Original		
				Format	Resolution	Source
Landsat-5TM	129/55	5:4:3	1990-01-31	TIFF	30 m	[11]
Landsat-8OLI/TIRS	129/55	6:5:4	2014-02-02	TIFF	30 m	[11]

^aR:G:B red:green:blue

The methodological approach used is displayed schematically in Fig. 2 and the details were discussed more in “Image processing and Geographic information system (GIS) approach” and “The CA-Markov model” as following;

The number 4822II at a 1:50000 scale, which derived from the Royal Thai Survey Department (RTSD) topographic map sheet series L7018, and land use digital files (vector), which is from the Land Development Department (LDD), delivered the information become Geospatial information and it was used to prepare for land use reference base maps for each year and to detect changes.

Image Processing and GIS Approach

In the year 1990 and 2014, Landsat TM and OLI/TIRS data acquired were manipulated in this study. All images were adjusted to a common Universal Transverse Mercator coordinate system based on the 1:50000 topographic maps which is from the Royal Thai Survey Department (RTSD) topographic map sheet series L7018. As reference, Geometric correction was operated on all of the images using a Landsat TM image of the same area from 2007, and at least 20 ground control points (GCPs) were used to rectify images for that reason, a reference for image-to-image registration of all other was from the corrected image [12].

Each scene of Landsat images was improved for using the histogram equalization approach in order to earn a higher contrast in images. A supervised classification with the maximum possibility algorithm, depend on more than 60 ground control points which collected during the GPS-assisted field campaigns and almost 30 training

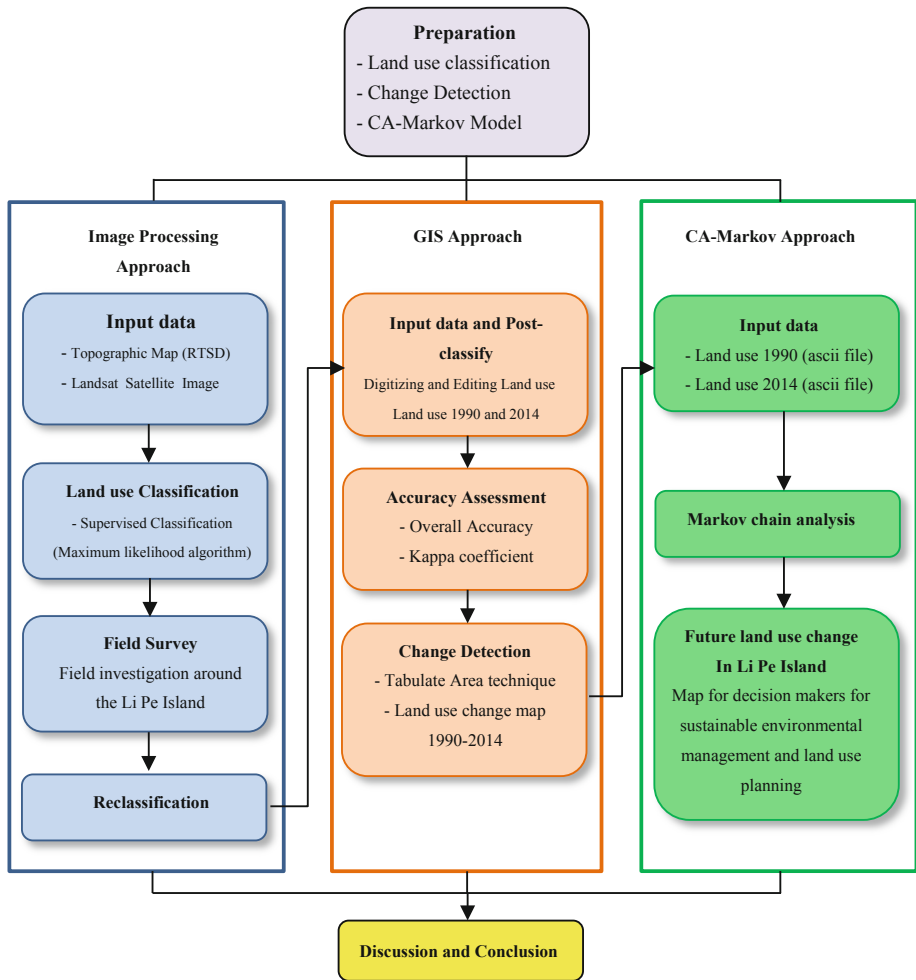


Fig. 2. Schematic flowchart summarizing the main methodological steps used in this research.

samples in total for all classes [13] was proceeded to classify the Landsat images using bands 5 (short-wavelength infrared), 4 (near-infrared), and 3 (red). The combination of fifth, fourth, and third uses TM 5 and the combination of sixth, fifth, and fourth uses OLI/TIRS 8, which largely consists of coastal and forest information for geospatial management [14, 15]. The maximum possibility classification is one of the statistical decision methods to define the possibility that specified pixels belong to a specific class [16]. This method has the assumption that individual input bands should be normally distributed. As additional calculations need to be done, it takes a long time to accomplish. The images were reclassified into 10 classes (5×5 raster grid resolution) based on the land use level. Landsat satellite imagery (RGB:543), as presented in Fig. 2, was analyzed using ERDAS Imagine software to classify land use. ArcGIS software was then used to overlay the derived land use maps from Landsat for each

year, and analyze previous secondary data and classify the final results. There are two main steps to employ the digital data analysis techniques in this study [17]. Firstly, image classification was performed by dividing pixels of the image into classes for representing different physical objects which the image classification is the process of making quantitative decisions from image data.

The classification procedure consisted of unsupervised and supervised classification and satisfied the three major attributes of the classification process [18]. The reference data and ancillary information were applied for selecting the training samples, for example, topographic maps (years 1990 and 2014) and land use digital files (vector format) from the Land Development Department (LDD) (years 1990 and 2014). Thirty to fifty training sites that are ranging in size from 10 to 50 pixels were used to train the images.

Classified image accuracy consists of two accuracy types; overall and user accuracy. Overall accuracy represents the accuracy of the entire product and the second is user accuracy which a map user has interested in. Accuracy represents the reliability of the map that represents the reality on the ground. The kappa coefficient is a measure of the difference between the actual agreement, between reference data and an automated classifier, and the chance agreement between the reference data and a random classifier. A qualitative classification of the overall accuracy values and kappa coefficient value of more than 0.61 indicate agreement (substantial agreement) as shown below [12, 19]:

<0	less than chance agreement,
0.01 – 0.40	poor agreement,
0.41 – 0.60,	moderate agreement,
0.61 – 0.80,	substantial agreement,
0.81 – 1.00,	almost perfect agreement.

In the Li Pe Island area, the land use changes were evaluated by importing the land use maps from 1990 and 2014 into the GIS database in raster format and then overlaying all two years and tabulating the area using spatial analysis. Each type of land use area was calculated and changed from 1990 to 2014 by using the cross-classification application. The change estimation was used for identifying the “from-to” change in land use and for quantifying the different rates and magnitudes of these changes. The annual change in land use was evaluated using Eq. 1 [20].

$$\Delta = [(A_2 - A_1)/A_1 \times 100]/(T_2 - T_1) \quad (1)$$

where Δ is the average annual rate of change (%), A_1 the amount of a land use type at time 1 (T_1) and A_2 the amount of a land use type at time 2 (T_2).

The CA-Markov Model

The CA-Markov model is a multi-scale, dynamic, spatially explicit and raster-based model that has the potential to identify areas with high probability of future changes in land use [20]. The CA-Markov model is the non-spatial demand module while, the changes in land use are estimated for a series of years at the aggregate level. Markov chain analysis is a stochastic process describing certain types of conditions which

change in sequential steps through the land use geospatial dataset. It was constructed using the land use distributions at the beginning (X_t) and at the end (X_{t+1}) of a discrete time period, along with a transition matrix (X_{LU}) which representing the land use changes that occurred during that period. The matrix cell values are derived directly from the classification of the three multi-spectral Landsat scenes using the maximum possibility algorithm, based on expressed as each proportions of land use. The CA-Markov module is available in the IDRISI software and can be used to generate such a transition probability matrix in which it takes two LULC maps as input data and then produces the following output: (1) transition probability matrix, (2) transition areas matrix, and (3) set of conditional probability maps [21].

Then, the matrix has created to form a ‘link’ in the Markov chain using as the following Eq. 2 [22]:

$$X_{LU} \times X_t = X_{t+1}, \quad (2)$$

$$\begin{bmatrix} LU_{uu} & LU_{ua} & LU_{uw} \\ LU_{au} & LU_{aa} & LU_{aw} \\ LU_{wu} & LU_{wa} & LU_{ww} \end{bmatrix} \begin{bmatrix} U_t \\ A_t \\ W_t \end{bmatrix} = \begin{bmatrix} U_{t+1} \\ A_{t+1} \\ W_{t+1} \end{bmatrix}$$

where U_t represents the probability of any given point being classified as urban at time t and LU_{ua} . The probability that an agricultural point at time t will change into urban land by $t + 1$, and so on.

3 Results and Discussion

3.1 Accuracy Assessment Result and Land Use Classification

Classification of land use map in Li Pe island area were evaluated by importing the Landsat satellite image from 1990 and 2014 into the Geo-spatial database in raster format and then overlaying two years and tabulating the area using spatial analysis. Accuracy assessment of land use classification was conducted for land use categories that were interpreted from Landsat-5TM satellite images in the year 1990 and 2014. This method was done by using 10 to 50 pixels sample points from Landsat-5TM and Landsat 8OLI/TIRS satellite images respectively in the year 1990 and 2014, and field investigations that were selected using stratified proportional random samplings. In this method, each land use category will be used as sampling measurement pixel. The result of overall accuracy assessment was 78.0% and 83.0% for year 1990 and 2014, respectively, with a kappa coefficient value of 0.76 and 0.81, in order as shown in Table 2.

According to the land use classification processes by Landsat-5 TM satellite images in 1990, there were 5 land use categories were identified, namely, beach, cultivated land, forest land, reef, and villages. Land use classification processes by Landsat-8 OLI/TIRS satellite images in 2014 could identify 10 land use categories, namely, beach, commercial and services area, construction area, cultivated land, forest land, institutional, reef, resorts, villages, and waterbodies. The trends of land use changes of the area during 1990 to 2014 were presented in Table 2, Figs. 3 and 4.

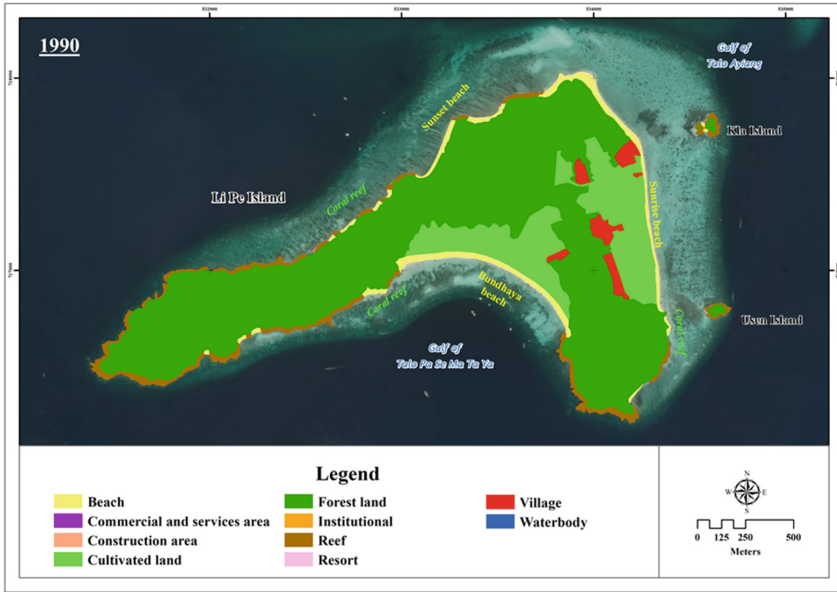


Fig. 3. Classification of land use categories in Li Pe Island area in 1990.

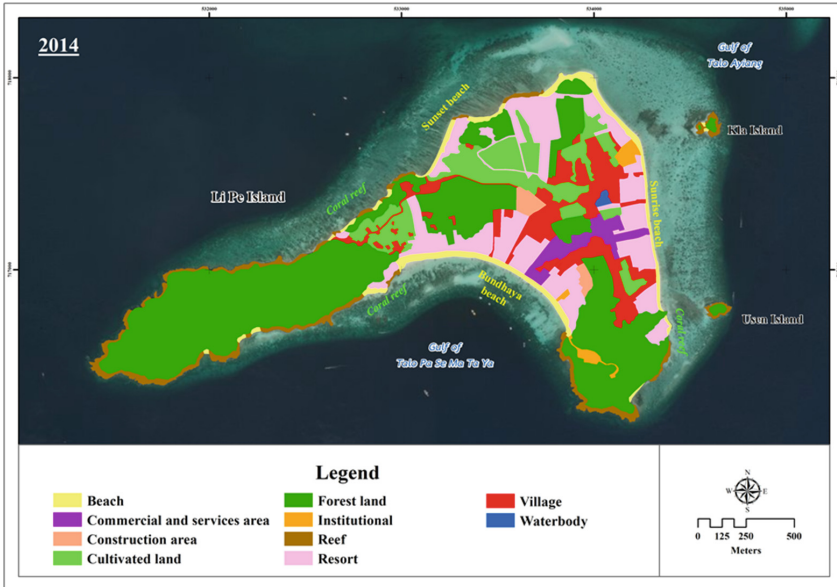


Fig. 4. Classification of land use categories in Li Pe Island area in 2014.

Table 2. Comparative land use in Li Pe island area, as derived from the Landsat-5TM in 1990 and Landsat-8OLI/TIRS in 2014.

Land use	1990		2014	
	km ²	%	km ²	%
Beach	0.09	4.33	0.09	4.33
Commercial and services area	0	0	0.06	2.72
Construction area	0	0	0.02	1.13
Cultivated land	0.35	16.84	0.22	10.65
Forest land	1.49	71.59	0.98	47.10
Institutional	0	0	0.02	1.09
Reef	0.10	4.91	0.10	4.91
Resort	0	0	0.36	17.28
Village	0.05	2.33	0.22	10.58
Waterbody	0	0	0.004	0.21
Total	2.08	100.00	2.08	100.00
Overall accuracy		78.0		83.0
Kappa coefficient (<i>KHAT</i>)		0.76		0.81

3.2 Detection of Land Use Changes in the Li Pe Island Area During 1990–2014

Detecting of land use changes in the Li Pe island was conducted by import map of land use in the year 1990 and 2014 into GIS database as raster format to overlay with land use map for two years by using tabulate area in spatial analysis.

The result revealed that the change detection for the land use classification in year 1990 and 2017, it could be seen that resorts, villages, commercial and services area, and construction area were increasing over time, whereas forest land and cultivated land tended to decrease. The trends of land use changes of the area during 1990-2014 were presented in Table 3 and Figs. 5 and 6.

Table 3. Matrix of land use changes in Li Pe island area, 1990–2014 (km²).

		2014									
Land use		Beach	Commercial and services area	Construction area	Cultivated land	Forest land	Institutional	Reef	Resort	Village	Water body
1990	Beach	0.090	0.000	0.000	0.000	0.000	0.000	0.000	0.000	0.000	0.000
	Cultivated land	0.000	0.031	0.000	0.017	0.015	0.002	0.000	0.171	0.112	0.004
	Forest land	0.000	0.008	0.023	0.204	0.965	0.010	0.000	0.189	0.089	0.000
	Reef	0.000	0.000	0.000	0.000	0.000	0.000	0.102	0.000	0.000	0.000
	Village	0.000	0.018	0.000	0.000	0.000	0.011	0.000	0.000	0.019	0.000

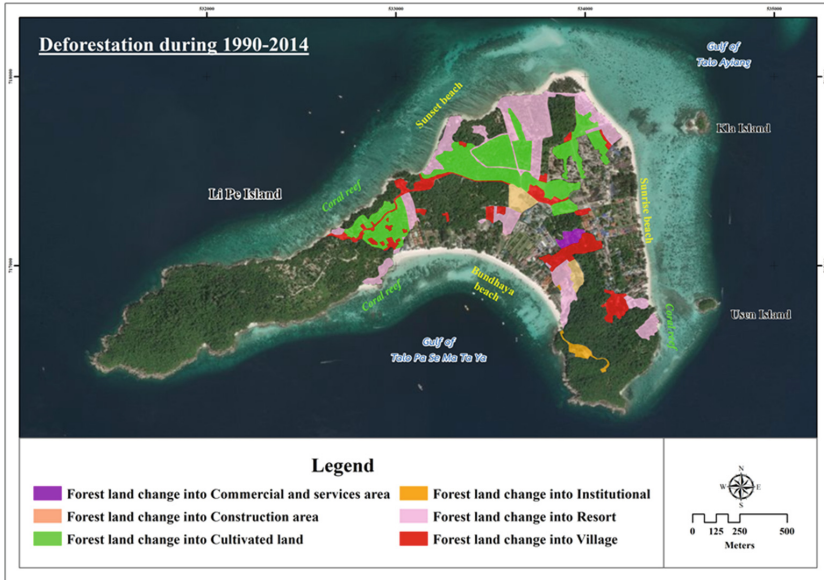


Fig. 5. Deforestation during 1990–2014 in Li Pe island area.

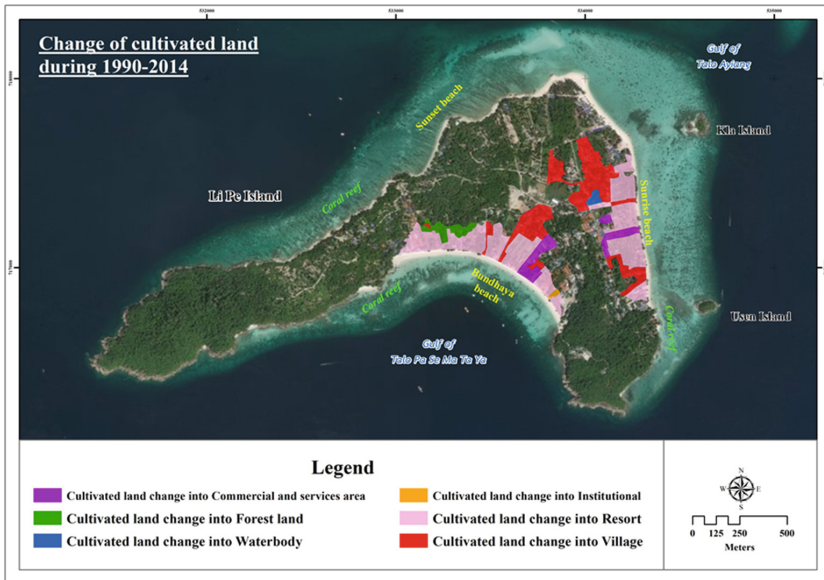


Fig. 6. Change of cultivated land during 1990–2014 in Li Pe island area.

The land use change during 1990–2014 revealed a rapid decreased in forest land area from 1.49 km² (71.59%) to 0.98 km² (47.1%) as shown in Table 3. It was found that 0.204 km² of forest land has been transformed to cultivated land, followed by

transforming to resort area (0.189 km^2) in the northern and central part of island because this area was easy to access and used to be habitation of primitive villagers (Fig. 5). Moreover, trespassing of entrepreneur groups in the forest land to build resorts and hotels are also happened in the northern part of island which is the area of Sunset beach, and another area in the southeastern area of Sunrise beach. These areas were objects of desire of entrepreneur groups because of beautiful tourist attractions.

Cultivated land area is rapidly decreased by the last 25 years (Table 3). Result reveals that 0.171 km^2 of cultivated land has been transformed to village around Bundhaya beach, located in the eastern part of the island as shown in Fig. 6. The important factors which caused transformation of land use in cultivated land area to other uses is fishermen adapted their traditional way of life from fisheries and agriculture to service industry. Some of them have divided their cultivated land and sold to entrepreneur groups to build resorts and hotels for tourism business purpose. Some fishermen have changed their occupation to service industry such as accommodation and coral reef dive, which gain more revenue comparing to the previous career.

3.3 Predicting Future Land Use Patterns

The CA-Markov model was used to simulate the land use patterns in Li Pe island area which use the information of the proportion of land use change from 1990–2014 to predict the pattern of land use in the next 25 years.

From the study, we found that there was change of pattern of land use of resort and village area expanding to western part of the island along Sunset beach, while eastern

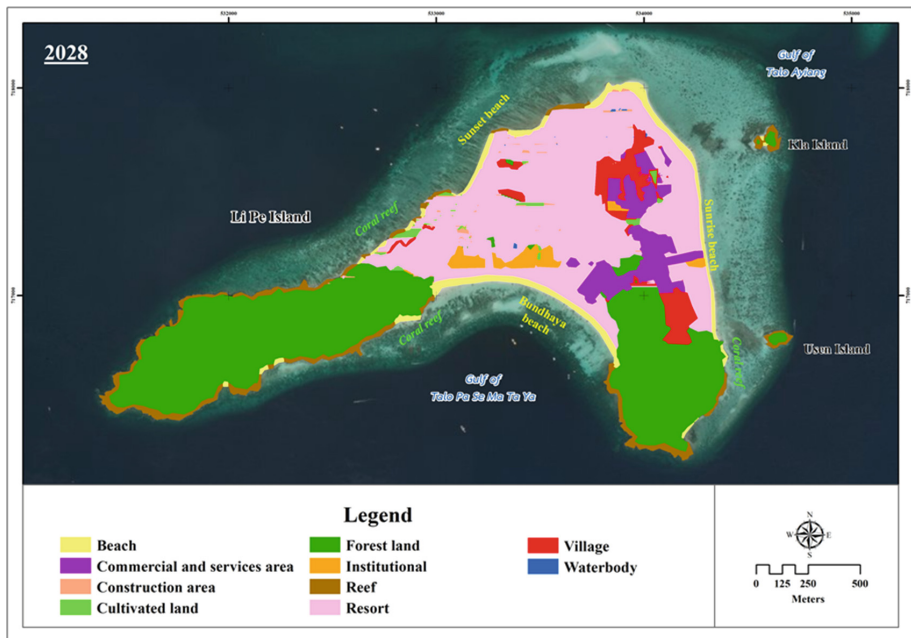


Fig. 7. Land use map in 2028 from the CA-Markov model.

part of the island around Sunrise beach area has been changed from traditional land uses to tourism businesses. Geographical characteristic of Li Pe island plays an important role in land use change because the central area of the island is wavy sand dune which helps to lessen strong wind from Southeast monsoon during May-September as shown in Fig. 7. Map of land use change between 1990–2018 is illustrated in Fig. 8.

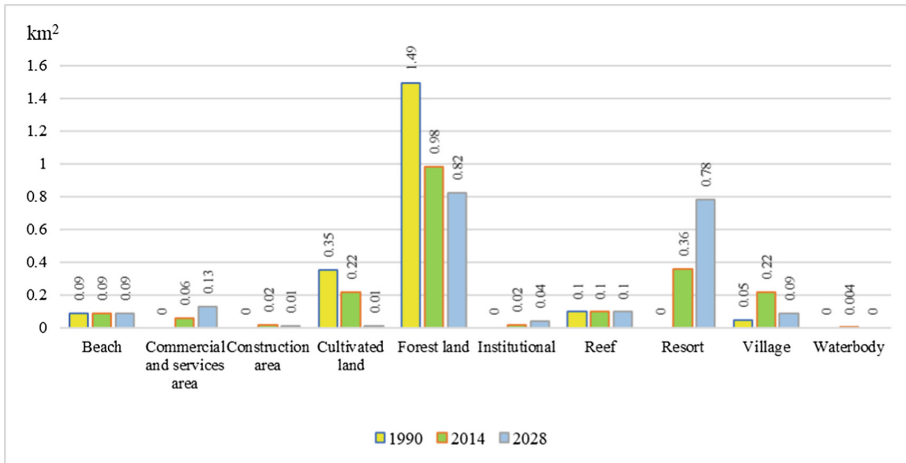


Fig. 8. Trend of land use changes in Li Pe island during 1990 to 2028.

According to the result of CA-Markov modelling, it can infer land use change could occur in the future. All stakeholders should focus on nature based solution which entails on co-benefits among businesses, natural resources and local community to ensure sustainability. Lastly, this information can be used as baseline information to assists policy makers to make a comprehensive decision making for sustainable development.

4 Discussion

The study of the CA-Markov model enables stakeholders to know about land use change in 2028. The area prone to such changes is located in the center of Li Pe Island (see Fig. 7). Results of the model reveal that changes in 2028 land use concern loss of a combination of the forest area and the cultivated land whereas the village area will be replaced by the commercial and service industries. Moreover, the area where resorts are situated will be extended to cover almost all of the center of the island – from 0.36 km² in 2014 to 0.78 km² in 2028 (Fig. 8). Land use change results from tourism industry development and promotion in Thailand and the Li Pe Island’s natural marine resources remain fertile, attracting more visitors every year. The number of Thai and foreign tourists visiting Satun Province increased from 582,057 in 2005 to 1,412,245 in 2017

[23], which is equivalent to 242.63% increase during 12 years. Out of 20% of all tourists visiting Satun tend to come to visit the island. If existing patterns still continue, especially in terms of resorts and accommodations, the island will become deteriorated and populated with a lot of buildings and built-up area similar to the tombolo connecting Phi Phi islands in Krabi Province at present. Therefore, the Li Pe Island should formulate some measures for urban planning and land utilization to prevent misuse of land which ever been happened earlier in marine natural resources of Tarutao National Marine Park, which is located only a kilometer away.

5 Conclusions

Land use planning plays an important role in sustainable land management. It was a significant tool in land use policy to plan for the future use of land resources. Result demonstrates that Landsat classification could be used to produce accurate land use change maps and statistics. In Li Pe island, General trends and patterns of land use change was evaluated by: (1) classifying the amount of land use in this area that was converted from forest land and cultivated land use for resorts, commercial and services industry purposes during four periods from 1990 to 2014 and 2014 to 2028; (2) quantitatively assessing the accuracy of change detection maps; and (3) analyzing the change detection to explore the expansion of entrepreneurs. This study quantifies change in pattern of land use in the Li Pe island and demonstrates the potential of multi-temporal Landsat data and the CA-Markov model in order to give an accurate, extrapolated and economical means to the map not only that, but also analyze the changes in land use over time that can be used as inputs to track land use changes for many different agencies to solve natural resources and socio-economic problems, including making a plan for sustainable land management.

References

1. Coppin, P., Jonckheere, I., Nackaerts, K., Muys, B., Lambin, E.: Digital change detection methods in ecosystem monitoring. *Int. J. Remote Sensing* **25**, 1565–1596 (2004)
2. Xian, G., Homer, C., Fry, J.: Updateing the 2001 national land cover database land cover classification to 2006 by using Landsat imagery change detection method. *Remote Sensing Environ.* **113**, 1133–1147 (2009)
3. Gilani, H., Shrestha, H.L., Murthy, M., Phuntso, P., Pradhan, S., Bajracharya, B., Shrestha, B.: Decadal land cover change dynamics in Bhutan. *J. Environ. Manage.* **148**, 91–100 (2015)
4. Liu, Y., Huang, X., Yang, H., Zhong, T.: Environmental effects of land-use/cover change caused by urbanization and policies in Southwest China Karst area – a case study of Guiyang. *Habitat Int.* **44**, 339–348 (2014)
5. Kanianska, R., Kizekova, M., Novacek, J., Zeman, M.: Land-use and land-cover changes in rural areas during different political systems: a case study of Slovakia from 1782 to 2006. *Land Use Policy* **36**, 554–566 (2014)
6. Tarutao National Marine Park. <https://www.thainationalparks.com/tarutao-national-marine-park>. Accessed 8 Feb 2018

7. Mahidol University Project on Education and Research on Environment: Report on preliminary survey of Tarutao National Marine Park, Mahidol University, Bangkok (1974)
8. Groot, J.Y.: *Urak Lawoi' Language and Social History*. Prince of Songkla University, Phuket (2012)
9. Pukkalanun, N., Inkapatanakul, W., Piputsitee, C., Chunkao, K.: An analysis of the environmental vulnerability index of a Small Island: Lipe Island, Kho Sarai Sub-District, Mueang District, Satun Province, Thailand. *Mod. Appl. Sci.* **7**(2), 33–38 (2013)
10. Groot, J.Y.: The legend of To Kiri: unraveling an oral tradition about the homeland of the Urak Lawoi. *J. Int. Stud.* **1**, 79–93 (2011)
11. U.S. Geological Survey. <https://earthexplorer.usgs.gov/>. Accessed 14 May 2018
12. Waiyasusri, K., Yumuang, S., Chotpantararat, S.: Monitoring and predicting land use changes in the Huai Thap Salao Watershed area, Uthaitхани Province, Thailand, using the CLUE-s model. *Environ. Earth Sci.* **75**, 533 (2016)
13. Munthali, K.G.; Murayama, Y.: Land use/cover change detection and analysis for Dzalanyama forest reserve, Lilongwe, Malawi. In: *International Conference: Spatial Thinking and Geographic Information Sciences*, vol. 21, pp. 203–211. *Procedia Social and Behavioral Sciences*, Tokyo, Japan (2011)
14. U.S. Geological Survey. <https://landsat.usgs.gov/landsat-8>. Accessed 6 Apr 2018
15. Islam, K., Jashimuddin, M., Nath, B., Nath, R.K.: Land use classification and change detection by using multi-temporal remotely sensed imagery: the case of Chunati wildlife sanctuary, Bangladesh. *Egypt. J. Remote Sensing Space Sci.* **21**, 37–47 (2018)
16. Bake, N., Weindorf, D.C., Bahnassy, M.H., Marei, S.M., El-Badawi, M.M.: Monitoring land cover changes in a newly reclaimed area of Egypt using multi-temporal Landsat data. *Appl. Geogr.* **30**, 592–605 (2010)
17. Rawat, J.S., Biswas, V., Kumar, M.: Changes in land use/cover using geospatial techniques: a case study of Ramnagar town area, district Nainital, Uttarakhand, India. *Egypt. J. Remote Sensing Space Sci.* **16**, 111–117 (2013)
18. Kolois, S., Stylios, C.D.: Identification of land cover/land use changes in the greater area of the Preveza peninsula in Greece using Landsat satellite data. *Appl. Geogr.* **40**, 150–160 (2013)
19. Lillesand, T.M., Kiefer, R.W., Chipman, J.W.: *Remote Sensing and Image Interpretation*. Wiley, New Jersey (2015)
20. Peng, L., Chen, T., Liu, S.: Spatiotemporal dynamics and drivers of farmland changes in Panxi mountainous region, China. *Sustainability* **8**(11), 1209 (2016)
21. Markov, A.: Extension of the limit theorems of probability theory to a sum of variables connected in a china. *The Notes of the Imperial Academy of Sciences of St. Petersburg*, VIII Series. *Physio Mathematical College* **1**(9), 9 (1907)
22. Muller, M.R., Middleton, J.: A Markov model of land-use change dynamics in the Niagara, Ontario, Canada. *Landscape Ecol.* **9**(2), 151–157 (1994)
23. The National Statistical Office of Thailand: *Statistical Yearbook Thailand 2017*. National Statistical Office, Ministry of Digital Economy and Society, Bangkok (2017)



Sustainable Cultivation Planning in Ban Phaeo District, Samut Sakhon Province with Goal Programming and Geographic Information System

Talisa Niemmanee^(✉) and Walaiporn Phonphan

Faculty of Science and Technology, Suan Sunandha Rajabhat University,
Bangkok, Thailand

talisa.ni@ssru.ac.th

Abstract. Ban Phaeo District's geological conditions are highly fertile and suitable for fruit tree cultivation. Hence, it is one of the importance places for fruit agriculture in a province. However, the decrease in agricultural land leads to difficulty in agriculture land use planning. This study aims at; (1) to plan about sustainable cultivation with goal programming, (2) to categorize area for 6 essential plants and create map. Goal programming is used to determine the goal according to the concept of sustainable agriculture. The goals are the highest average net return with lowest environmental impact quotient from the use of agricultural chemicals and the lowest working hours of labors. This study was conducted with 6 selected plants including mango, aromatic coconut, dragon fruit, guava, lemon and longan. The findings reveal that Ban Phaeo District had 5 alternatives and it was recommended to grow at least 2 plants while aromatic coconuts were not recommended in every alternative. According to the result of Geographic Information System (GIS) analysis, cultivation areas of coconut were highest in Ban Phaeo District. Therefore, coconuts plantation area should be preserved in the area.

Keywords: Sustainable cultivation · Goal programming · Geographic Information System (GIS) · Ban Phaeo District

1 Introduction

Agricultural sector plays a vital role in Thailand because nearly half of all Thailand's labor workers are employed in agricultural related industry. Agriculture products can be a source of raw materials for agroindustry and service sectors, generating more revenue and contributing to local livelihood, wisdom and culture for a long time in Thai societal. However, due to the transition of economy away from agriculture to commercial, including focusing more on a single crop agriculture which uses chemical fertilizer, pesticides, etc. It causes toxic contamination in the environment and health problems. Agricultural practice is mostly depended on external factors, leading to high investment cost while product prices are low and uncertain. Such problems occur in several agricultural areas nationwide including Samut Sakhon province.

Samut Sakhon Province occupies an area of 545,216 Rai with fertile soil condition. Tha chin River serves as a main source of water for an agricultural area in 3 districts which accounted for 55.60% of total area. A development plan of Samut Sakhon Province from 2014–2017 focuses on two directions of sustainable development pathway; environmentally friendly city with food security and ecological industrial development” and stipulates agricultural strategy. The 1st strategy is to develop industry, fishery, agriculture and to meet the international standard and the 2nd strategy is to promote and develop a province as the world kitchen of seafood and agriculture. However, with success of the province’s development, it was found that in 2014, Samut Sakhon’s Gross Primary Production (GPP) was 359,566 Thai Baht/person/year, being the 7th rank comparing to other provinces. Most production revenues were derived from industrial sector (67.4%). This leads to major agricultural problems by transforming agricultural area into industrial premises and current agricultural area remains only 97,486 Rai accounted for 17.88% of the entire area [1]. Most important agricultural area of the province is located in Ban Phaeo District.

Ban Phaeo District occupies area of 153,144 Rai and suitable for cultivating vegetables and fruits such as coconut, lemon, orchids etc. Hence, This district plays a crucial role in agricultural production with the agricultural area of 73.74% of the entire area of the province [2]. Currently, Ban Phaeo faces the decrease in agricultural area due to several reasons such as industrial development in nearby districts, reduced in soil fertility, outbreak of pests as well as environmental contamination [1]. If such problems are not hurriedly resolved, cultivation areas of the province will be transformed to other purposes, leading to a decline of agricultural products and affecting the food security of the nation and international level. Of the solution to solve this problem is to control and protect the cultivation area by promoting a sustainable agricultural system with appropriate agricultural planning. Sustainable agriculture for small-scale farmers in Thailand implies an agricultural system that will lead farmers to self-sufficiency, and also maintain a favorable ecological balance and stable farm communities. The first step to attain the sustainable agriculture in general is to move from monoculture to crop diversified or mixed farming. The next step is to choose crops that generates high income [3]. Production planning in the agricultural sector is another way to solve agricultural problems because it could identify which crops could make a high profit return and in what amount under limitations of production resources. A useful instrument to be applied in this research is goal programming which based on multiple criteria analysis to maximize economically and socially benefit while minimize environmental impact [4–6]. Therefore, sustainable agriculture in Ban Phaeo District, Samut Sakhon Province should consider economic, society, and environment aspects when planning for agricultural practices. Geographic Information System (GIS) is applied for agricultural planning support to ease data collection, data analysis and map visualization.

2 Conceptual Framework

A framework starts with problems in Ban Phaeo Sub-district such as rapid industrial and commercial development which attracts a number of farmers become workers in new industries. Furthermore, economic-based agricultural system with emphasis on single crop and chemical use for agriculture could lead to environmental problems. Thus, it is necessary to investigate those problems in terms of economic, society and environment. Problems should be considered to determine a pattern of agricultural system with effective agricultural production planning based on the economic, society and environment. Results will reveal a current cultivation area and agricultural sustainability (see Fig. 1).

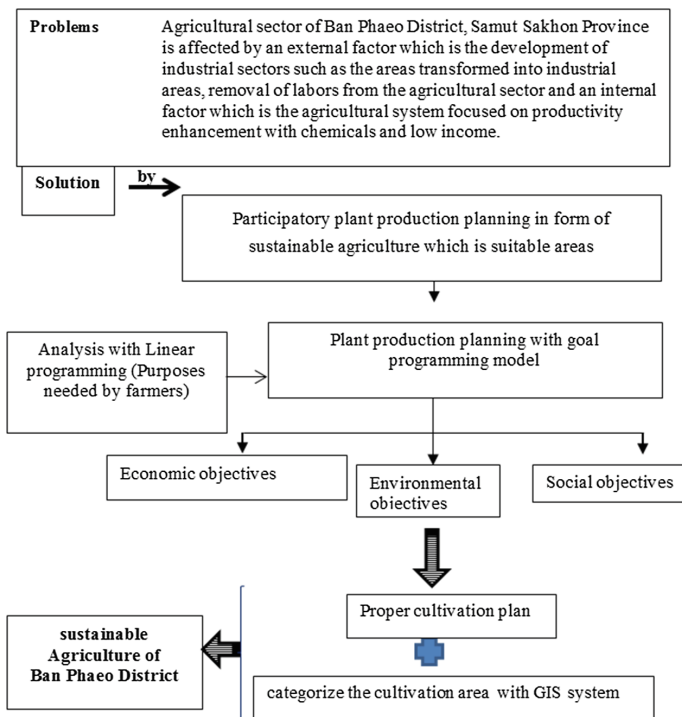


Fig. 1. Conceptual framework of the research.

3 Methodology

This study contains secondary data from 2016–2018 which is collected in areas of Ban Phaeo District, Samut Sakhon Province. Data is divided into 2 parts as the following;

3.1 Cultivation Planning for Sustainable Agriculture with Goal Programming

To plan suitable plants production requires goal programming which is a model of Multi-Goal Programming to consider 6 plants appropriately grown in the area including mango, aromatic coconut, dragon fruit, guava, lemon and longan.

Structure of Goal Programming

The model of goal programming contains objective function and limitations provided that objective functions of the goal programming consist of no decision variables, but they contain a deviational variable which is a value deviated from the goal. Any goal comprises 2 deviational variables including positive and negative deviation. Therefore, the objective function is to find the minimum sum score of deviations from the goal by following the general mathematical format of the goal programming [7] see Eq. 1.

$$\text{Objective function Minimize } Z = \sum_{i=1}^n (d_i^- + d_i^+) \tag{1}$$

Under limitation

$$AX + d^- - d^+ = b$$

$$X, d^-, d^+ \geq 0$$

Above equation can be written in matrix form as follows

Objective function Minimize $Z = [d_1^- + d_2^- + \dots + d_n^-] + [d_1^+ + d_2^+ + \dots + d_n^+]$
 under limitation

$$\begin{bmatrix} A_{11} & A_{12} & \dots & A_{1n} \\ A_{21} & A_{22} & \dots & A_{2n} \\ \vdots & \vdots & \vdots & \vdots \\ A_{m1} & A_{m2} & \dots & A_{mn} \end{bmatrix} \begin{bmatrix} X_1 \\ X_2 \\ \vdots \\ X_n \end{bmatrix} + \begin{bmatrix} d_1^- \\ d_2^- \\ \vdots \\ d_n^- \end{bmatrix} - \begin{bmatrix} d_1^+ \\ d_2^+ \\ \vdots \\ d_n^+ \end{bmatrix} = \begin{bmatrix} b_1 \\ b_2 \\ \vdots \\ b_n \end{bmatrix}$$

$$\begin{bmatrix} X_1 \\ X_2 \\ \vdots \\ X_n \end{bmatrix}, \begin{bmatrix} d_1^- \\ d_2^- \\ \vdots \\ d_n^- \end{bmatrix}, \begin{bmatrix} d_1^+ \\ d_2^+ \\ \vdots \\ d_n^+ \end{bmatrix} \geq 0$$

Where

- z** is a deviation from set goal objective (Deviational Variables).
- d_i^- is deviation of the objective at i making it lower than the goal.
- d_i^+ is deviation at i making it higher than the goal.
- n** is the number of objectives defined in production planning.
- X** is activities for production planning.
- A** is coefficient showing the relationship between product and production factor.
- b** is a limited production factor or conditions to achieve production planning.

The model used in this study is defined to contain 3 objectives including the economic, society, and environment by weighing each aspect equally as explained below;

- (1) Economic objective is the highest net present value specified as e_1 . This objective is to obtain a result similar to the defined value in the objective. The negative deviation is equal to d_1^- – the suitable production plan will contain the least d_1^- – that is, the suitable production plan will create net present value closest to e_1 .
- (2) Social objective is to use labor in producing plants. The targeted labors (e_2) depend on a number of household members and employed workers and the suitable production plan will try to make deviation negative (d_2^-) that the farmers do not have sufficient workers to be the lowest value.
- (3) The environmental objective is the level of environmental impacts from pesticide use in farms (EIQ field use rating). The objective is to make EIQ field use rating lowest. The goal value (e_3) of this objective is the EIQ field use rating and the suitable production plan will attempt making the deviation positive. In other ways, EIQ field use rating is higher than specified (d_3^+) with the lowest value. That is, the suitable production plan will try to make EIQ field use rating equal to e_3 .

Limitation and Condition

Agricultural areas (b1): cultivation areas for fruit trees-perennial plants for 45,386 Rai [2].

Number of household and community workers (b2): number of workers is calculated from an average number of household workers for 3 persons working 8 h a day and 20 days a month. So, working hours in the District are 28,800,000.00 h/year.

Household investment (b3): Investment that the farmers can use to produce plants is from 2 sources (1) saving of farmers, according to the survey, about 100,000 Baht/household with the total investment of 500,000,000.00 Baht/year and secondly, investment from borrowing in model equal to 7% per year.

The Coefficient Used in the Model

The coefficient in the model of cultivation activities is obtained from the following cases

- (1) An average annual value of NPV is derived from the NPV multiplied by the capital recovery factor (CRF).
- (2) Environmental data.

It is considered from the level of environmental impacts from pesticide use (EIQ Field Use Rating) because it is calculated from EIQ or Environment Impact Quotient as the indicator to consider impacts of pesticides on environmental generally. It is examined from the affected group including (1) impact on humans with illness, (2) acute toxicity in birds, (3) toxicity in fish, (4) toxicity in bees, (5) acute toxicity on skin, (6) long-term health impacts, (7) contamination in soil, (8) contamination in plant's parts, (9) toxicity in other organisms beneficial to plants, and (10) contamination in underground water. It can be seen from the fact that EIQ is an indicator emphasized on 3 main groups in agricultural production system including workers in

agricultural areas, consumers, and ecosystem [8]. Thus, it reflects environmental issues better than consideration of only chemical use.

(3) Society data

Economic, environmental and society data are used to define coefficient in goal programming including 1. net present value per annum, 2. EIQ Field Use Rating and 3. The number of working hour/rai for 6 plants in Ban Phaeo District, Samut Sakhon Province as shown in Table 1.

Table 1. Average annual value of NPV//Rai, EIQ Field Use Rating and the number of working hour/rai for 6 plants in Ban Phaeo District, Samut Sakhon Province

Type	Net present value/Rai	Average annual value of NPV//Rai	EIQ Field Use Rating/Rai	Working hour/Rai
Aromatic coconut	671,914.39	54,156.30	17.24	27.58
Mango	87307.35	7,036.97	28.02	109.47
Dragon fruit	329824.40	26,583.85	8.26	229.03
Guava	1,127,576.70	90,882.68	15.73	309.90
Lemon	1,098,369.37	88,528.57	81.48	408.80
Longan	1,680,793.41	135,471.95	16.80	88.22

Source: [9]

3.2 Studying Land Use with GIS

A purpose of including land use data is to provide an overview of location of cultivated areas of six plants as Aromatic coconut Mango, dragon fruit, guava, lemon and Longan. Land use data generated by aerial photographic interpretation with updates from LANDSAT satellite imagery. The supervised classification technique was performed using maximum likelihood algorithm to determined land use. Six essential plants were identified and to calculate the size and location of each plant and was created essential map.

4 Result and Discussion

4.1 Sustainable Cultivation Planning with Goal Programming

To plan multiple-objective cultivation with goal programming is to determine equal objectives and consider providing a model simultaneously including objective 1: highest net present value from plant production, objective 2: lowest EIQ Field Use Rating/Rai and objective 3: lowest working hours under the limitation of investment for

300,000 Baht, 200,000 Baht and 100,000 Baht without loaning and 100,000 Baht loan on 45,386-Rai cultivation area.

A goal of each objective and limitations are as follows

- (1) The goal of net present value from plant production is 50% of the highest net present at 6,148,529,870.51 Baht calculated from a linear program or 3,074,264,935.26 Baht.
- (2) The goal of EIQ Field Use Rating is equal to mean of EIQ Field Use Rating of 6 plants/45,386-Rai area at 1,266,269.40.
- (3) The goal of working hour by focusing on a concept of household workers. The average number of household workers is 3 persons working 8 h a day and 20 days a month in 5,000 households. Therefore, the working hours are 28,800,000.00 h/year.
- (4) The limitation is the investment of 300,000 Baht, 200,000 Baht and 100,000 Baht which is the average investment from field data collection.
- (5) Limitation of the loan, not over 100,000 baht and no loaning.
- (6) 45,386-Rai land.

The findings reveal that plant production planning with such targeted value and limitations generates following alternatives for local farmers.

1st alternative: growing mango 21,435.70 Rai, lemon for 4,299.27 Rai and longan for 18,770.05 Rai, totally 44,505.01 Rai. Following this plan will create net present value for 3,074,264,935.26 Baht. It requires workers for 28,800,000.00 h with EIQ Field Use Rating 1,266,269.40 and investment of 1,073,953,115.67 Baht without borrowing.

2nd alternative: growing mango for 22,244.26 Rai, guava for 103.18 Rai, lemon for 3,931.89 Rai and longan for 19,106.67 Rai, totally 45,386.00 Rai. Following this plan will create the net present value of 3,067,411,601.40 Baht and it requires workers for 28,800,000.00 h with EIQ Field Use Rating at 1,266,269.40 and investment of 589,196,357.98 Baht as well as 500,000,000.00 Baht loan.

3rd alternative: growing mango for 12,238.67 Rai, lemon for 7,059.10 Rai and longan for 17,393.68 Rai, totally, 36,691.46 Rai. Following this plan will create net present value of 3,067,411,601.40 Baht and it requires workers for 28,800,000.00 h with EIQ Field Use Rating at 1,266,269.40 and 1,000,000,000.00 Baht loan.

4th alternative: growing lemon for 10,682.31 Rai and longan for 15,790.89 Rai, totally 26,473.19 Rai. Following this plan will create the net present value of 3,049,911,601.40 Baht. It requires workers for 28,800,000.00 h with EIQ Field Use Rating at 1,266,269.40, investment of 405,355,034.01 Baht and 500,000,000.00 baht loan.

The 5th alternative: growing longan for 18,977.10 Rai, totally 18,977.10 Rai. Following this plan will create the net present value of 3,049,911,601.40 and it requires workers for 28,800,000.00 h with EIQ Field Use Rating at 1,266,269.40 and investment of 500,000,000.00 Baht.

4.2 Cultivation Area Classification for 6 Major Plants

To classify cultivated area for 6 essential plants including mango, coconut, dragon fruit, guava, lemon and longan, when calculated size of cultivation areas, it was found that plants those share the highest cultivated area is for 31,228 Rai. (see Table 2 and Fig. 2).

Table 2. Cultivation areas

Type	Area (Rai)
Coconut	31,228
Mango	8,779
Dragon fruit	1,975
Guava	4,024
Lemon	5,831
Longan	2,235
Total area	54,072

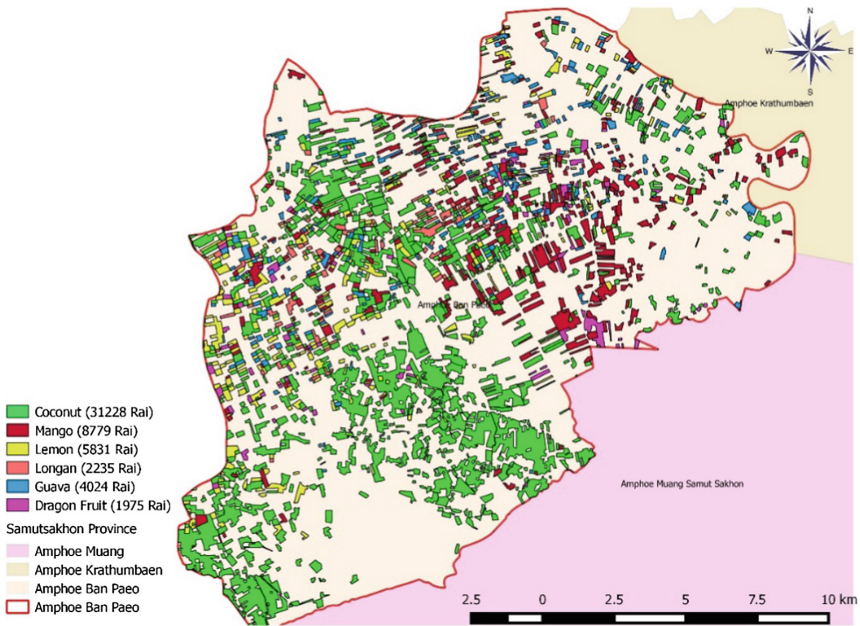


Fig. 2. Location of mango, aromatic coconut, dragon fruit, guava, lemon and longan

4.3 Planning Sustainable Cultivation by Considering Data Obtained from Goal Programming and GIS

From multiple-objectives plant production planning with goal programming, coconuts are not recommended in comparison with 5 alternatives, but agricultural land use data indicated that coconut's cultivation area occupies the highest area comparing to other trees. According to government data, Ban Phaeo aromatic coconut is registered as the geographical indication (GI). Therefore, aromatic coconut should be preserved, and other plants should be promoted according to the plan derived from goal programming results to promote other fruit cultivations.

5 Recommendations

5.1 Recommendations from the Research

- (1) Encouraging farmers to try mixed farming according to the suggested plants. Plant diversification will lead to agriculture in term of economic and environmental sustainability.
- (2) Promoting farmers to use organic fertilizers to enhance soil fertility. Application of fertilizer can reduce the cost of chemical use, resulting in the decrease of production cost and prevention of environmental problems from chemical uses.

5.2 Recommendations for Further Research

Additional factors related to plant cultivation should be examined such as soil characteristics and community need to determine suitable cultivation district. Online information platform related to land suitability should be created to provide central information of agricultural database.

References

1. Sakhon, S.: <http://www.samutsakhon.go.th>. Accessed 15 Jan 2016
2. Ban Phaeo District Agricultural Office. Agricultural Planning 2017–2021 (2007)
3. Kyuma, K.: What is Soil? pp. 276–285. Kyoto University Academic Publisher (2005)
4. Praneetwatakul, S., Sirijinda, A.: Sustainable Agricultural System Planning on Northern Highlands of Thailand. Thai Research Fund, Bangkok (2003)
5. Tantiyanukul, P.: Agricultural production planning with linear program under the concept of sufficiency economy in Samut Sakhon Province. *SDU Res. J. Sci. Technol.* **8**(1), 161–174 (2011)
6. Sinchaiyakul, S.: Optimal patterns for integrated farming systems in Chiang Mai lowlands. Thesis of Master Degree, Chiang Mai University (2004)
7. Niemmanee, P.: Resource Allocation Model, 1st edn
8. Kovach, J., Petzoldt, C., Degnil, J., Tette, J.: A method to measure the environmental impact of pesticides. *New York's Food Life Sci. Bull.* **139**, 1–8 (1992)
9. Niemmanee, T.: Doctoral Dissertation, Kasetsart University (2017). Thai Pattana Raiwan Press Co., Ltd., Bangkok (2009)



Drought Assessment During Dry Season Derived from LANDSAT Imagery Using Amplitude Analysis in Sa Kaeo, THAILAND

Tawatchai Na-U-Dom¹(✉), Prasarn Intacharoen²,
Thippawan Thodsan³, and Sirirapha Jangkorn¹

¹ Faculty of Science and Social Science, Burapha University, Sa Kaeo Campus,
Sa Kaeo 27160, Thailand

tawatchai.na@buu.ac.th

² Department of Aquatic Science, Faculty of Science, Burapha University,
Chonburi 20131, Thailand

³ Hydro Informatics Division, Hydro and Agro Informatics Institute,
Bangkok 10400, Thailand

Abstract. This research aims to assess the spatio-temporal of agriculture drought during dry season (November – April) in Sa Kaeo. The anomaly of normalized difference vegetation index (NDVI) and the anomaly of normalized difference moisture index (NDMI) derived from LANDSAT imagery during dry season in 2001–2002 to 2016–2017 were used to map the drought assessment using amplitude analysis. Function of Mask (Fmask) algorithm and Inverse Distance Weighted (IDW) interpolation were applied to remove the atmospheric noise. The result showed that slight and moderate drought normally occur during dry season, but severe and extreme drought occurred during dry season from late 2001 to early 2002. In addition, drought effect was widely distributed during last five years. The spatial trend of the amplitude value also showed dryer trend in the southern Sa Kaeo, while it showed wetter trend in the northern and northeastern Sa Kaeo, especially in the forest ecosystem. For the environmentalists and ecosystem managers, this research could benefit them as it provides maps related with drought assessment and its spatial distribution, which leads to more effective plans of water management, ecosystem management and mitigation plans of drought during dry season in the Sa Kaeo.

Keywords: Amplitude analysis · Drought · LANDSAT · Normalized difference vegetation index · Normalized difference moisture index

1 Introduction

Nowadays, it is well known that climate change has an intense effect on global ecosystems. Climate change, especially from human activities, is a major factor that intensifies the effect on food production worldwide [1]. Several climate models have found a connection between global warming and the occurrence of climatic extreme events, such as drought, in frequency, intensity, and duration [2].

Drought has a large impact on crop yield, is more sensitive to precipitation than temperature [1], and food security. Hence, It is vital to assess and monitoring drought impact. Nevertheless, using field- or ground- based observation to assess drought impact is generally difficult and expensive to apply in the large scale, while satellite data is effective option for assessing drought impact [3], because it can apply in the large area and multi-temporal scale. For example, the moderate resolution imaging spectroradiometer (MODIS) were applied to assess drought impact in the western Liaoning, China, and found that the anomalies of NDVI and NDMI are effective to assess drought condition from the vegetation and soil moisture [4].

Using drought indices from satellite data to assess spatial extent of drought have been widely applied, such as NDVI [3, 5], Normalized Difference Water Index (NDWI) [6], Vegetation Condition index (VCI) [7], etc., but the weakness of them is solely consider either vegetation or soil moisture.

The objective of this study was to assess and monitoring drought impact in Sa Kao, Thailand, during dry season using the amplitude analysis, which was estimated from the anomalies of NDVI and NDMI in order to focus on vegetation condition and soil moisture. The study was focused on spatial distribution of drought in dry season during 2002 to 2017. In addition, the spatial trend of the amplitude value was also consider in order to detect trend and magnitude of drought. The results could benefit environmentalists as it provides maps related with drought assessment and its spatial distribution, which leads to more effective plans of water management, ecosystem management and mitigation plans of drought during dry season in the Sa Kao.

2 Materials and Methods

2.1 Study Area

The study area is Sa Kao (Fig. 1), a province of eastern Thailand, which cover 101.5° E to 103° E and 13° N to 14.5° N. The northern part of the area includes part of the Thaplan National Park. Cropland, such as rubber, eucalyptus, rice and cassava, are cultivated in the central and the southern Sa Kao. The rice cultivation area is flat land with an elevation varying between 10 m and 100 m. The main crop for dry season are cassava and maze, while rice cultivation is less important because of lack of water [8].

2.2 Satellite Data and Pre-processing

In this study, we use the Landsat 4-5TM, 7ETM and 8OLI to retrieve images during dry season (November to April) from 2002 to 2011, 2012 and 2013–2017, respectively. Dark Object Subtraction (DOS) method was used for atmospheric correction using Semi-Automatic Classification plugin [10] in QGIS, and Function of Mask (Fmask) were applied in order to remove the atmospheric noise, such as cloud and cloud shadow, using Cloud Masking plugin [11] in QGIS. We used NDVI and NDMI to evaluate vegetation condition and soil moisture. NDVI is widely used to monitoring vegetation greenness, biomass, inter-annual and seasonal vegetation productivity [1–5].

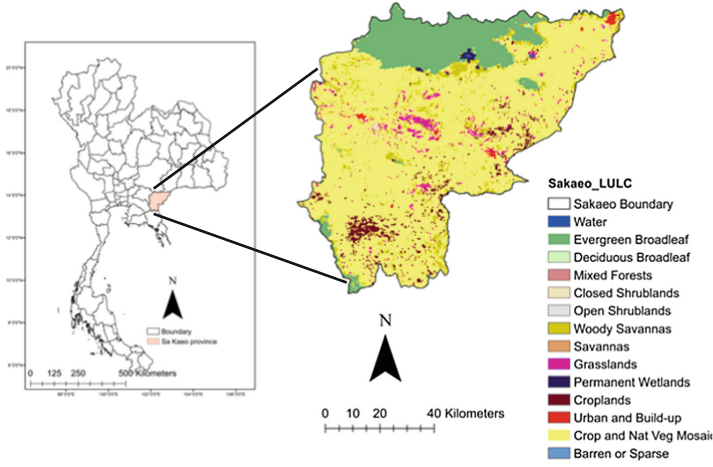


Fig. 1. Sa Kaeo in Thailand and its land cover (MCD12Q1) [9]

NDVI is calculated using two satellite imagery bands, which are red (RED) and near-infrared (NIR), as follows:

$$NDVI = (NIR - RED) / (NIR + RED) \quad (1)$$

NDMI were evaluated using mid-infrared (MIR) and NIR, as showed in Eq. 2, which are sensitive to leaf structure and water content.

$$NDMI = (NIR - MIR) / (NIR + MIR) \quad (2)$$

Then, the Inverse Distance Weighted (IDW) interpolation were applied to NDVI and NDMI imagery in order to fill blank pixels, which were formerly cloud and cloud shadow.

2.3 NDVI and NDMI Anomalies and Amplitude Analysis

NDVI and NDMI anomalies are the departure of the long-term average NDVI and NDMI for a specific time, which could indicate drought condition in the specific time. The anomalies of NDVI and NDMI (NANO and MANO, respectively) in year k for pixel ij could be defined as Eqs. 3 and 4.

$$NANO_{ijk} = \overline{NDVI}_{ij} - NDVI_{ijk} \quad (3)$$

$$MANO_{ijk} = \overline{NDMI}_{ij} - NDMI_{ijk} \quad (4)$$

Where \overline{NDVI}_{ij} and \overline{NDMI}_{ij} are the multiyear average NDVI and NDMI for pixel ij , and $NDVI_{ijk}$ and $NDMI_{ijk}$ are NDVI and NDMI in year k for pixel ij , respectively. Then, amplitude value in year k for pixel ij ($Amplitude_{ijk}$) was estimated using Eq. 5 [4].

$$Amplitude_{ijk} = \sqrt{(NANO_{ijk})^2 + (MANO_{ijk})^2} \quad (5)$$

Next, we average all period (November to April) to represent the vegetation (NDVI) and soil moisture (NDMI) conditions in the period. For example, amplitude value in 2001 to 2002 was an average value from November 2001 to April 2002.

2.4 Trend Analysis Based on Linear Regression

To predict linear trend, linear regression analysis was applied as Eq. 6.

$$Slope = \frac{n * \sum_{k=1}^n * Amplitude_{(k)} - (\sum_{k=1}^n k) * (\sum_{k=1}^n Amplitude_{(k)})}{n * \sum_{k=1}^n k^2 - (\sum_{k=1}^n k)^2} \quad (6)$$

Where *Slope* is the slope of regression equation, *n* is the number of years, *k* is the year sequence in the study period, ranging from 1 to *n*, $Amplitude_{(k)}$ is the amplitude value of year *k*. If *Slope* > 0.00 (<0.00), the amplitude value shows increasing (decreasing) trend. On the other hand, if *Slope* = 0.00, amplitude value does not change.

3 Results

3.1 Spatial and Temporal of Drought Severity

Spatial and temporal of drought severity in different periods, from 2001–2002 to 2016–2017, are showed in Fig. 2. The results show that drought during summer in Sa Kaeo is normally slight (0.00–0.10) to moderate (0.10–0.15), especially in 2010–2011 and 2011 to 2012, which coherence with other areas. In 2001–2002, it obviously shows that severe drought (>0.15) distributed almost entire of Sa Kaeo, while severe drought occurred in the evergreen forest ecosystem in 2002–2003 and 2008 – 2009. During last five years (2012–2013, 2013–2014, 2014–2015, 2015–2016 and 2016–2017), drought effect are more distribute and evergreen forest and cropland in the north and central of Sa Kaeo experienced with moderate to severe drought, especially in 2013–2014 and 2014–2015.

3.2 Trend Analysis of Drought Severe

Positive and negative summer mean amplitude value trends from 2002–2003 to 2016–2017, across the Sa Kaeo, are showed in Fig. 3. The trends were represented in amplitude value units/year. Green (Red) represents negative (positive) trend, which mean wetter (drier) over time.

The result showed that amplitude value increased at around 0.002 to 0.003 amplitude value units per year; most clearly seen in the central of Sa Kaeo. The highest positive slope, around 0.005 to 0.01, was showed in the south of Sa Kaeo, which is covered by cropland. The wetting trend (< –0.005) found in the forest biome and cultivation area in the north and northeast of Sa Kaeo.

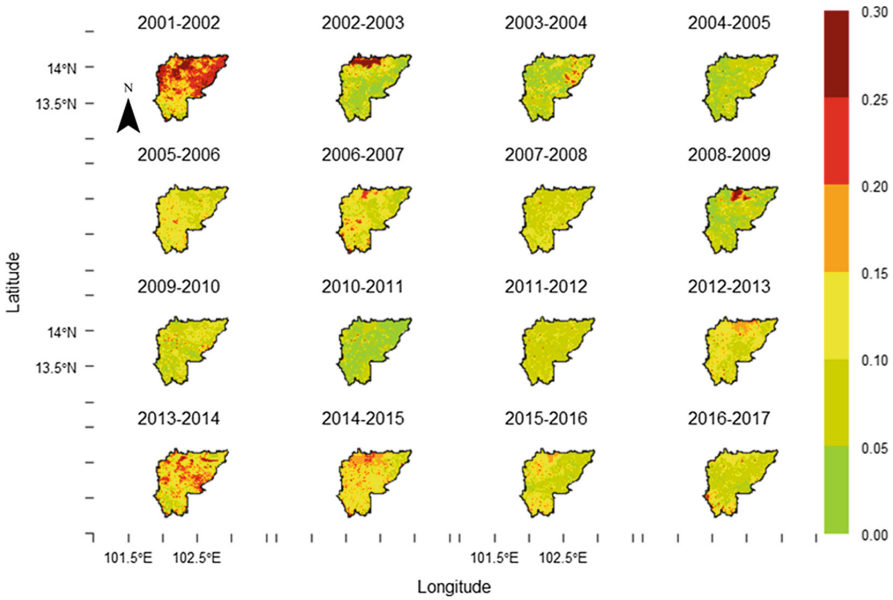


Fig. 2. Spatial and temporal of drought severity in Sa Kaeo in 2001–2002 to 2016–2017 while colored bar represents drought severity

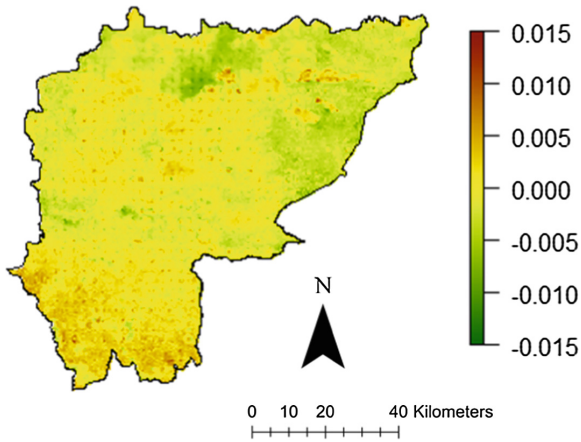


Fig. 3. Spatial distribution of amplitude value trend analysis (amplitude value unit/year)

4 Discussion

Assessment of drought impact is vital and has significance in environmental, agricultural and ecological planning. In previous researches, many techniques were used to evaluate impact of drought in several regions, but the weakness of them is solely

consider either vegetation or soil moisture. Hence, in the research, amplitude analysis were used to evaluate spa-temporal distribution drought dynamics in the Sa Kaeo.

Drought during dry season in Sa Keao, severe drought occurred in 2001–2002, 2008–2009 and 2012–2013, which corresponded with Laosuwan et al. [5]. They discovered severe drought in Mahasarakham, is located in the north-east Thailand, during 2007, 2010 and 2012. Moreover, the minimum and maximum temperatures in Thailand showed significant increasing trend [12], which is positively related to high evaporation [13].

However, drought during dry season in Sa Keao was different in both spatial and temporal scale, and the amplitude was also showed increasing trends, especially in the central and south of Sa Keao. The appropriate irrigation plans and managements are vital for mitigate drought impact in this region. Hao et al. [14] also suggested that anthropogenic activities affected to ecosystems. Na-U-Dom et al. [15] showed that cropland was benefit to human activities, i.e. irrigation and fertilization, while forest showed negative trend with human activities, i.e. deforestation. Hence, appropriate human activities and extreme weather, i.e. drought, impact in the regional scale with different ecosystems are vital for future researches, which are benefit ecological and environmental restoration program in the future.

5 Conclusion

Drought during dry season in Sa Kaeo was spatial and temporal change over years. Slight and moderate drought normally occur during dry season, but severe and extreme drought occurred during dry season from 2001–2002, 2008–2009 and 2012–2013. The forest biome, in the north Sa Kaeo, is sensitive to drought during dry season, which may lead to fire forest. Cropland was located in slight drought zone. It was probably due to the irrigation system. During dry season in last five years, drought effect wildly distributed. Moreover, the amplitude trend showed dryer trend in the southern Sa Kaeo, which was covered by cropland and forest, while other parts of Sa Kaeo tend to be wetter during dry season, especially the forest biome in the northern and northeastern Sa Kaeo.

For the environmentalists and ecosystem managers, this research could benefit them as it provides maps related with drought assessment and its spatial distribution, which leads to more effective plans of water management, eco-system management and mitigation plans of drought during dry season in the Sa Kaeo.

References

1. Kang, Y., Khan, S., Ma, X.: Climate change impacts on crop yield, crop water productivity and food security - a review. *Prog. Nat. Sci.* **19**, 1665–1674 (2009)
2. Field, C.B., Barros, V., Stocker, T.F., Qin, D., Dokken, D.J., Ebi, K.L., Mastrandrea, M.D., Mach, K.J., Plattner, G.-K., Allen, S.K., Tignor, M., Midgley, P.M.: *Managing the Risks of Extreme Events and Disasters to Advance Climate Change Adaptation*. Cambridge University Press, Cambridge (2012)

3. Legesse, G., Suryabagavan, K.V.: Remote sensing and GIS based agricultural drought assessment in East Shewa Zone, Ethiopia. *Trop. Ecol.* **55**, 349–363 (2014)
4. Lin, M.L., Wang, Q., Sun, F., Chu, T., Shiu, Y.: Quick spatial assessment of drought information derived from MODIS imagery using amplitude analysis. *Int. J. Geol. Environ. Eng.* **4**, 271–275 (2010)
5. Laosuwan, T., Sangpradid, S., Gomasathit, T., Rotjanakusol, T.: Application of remote sensing technology for drought monitoring in Mahasarakham Province. *Int. J. Geoinform.* **12**, 17–25 (2016)
6. Zhang, X., Yamaguchi, Y., Li, F., He, B., Chen, Y.: Assessing the impacts of the 2009/2010 drought on vegetation indices, normalized difference water index, and land surface temperature in southwestern China. *Adv. Meteorol.* **2017**, 1–9 (2017)
7. Zhang, A., Jia, G.: Monitoring meteorological drought in semiarid regions using multi-sensor microwave remote sensing data. *Remote Sens. Environ.* **134**, 12–23 (2013)
8. Wijesingha, J.S.J., Deshapriya, N.L., Samarakoon, L.: Rice crop monitoring and yield assessment with MODIS 250 m gridded vegetation product: a case study in Sa Kaeo Province, Thailand. In: Schreier, G., Skrovseth, P.E., Staudenrausch, H. (eds.) 36th International Symposium on Remote Sensing of Environment, vol. 40, pp. 121–127. Berlin, Germany (2015)
9. Friedl, M.A., Sulla-Menashe, D., Tan, B., Schneider, A., Ramankutty, N., Sibley, A., Huang, X.: MODIS collection 5 global land cover: algorithm refinements and characterization of new dataset. *Remote Sens. Environ.* **114**, 168–182 (2010)
10. Semi-Automatic Classification Plugin Documentation. <https://media.readthedocs.org/pdf/semiautomaticclassificationmanual-v3/latest/semiautomaticclassificationmanual-v3.pdf>. Accessed 15 Jan 2018
11. Cloud Masking Qgis plugin (Version 17.6.30). <https://smbyc.bitbucket.io/qgisplugins/cloudmasking>. Accessed 15 Jan 2018
12. Limsakul, A., Limjirakan, S., Sriburi, T., Suttamanuswong, B.: Trends in temperature and its extremes in Thailand. *Thai Environ. Eng. J.* **25**(1), 9–16 (2011)
13. Kosa, P.: Air temperature and actual evapotranspiration correlation using Landsat 5 TM satellite imagery. *Kasetsart J.* **43**, 605–611 (2009)
14. Hao, W., Liu, G., Li, Z., Ye, X., Fu, B., Lv, J: Impacts of drought and human activity on vegetation growth in the grain for green program region, China. *Chin. Geogr. Sci.* **28**(3), 470–481 (2018)
15. Na-U-Dom, T., Mo, X., García, M: Assessing the climatic effects on vegetation dynamics in the mekong river basin. *Environments* **4**(1), 1–17 (2017)



Determination Critical Rainfall Threshold for the Initiation of Landslides Using Rainfall-Infiltration Model and Infinite Slope Stability Model

Thapthai Chaithong^(✉) 

Tohoku University, Sendai, Miyagi 980-0866, Japan
Four.qed@gmail.com

Abstract. Landslides or slope failures may occur during or immediately after heavy or prolonged rainfall. The amount of rainwater that infiltrates into the slope is one of the most significant triggering factors; in addition, the antecedent moisture content of the soil slope is an important control factor for landslide or slope failure. Hence, the aim of this study is to determine the critical rainfall threshold for an early warning system that can mitigate the loss of life and property. A modified GIS-based Green-Ampt infiltration model and infinite slope stability model were applied to determine the critical rainfall threshold. This study was performed to validate the efficiency of the critical rainfall threshold using the case of the Fukuoka landslide in 2017 by comparing the three-day antecedent precipitation index and the critical rainfall threshold in terms of the rainfall triggered ratio.

Keywords: Critical rainfall threshold · Landslide · Infinite slope stability model · Extreme rainfall

1 Introduction

Landslides are natural disasters, common in mountainous areas, which can destroy infrastructure and homes and lead to the loss of human life. The loss of property and human life caused by landslides is on the rise because of the expansion of residential and economic districts into mountainous and forested areas. When considering the causes of landslides, rainfall is the principal trigger parameter [1, 2]. Rainfall-induced landslides often occur during or immediately after heavy or prolonged rainfall in the monsoon season [3]. In addition, previous studies have shown that the infiltration of rainwater play a key role in pore water pressure changes [4, 5]. The mechanism behind shallow landslide triggered by rainfall is a rising positive pore water pressure on a slope due to rainwater infiltration. It may reduce the effective stress and leads to a reduction in shear strength on the failure plane. These changes may lead to shallow landslide. Landslide mitigation tools are an important component of the strategy for reducing the risk posed by landslides to both the public and private sectors. One such mitigation tool that has proved useful is the landslide early warning system [6]. However, the critical rainfall threshold significantly influences the accuracy of the system. Numerous

methods have been used to calculate the critical rainfall threshold, such as the statistical technique (intensity–duration threshold) or a combination of seepage analysis and slope stability analysis [7–9]. The spatial condition is critical to the proper functioning of the early warning system. Therefore, the purpose of this study is to develop the spatial critical rainfall threshold using a physically based model (which combines the infiltration and infinite slope analysis models) in conjunction with geographic information system software.

2 Method

2.1 Critical Rainfall Threshold Model

The critical rainfall threshold is the amount of rainwater that causes a shallow landslide and slope failure. A rainfall-induced landslide occurs when rainwater infiltrates the hillslope to generate positive pore water pressure or groundwater table and the shear strength on the potential failure plane is reduced. This may lead to landslides or slope instability. Therefore, the main concept of the critical rainfall threshold model is to calculate the amount of rainwater available to seep into the hillslope that decreases the safety factor of the slope to 1. There are three significant assumptions. First, the mode of failure is based on the infinite slope stability analysis model because it is similar the characteristics of shallow landslides and the saturation condition of soil will destabilize the hillslope. Second, the initial water content of the ground prior to rainfall is equal to the volumetric water content at field capacity (suction = 33 kPa). Third, the critical depth of the slope is a depth of wetting front of infiltration process [10, 11].

Figure 1a shows the water content profile for a soil slope of modified Green-Ampt infiltration model. The wetting front is a sharp boundary of saturated soil layer. The wetting front can be calculated based on the cumulative infiltration depth, as shown in Eq. (1) [11, 12].

$$I = (\theta_s - \theta_i) \times (Z_f \cos \beta) \quad (1)$$

where I is the cumulative infiltration depth, θ_s is the saturated volumetric water content, θ_i is the initial volumetric water content, Z_f is the wetting front depth and β is the slope angle.

Figure 1b shows the modelling of the infinite slope stability analysis. The infinite slope stability analysis model is commonly used in shallow landslide analysis [13, 14]. The stability of the slope is presented in the form of a safety factor, which is the ratio of the shear strength of the slope, based on the Mohr–Coulomb failure criteria, to the shear stress applied to the slope, as shown in Eq. (2) [15, 16].

$$F_s = (c' / \gamma_t H \sin \beta \cos \beta) + (\tan \phi' / \tan \beta) \quad (2)$$

where F_s is the safety factor of slope, c' is the soil cohesion, ϕ' is the friction angle of soil, γ_t is the total unit weight of soil, and H is the failure depth of slope.

According to Eq. (2), the depth of the slope at a safety factor of 1 is referred to as the critical depth of the slope (H_{cr}). Based on the second and third assumptions, the

critical rainfall threshold can be calculated by combining Eqs. (1) and (2), as shown in Eq. (3).

$$R_c = [c' / (\gamma_t \sin \beta \cos \beta (1 - (\tan \phi' / \tan \beta)))] \times [(\theta_s - \theta_f) \cos \beta] \tag{3}$$

where R_c is the critical rainfall threshold.

The predictive equations used to estimate volumetric water content at saturated capacity and at field capacity are based on soil texture, as proposed by [17]. For simplified calculation, this study ignores the organic content of the soil. The term of can calculate by Eq. (4).

$$\theta_s - \theta_f = \theta_{(s-33)t} + (0.636\theta_{(s-33)t} - 0.107) \tag{4}$$

where

$$\theta_{(s-33)t} = 0.278S + 0.034C - 0.584(S \times C) + 0.078 \tag{5}$$

where S is the percentage of sand by weight, C is the percentage of clay by weight. θ_s is the saturated volumetric water content, θ_f is the volumetric water content at field capacity.

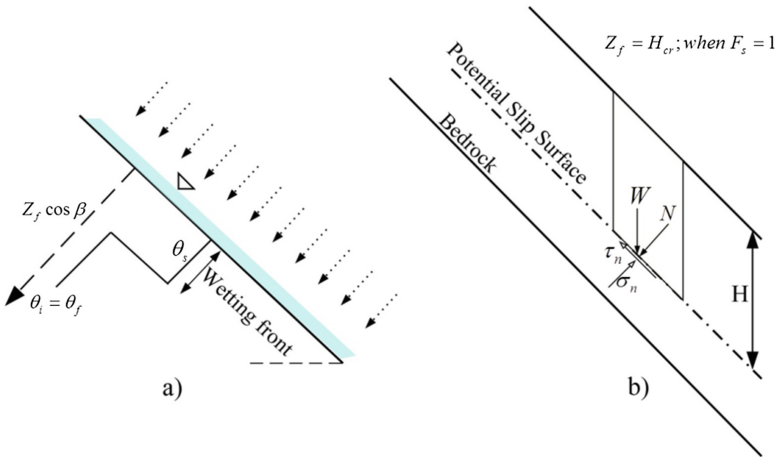


Fig. 1. (a) Water content profile for soil slope of modified Green-Ampt infiltration model. (b) Infinite slope stability model

2.2 Rainfall Triggered Landslide Ratio

The rainfall-triggered landslide ratio [18, 19] is the ratio of the critical rainfall amount to the antecedent precipitation index, as shown in Eq. (6). The rainfall-triggered landslide ratio is calculated to assess the possibility of the occurrence of a landslide as a

result of rain. In this study, if the value of the rainfall-triggered landslide ratio is less than 1.0, the slope will collapse.

$$RTL = (\text{critical rainfall/antecedent precipitation index}) = (R_c/API) \quad (6)$$

where RTL is the rainfall triggered landslide ratio, R_c is the amount of critical rainfall, API is the antecedent precipitation index.

The antecedent precipitation index is the index that indicates the antecedent moisture condition in the soil prior to a rainfall event. For shallow landslides triggered by rainfall, the cumulative moisture content in the soil is also an important factor increasing the probability of landslide occurrence. The antecedent rainfall decreases with time after the rain event [20], and is calculated by Eq. (7) [21]:

$$API_t = (API_{t-1} \times k) + R_t \quad (7)$$

where API_t is the antecedent precipitation index at time t , k is the recession coefficient, API_{t-1} is the antecedent precipitation index at time $t-1$, and R_t is the amount of rainfall at time t . The regression coefficient, which is related to potential evaporation and soil hydrological properties, [22, 23] can be calculated by Eq. (8):

$$k = \exp[-E_p/(z(\theta_f - \theta_w))] \quad (8)$$

where E_p is the potential evaporation, z is the soil depth, θ_w is the volumetric water content at the permanent wilting point,

The volumetric water contents at field capacity and at the permanent wilting point can calculate by Eqs. (9) and (10) [17].

$$\theta_w = \theta_{1500t} + (0.14\theta_{1500t} - 0.02); [\theta_{1500t} = -0.024S + 0.487C + 0.068(S \times C) + 0.031] \quad (9)$$

$$\theta_f = \theta_{33t} + [1.283(\theta_{33t})^2 - 0.374\theta_{33t} - 0.015]; [\theta_{33t} = -0.251S + 0.195C + 0.452(S \times C) + 0.299] \quad (10)$$

2.3 Description of Study Site

The study site is the city of Asakura in Fukuoka Prefecture, on the Island of Kyushu, Japan. The city of Asakura was affected by Tropical Storm Nanmadol in 2017. The storm made landfall on 4 July at 0.00 UTC near Nagasaki, on the island of Kyushu. The total rainfall in the city of Asakura between 4 and 6 July 2017 reached approximately 590 mm. The maximum hourly rainfall of 106 mm on 5 July 2017 was measured at Asakura station by the Japan Meteorological Agency. Figure 2 shows the location of the landslide scars in the city of Asakura. Figure 3 plots the hourly rainfall from 4 to 6 July 2017 at Asakura station.

2.4 Dataset

This study used the ASTER Global Digital Elevation Model, Version 2 (GDEM v2), to extract the elevation and slope angle data set. The ASTER GDEM was collaboratively developed by the National Aeronautics and Space Administration (NASA) and the Japanese Ministry of Economy, Trade, and Industry (METI). The horizontal resolution in this study is 100×100 m per grid. Figure 4 shows the slope angle of the city of Asakura. The soil engineering parameters for infinite slope stability analysis model such as soil cohesion 12.3 kN/m^2 ; soil friction angle 20° , total soil unit weight 18 kN/m^3 . The potential evaporation in July in Fukuoka Prefecture is approximately 84 mm/month [24].

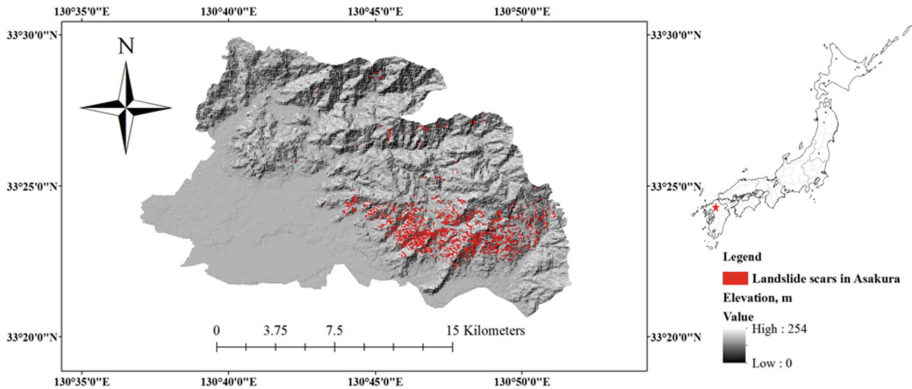


Fig. 2. Location of landslides in the city of Asakura, Fukuoka prefecture on the Island of Kyushu of Japan.

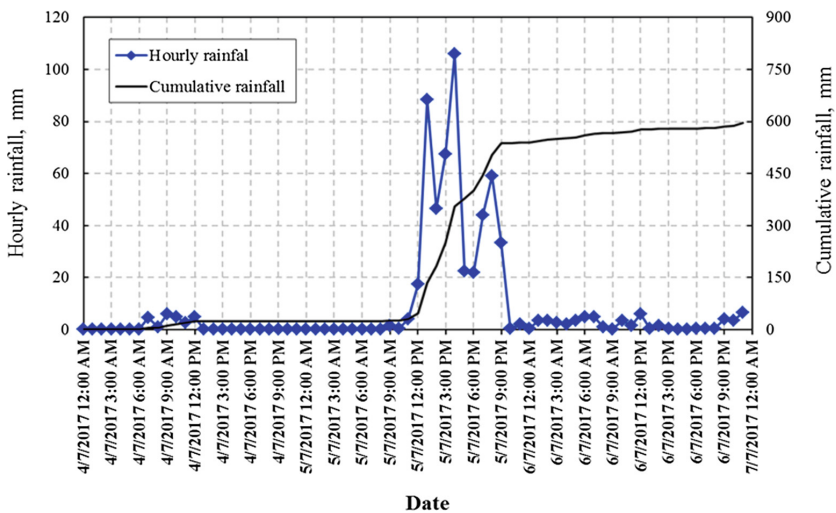


Fig. 3. Plots of hourly rainfall and cumulative rainfall at Asakura station.

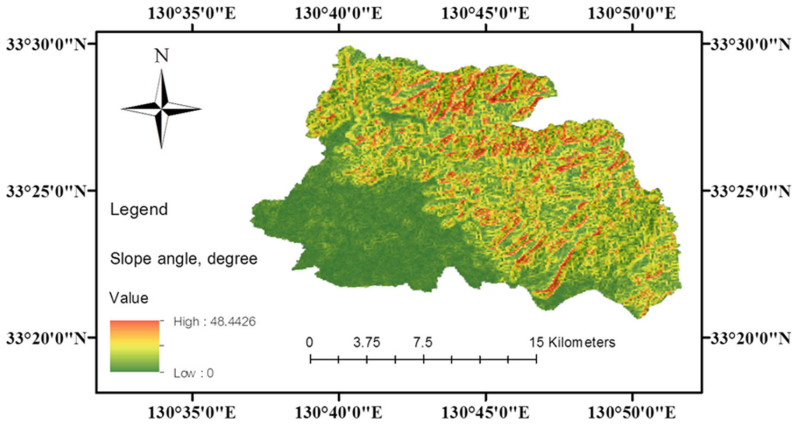


Fig. 4. Slope angle dataset of the city of Asakura, Fukuoka prefecture, Japan.

The soil hydrological data used global gridded hydrologic soil groups (HSGs) for curve-number-based runoff modelling [25]. The HYSOGs250m separates hydrological soil types into 14 groups based on USDA-based soil texture classes, depth of bedrock, and depth to groundwater table. Hydrological soil groups A, D, C and D correspond to low, moderately low, moderately high and high runoff, respectively, and dual HSGs are assigned to wet soils that, despite having the same soil texture, have a high rainfall runoff. Therefore, this study considers only the percentage of sand and clay present in soil to calculate the critical rainfall data. Table 1 sets out the description of the HYSOGs250m soil groups. Figure 5 shows the hydrological soil groups of the city of Asakura.

Table 1. Description of soil group of HYSOGs250m [26].

Pixel values	Description
1	HSG-A: low runoff potential (>90% sand and <10% clay)
2	HSG-B: moderately low runoff potential (50–90% sand and 10–20% clay)
3	HSG-C: moderately high runoff potential (<50% sand and 20–40% clay)
4	HSG-D: high runoff potential (<50% sand and >40% clay)
11	HSG-A/D: low runoff potential (>90% sand and <10% clay)
12	HSG-B/D: moderately low runoff potential (50–90% sand and 10–20% clay)
13	HSG-C/D: moderately high runoff potential (<50% sand and 20–40% clay)
14	HSG-D/D: high runoff potential (<50% sand and >40% clay)

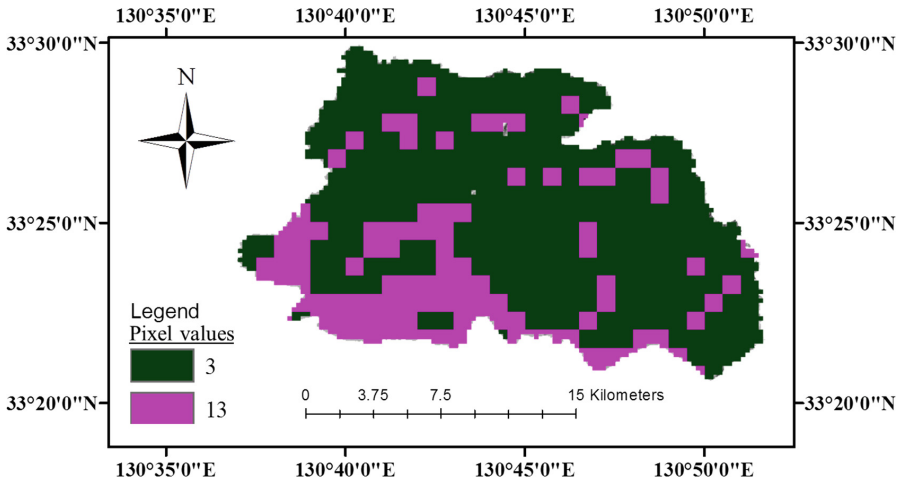


Fig. 5. Hydrological soil groups of the city of Asakura, Fukuoka prefecture, Japan.

3 Results and Discussion

Figure 6 shows the critical rainfall threshold of the city of Asakura. In this study, the percentages of clay and sand used to determine the volumetric water content for the critical rainfall threshold and antecedent precipitation index calculations are 30% and 40%, respectively. The value of $\theta_s - \theta_f$ is 0.13 for the critical rainfall calculation, giving a minimum critical rainfall threshold of approximately 200 mm. The critical rainfall threshold is lower in areas with steep slopes than in areas with gentle slopes. Figure 7 shows the API in the city of Asakura between 4 and 6 July 2017. The API for

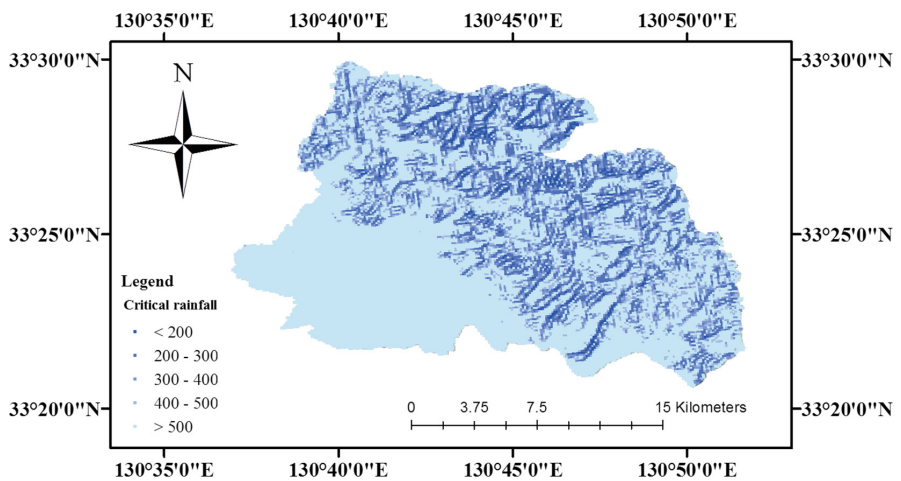


Fig. 6. Critical rainfall threshold of the city of Asakura, Fukuoka prefecture, Japan.

the period of 4 to 6 July 2017 was calculated using data from the 19 rain gauges situated throughout Fukuoka prefecture from the Japan Meteorological Agency's Automated Meteorological Data Acquisition System. The maximum antecedent precipitation index was approximately 587 in the Asakura rain gauge. To estimate an antecedent precipitation index distribution in this study, the IDW method in the Spatial Analyst Tool of ArcGIS was used. Figure 8 shows Asakura's rainfall-triggered landslide ratio (RTL) during this event. A review of the RTL reveals that grids with an RTL value lower than 1 are well correlated with the actual landslide scars of this event,

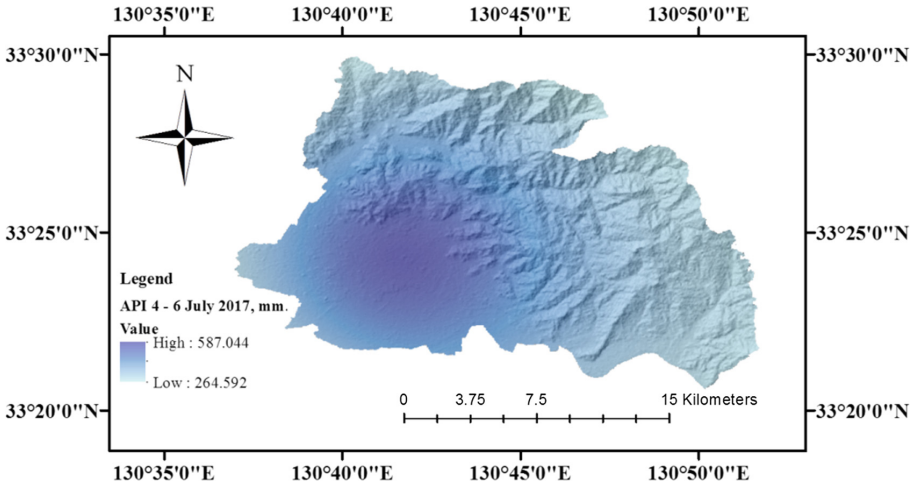


Fig. 7. Antecedent precipitation index in the city of Asakura, Fukuoka prefecture, Japan during 4 to 6 July 2017.

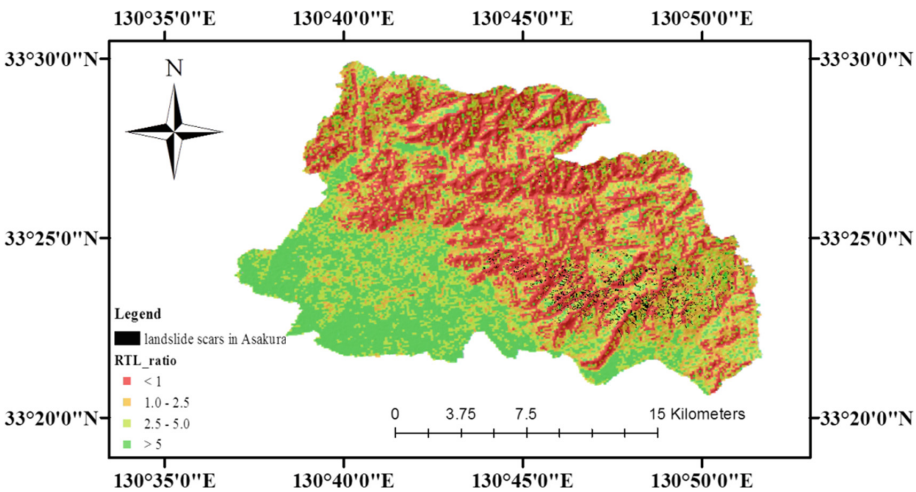


Fig. 8. Rainfall triggered landslide ratio (RTL) of the city of Asakura, Fukuoka prefecture, Japan in this event.

although the results of the RTL overestimate landslides in the study area. The actual landslide scars were obtained from aerial photographs provided by the Geospatial Information Authority of Japan.

4 Conclusions

This study applied a geographic information system to determine the critical rainfall threshold in the spatial condition. The critical rainfall model is based on the analytical concepts of the infiltration model and infinite slope stability model. The critical depth as determined by the infinite slope stability model is a wetting front of modified Green-Ampt infiltration model. Using the RTL, this critical rainfall model can calculate the amount of rainwater to provide an early warning system for landslides. This study is limited by the fact that only a single data set of soil engineering parameters was used. The important challenge is the spatial condition of soil engineering parameters.

Acknowledgments. The author is grateful to the Japan Meteorological Agency for rainfall data and the Geospatial Information Authority of Japan for the aerial photographs of landslides.

References

1. Jeong, S.S., Lee, K.W., Kim, J.H., Kim, Y.M.: Analysis of rainfall-induced landslide on unsaturated soil slopes. *Sustainability* **9**, 1–20 (2017)
2. Iverson, R.M.: Landslide triggering by rain infiltration. *Water Resour. Res.* **36**, 1897–1910 (2000)
3. Orense, R.P.: Slope failures triggered by heavy rainfall. *Philippine Eng. J.* **25**, 73–90 (2004)
4. Rahardjo, H., Leong, E.C., Rezaur, R.B.: Effect of antecedent rainfall on pore-water pressure distribution characteristics in residual soil slopes under tropical rainfall. *Hydrol. Process.* **22**, 506–523 (2008)
5. Tofani, V., Dapporto, S., Vannocci, P., Casagli, N.: Infiltration, seepage and slope instability mechanisms during the 20–21 November 2000 rainstorm in Tuscany, central Italy. *Nat. Hazards Earth Syst. Sci.* **6**, 1025–1033 (2006)
6. Intrieri, E., Gigli, G., Mugnai, F., Fanti, R., Casagli, N.: Design and implementation of a landslide early warning system. *Eng. Geol.* **147–148**, 124–136 (2012)
7. Guzzetti, F., Peruccacci, S., Rossi, M., Stark, C.P.: Rainfall thresholds for the initiation of landslides in central and southern Europe. *Meteorol. Atmos. Phys.* **98**, 239–167 (2007)
8. Soralump, S.: Geotechnical approach for the warning of rainfall-triggered landslide in Thailand considering antecedent rainfall data. In: *International Conference on Slope 2010: Geotechnique and Geosynthetics for Slopes*, Chiang Mai Thailand (2010)
9. Kanjanakul, C., Chub-uppakarn, T., Chalermyanont, T.: Rainfall threshold for landslide early warning system in Nakhon Si Thammarat. *Arab. J. Geosci.* **9**, 2–11 (2016)
10. Jotisankasa, A., Vathananukij, H.: Investigation of soil moisture characteristics of landslide-prone slopes in Thailand. In: *International Conference on Management of Landslide Hazard in the Asia-Pacific Region*, Sendai, Japan (2008)
11. Chaitong, T., Komori, D., Sukegawa, Y., Touge, Y., Mitobe, Y., Anzai, S.: Landslides and precipitation characteristics during the typhoon Lionrock in Iwate prefecture, Japan. *Int. J. Geomate* **14**(44), 109–144 (2018)

12. Chen, L., Young, M.H.: Green-Ampt infiltration model for sloping surfaces. *Water Resour. Res.* **42**, 1–9 (2006)
13. Muntohar, A.S., Ikhsan, J., Liao, H.J.: Influence of rainfall patterns on the instability of slopes. *Civil Eng. Dimension* **15**(2), 121–128 (2013)
14. Tarolli, P., Tarboton, D.G.: A new method for determination of most likely landslide initiation points and the evaluation of digital terrain model scale in terrain stability mapping. *Hydro. Earth Syst. Sci.* **10**, 663–677 (2006)
15. Rahardjo, H., Lim, T.T., Chang, M.F., Fredlund, D.G.: Shear strength characteristics of a residual soil. *Can. Geotech. J.* **32**, 60–77 (1995)
16. Zhang, L.L., Zhang, J., Zhang, L.M., Tang, W.H.: Stability analysis of rainfall-induced slope failure: a review. *Proc. Inst. Civ. Eng. Geotech. Eng.* **164**, 299–316 (2011)
17. Saxton, K.E., Rawls, W.J.: Soil water characteristic estimates by texture and organic matter for hydrologic solution. *Soil Sci. Soc. Am. J.* **70**, 1569–1578 (2006)
18. Polemio, M., Petrucci, O.: Rainfall as a landslide triggering factor: an overview of recent international research. *Landslides in research, theory and practice*, Thomas Telford, London (2000)
19. Chaithong, T., Soralump, S., Pungsuwan, D., Komori, D.: Assessing the effect of predicted climate change on slope stability in northern Thailand: a case of Doi Pui. *Int. J. Geomate* **13** (38), 38–48 (2017)
20. Ohtsu, H.M.: A study on rainfall infiltration into subsoil at a slope. In: *EIT-JSCE Joint International Symposium on International Human Resource Development for Disaster-Resilient countries*, Bangkok Thailand (2012)
21. Fedora, M.A., Beschta, R.L.: Storm runoff simulation using an antecedent precipitation index (API) model. *J. Hydrol.* **112**, 121–133 (1989)
22. Ide, J., Haga, H., Chiwa, M., Otsuki, K.: Effects of antecedent rain history on particulate phosphorus loss from a small forested watershed of Japanese cypress (*Chamaecyparis obtusa*). *J. Hydrol.* **352**, 322–335 (2008)
23. Choudhury, B.J., Blanchard, B.J.: A simulation study of the recession coefficient for antecedent precipitation index. *NASA Technical Memorandum* (1981)
24. Kondo, J., Nakazono, M., Watanabe, T., Kuwagata, T.: Hydrological climate in Japan(3)-evapotranspiration from forest. *J. Japan Soc. Hydrol. Water Resour.* **5**(4), 8–18 (1992)
25. Global Hydrologic Soil groups (HYSOGs250m) for curve Number-Based Runoff Modeling. <https://doi.org/10.3334/ORNLDAAAC/1566>. Accessed 09 May 2018
26. Global Hydrologic Soil groups (HYSOGs250m) for curve Number-Based Runoff Modeling (Get Data). https://daac.ornl.gov/SOILS/guides/Global_Hydrologic_Soil_Group.html. Accessed 12 May 2018



Comparison of Rice Phenology from MODIS and Ground Image Data in Sakaeo Province, Thailand

Wannaphorn Srichupieam^{1(✉)}, Narut Soontranon^{2(✉)},
and Sutatip Chavanavesskul^{3(✉)}

¹ Master's Program, Department of Geography, Faculty of Social Sciences,
Srinakharinwirot University, Bangkok, Thailand
wannaphorn.bb@gmail.com

² Dev Drone Mapper Co., Ltd., Chon Buri, Thailand
narut.soo@gmail.com

³ Department of Geography, Faculty of Social Sciences,
Srinakharinwirot University, Bangkok, Thailand
such2305@gmail.com

Abstract. This paper presents a study of vegetation phenology, which is used to monitor the state of rice fields. A well-known parameter, Normalized Difference Vegetation Index (NDVI) was created and based on the phenology of satellite images using Moderate Resolution Imaging Spectroradiometer (MODIS). Another parameter, Excessive Green Index (ExG), is also utilized to obtain the phenology from the field camera using visible range images. This study compares two phenological graphs. The results found a significant correlation between two phenology graphs on four observed rice fields. It should be noted that the field data was used as a validation data because it is a type of near field acquisition (high resolution, without atmospheric interference). In comparison to the field data, the results showed that the phenology obtained from MODIS was also used to analyze and estimate the different states of a rice field (e.g. seeding, heading and harvesting). Given the MODIS data in a wide area, we can monitor the status of several rice fields. It can be useful in terms of agricultural management (e.g. planning, demands, supplies and an environmental purpose, the campaign to reduce rice stubble burning).

Keywords: Phenology · Normalized Difference Vegetation Index · Excessive Green

1 Introduction

The Sakaeo province is located in the east of Thailand. It is a special economic zone between Thailand and Cambodia border which produces many agricultural products. With regard to rice products [1], the cultivation area has decreased since 2013 due to price decreases in the market. It results in rice farmers changing their agricultural activity from rice to other crops. Rice is one of the major economic crops of Sakaeo. It is an evident that rice is important to the Sakaeo province in terms of the export industry.

According to the recent geographic technology, remote sensing and its applications can be used to develop the rice monitoring process. Using the satellite data, it was easy to observe rice fields in a large area. The study aimed to create and compare two phenological graphs of rice fields, obtained from MODIS (Terra) and field data taken with a digital camera, respectively. Firstly, using the satellite data, we compute the phenology by using Normalized Difference Vegetation Index (NDVI). Secondly, using the field data, we obtain the phenology using Excessive Green Index (ExG). It should be noted that the field data will be used for the purpose of validation. The results may provide a correlation value between two phenological graphs (the satellite and field data). Based on the phenology, the results of the analysis showed that we can also determine the state of the rice field (e.g. cultivation, non-cultivation, seeding and harvesting). This study can be a part of precision farming in the future. It will be used for planning, demands, supplies and estimating yield, planting, the crop calendar, etc.

In this study, we are motivated to initially develop a model for monitoring rice fields in the Sakaeo province. The developed model will be used to support local farmers in the near future.

2 Technical Background

In this section, we provide technical background presented in three parts related to this work, vegetation index, phenology, and data acquisition.

2.1 Related Work

The satellite data used for agricultural application and referred to as MODIS used for monitoring agriculture activities. A predictive model was used to compute planting schedules based on a wavelet as a filtering approach. The results provided the information, which determined factors such as planting date, heading date, harvesting date and growing period [2]. MODIS is a type of time series data, it is required a pre-processing method in order to deal with noise (atmospheric and other). The paper [3] proposed a curve fitting technique used for MODIS's NDVI. The curve fitting technique was used to minimize the noise from atmospheric and sensor effects. Another analysis of time-series data obtained from MODIS [4] showed that Vegetation Index (VI) of MODIS could be used to analyze for a large area. An objective was to improve Land Use/Land Cover (LULC) crop classification in the Central Great Plains of the U. S. [5] studied on an automatic acquisition system used to obtain weather and field data. Using the automatic acquisition system, the data was obtained close to real time.

2.2 Vegetation Index and Phenology

The vegetation index is a parameter used to monitor level of green plants. One of the popular vegetation index is referred to NDVI and applied in several works [6]. In general, NDVI is required both near-infrared and red bands for computation. Referring

to the MODIS data used in our study, Mod 13 A1.005 Resolution 500 m [7] provided NDVI computation. It can be used to create phenology relying on the cultivation time in the observed rice fields. It should be noted that NDVI obtained from MODIS was normalized to a value between -1 (lowest) and 1 (highest). In terms of the field data, the images are acquired from a digital camera which generally provide red, green and blue bands. Using visible range images, another vegetation index used in this study, known as ExG (Excessive Green). ExG computed each image by selecting rice fields as a Region of Interest (ROI). In order to compare with the satellite data, ExG will also be normalized to a value between -1 and 1 .

ExG was computed as follows:

$$\text{ExG} = 2g - r - b \quad (1)$$

Where

ExG = Excessive Green (For the ExG value, a high value means high level of green plants).

$r = R/(R+G+B)$ Normalized composition of the red band.

$g = G/(R+G+B)$ Normalized composition of the green band.

$b = B/(R+G+B)$ Normalized composition of the blue band.

2.3 Data Acquisition

To observe four rice fields in Sakaeo province, the data used in this study can be separated into two aspects, satellite and field data. MODIS (Terra) Vegetation Indices Mod 13 A1.005 Resolution 500 m [8]. The product provided satellite data composition for 16 consecutive days. The specific WRS-2 paths and rows NDVI was selected and used as the vegetation index to create the phenology. The observation period was from April 2017 to November 2017.

Study area: There were four rice fields in Sakaeo Province which were studied as seen in Table 1 and Fig. 1.

Table 1. Coordinates of study area

Rice field	Sub-district	Coordinates
1	Tapraya	264426, 1548699
2	Tuprach	264456, 1548726
3	Tuprach	264472, 1548746
4	Tuprach	264344, 1548663

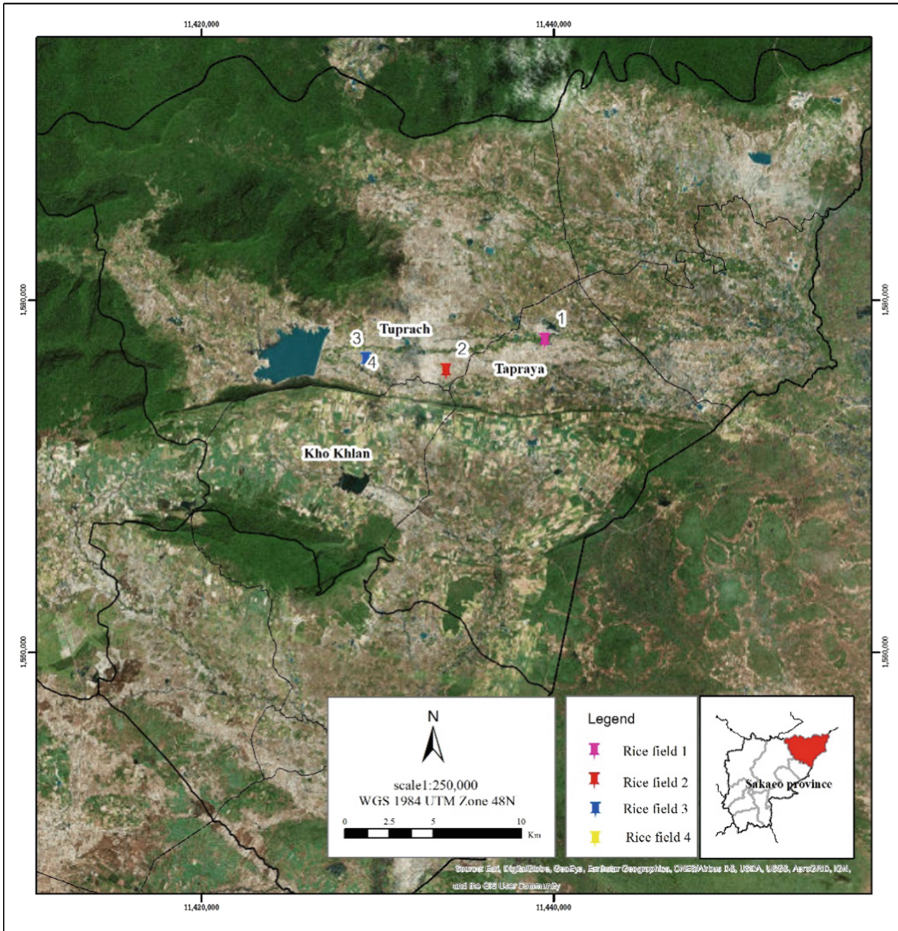


Fig. 1. Study area

Field data: The images are captured by field staff every 16 days. A digital camera (Nikon, D3100) is used to collect the images. The observation period is started from April 2017 to November 2017 as shown seeding, heading, harvesting in Fig. 2.

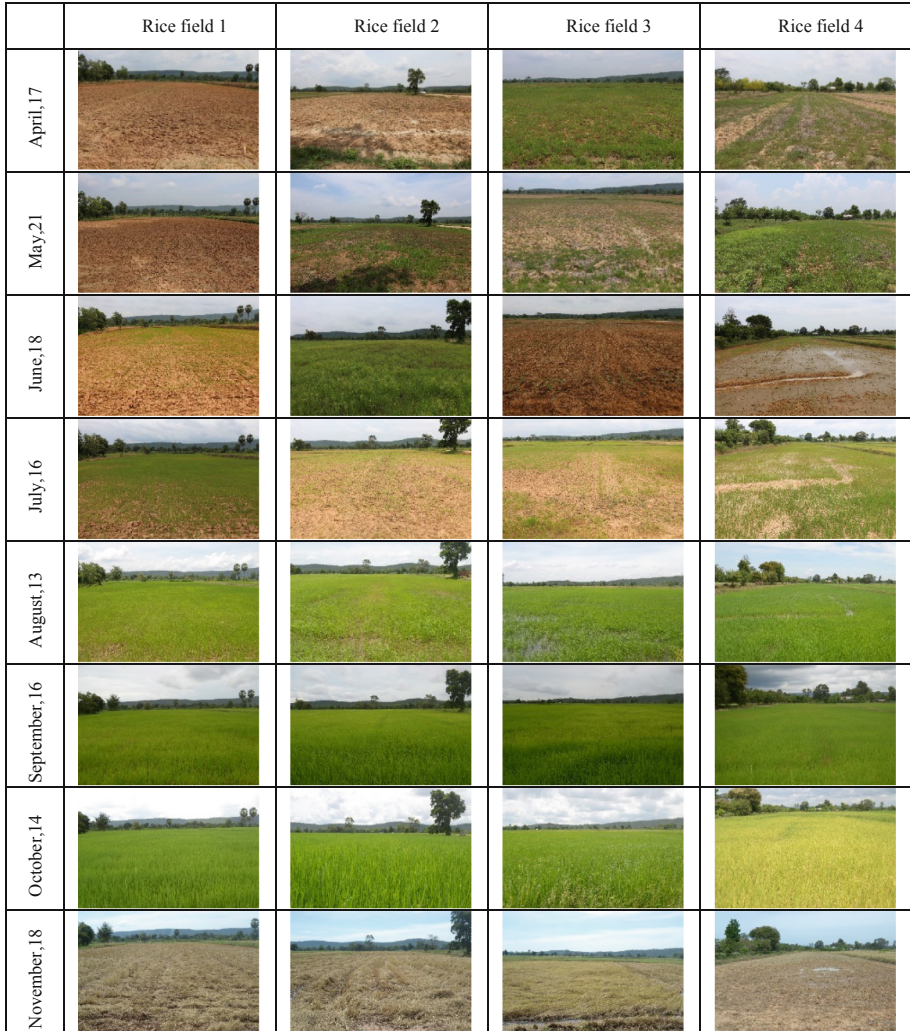


Fig. 2. The field images were obtained from the digital camera in four rice fields.

3 Methodology

An overview diagram is presented in Fig. 3, which can be separated into two parts: field collection and MODIS data. To select appropriate rice fields, the prior information was pre-analyzed, such as estimated area, existing cultivation and location. The estimated area should be larger than MODIS spatial resolution (500 m). The locations should be distributed in the study area with less bias. The field staff collected data approximately every 16 days during the cultivation period. The field images were used to compute the vegetation index and phenology. It should be noted that Excessive Green (ExG) can be calculated from RGB images. To obtain MODIS data, the selected

product is MOD13 A1.005 at 500 m resolution. The similar location (latitude and longitude) collected from the rice field and used to identify the right pixel for analysis. The selected MODIS product provides NDVI and its quality depending on the acquisition day (good, moderate or bad). The NDVI quality was excluded for the purpose of phenology computation. In order to compare the two phenological graphs (field and MODIS), a filtering process is required to obtain smooth curves.

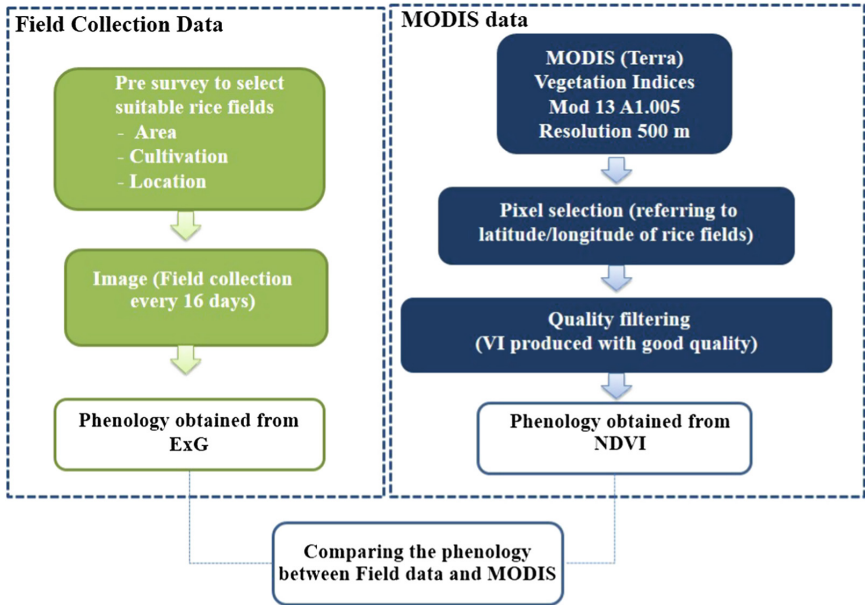


Fig. 3. An overview diagram of phenology comparison between field and MODIS data.

4 Experiments

Given the data from the rice field, two phenological graphs were created and compared. The first phenology created from MODIS, NDVI was computed for each time series image. It was noted that MODIS products used in our analysis had 500 m for spatial resolution and 16 days for temporal resolution. To obtain the phenology of a rice cycle (140–177 days), Vegetation Index images of MODIS were required. The second data was created by digital camera and the ExG was computed for each rice field image when RoI was preliminarily selected (rice area) as show in Fig. 4(a, b, c and d). The filed image provides higher spatial resolution compared with MODIS. In a crop cycle, time series images were acquired every 16 days at midday by the field staff. With regard to the MODIS data, it provided quality in terms of acquisition (good, moderate and bad). The best quality information was used to compute the phenology. For the filed data, better quality images were processed. Then, the linear interpolation was applied and presented the phenological graphs on the Day of Year axis (DoY).

The results are compared in Fig. 4(a, b, c and d). Graph phenology of rice with Normalized Difference Vegetation Index (NDVI) and Excessive Green Index (ExG) in the province.

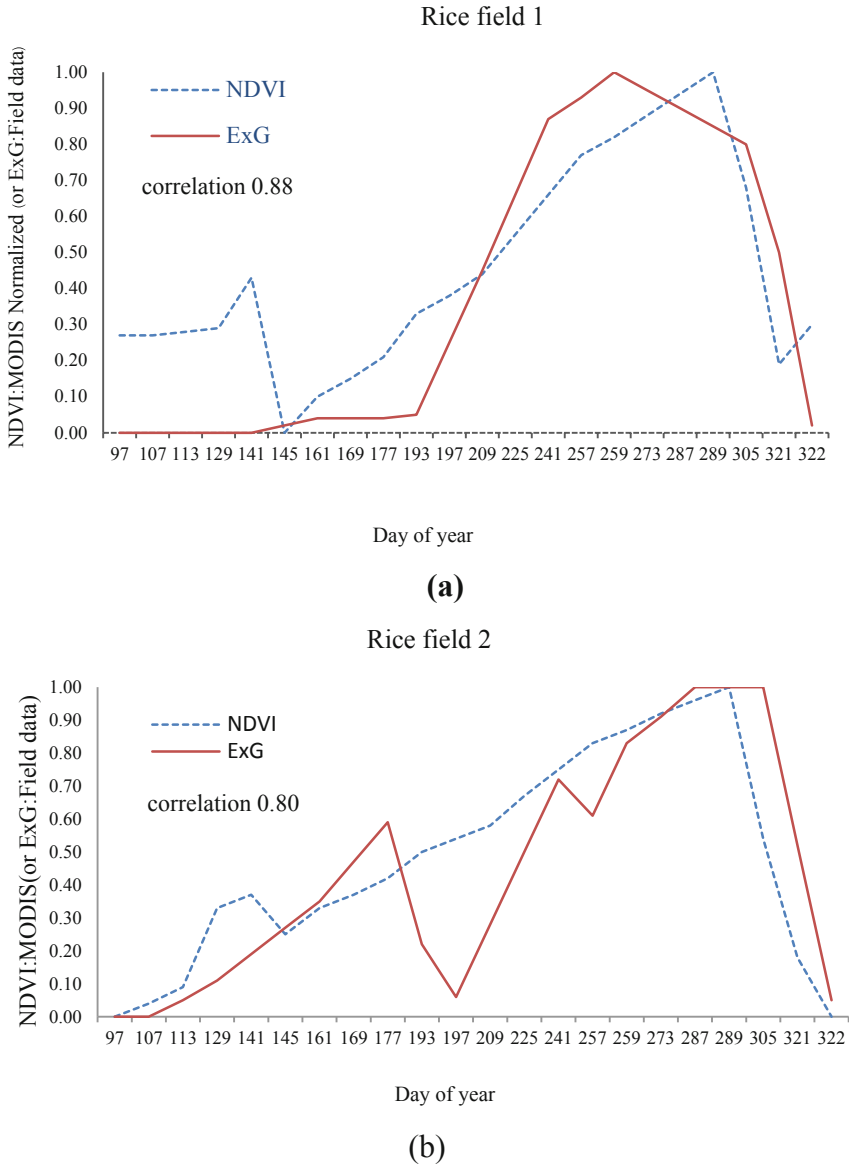
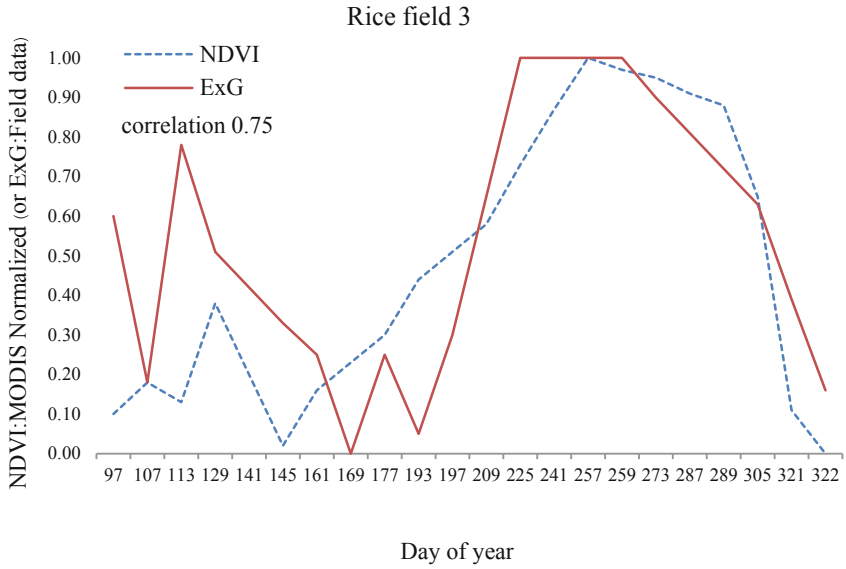
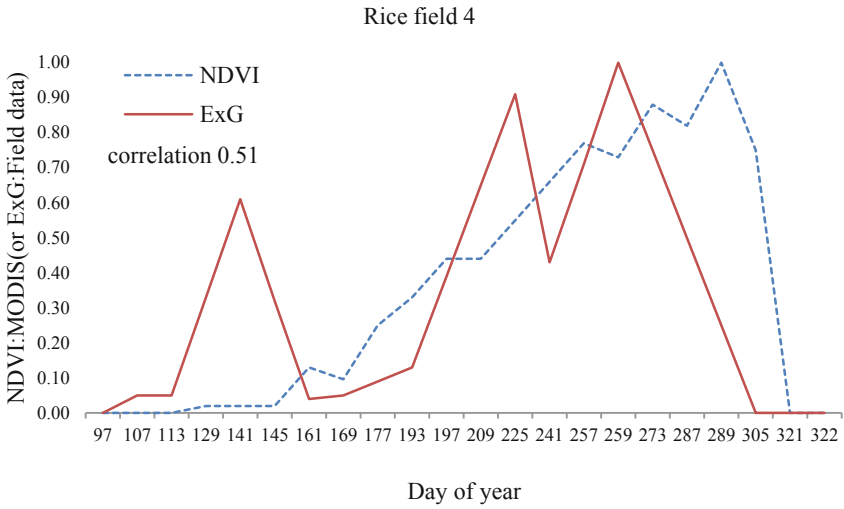


Fig. 4. Four graphs (a–d) show the phenology of the rice fields obtained from MODIS and field data.



(c)



(d)

Fig. 4. (continued)

Table 2. Correlation between MODIS and field data computed from four rice fields in the study area.

Rice field	Correlation score	Correlation level
1	0.88	High
2	0.80	High
3	0.75	High
4	0.51	Moderate

We obtained the high correlation level on 3 rice fields (Rice fields 1–3), which presented a high confidence in using MODIS to monitor the rice fields. Rice field 4 provided moderate correlation levels due to variations of the light on the acquisition day (cloudy). However, the phenology pattern was still efficient enough to represent significant rice stages, for example, the start, middle and the end of cultivation (Table 2).

5 Conclusions

In this study, the comparative results between two phenological graphs were presented. The data was obtained from a satellite (MODIS) and a field survey, respectively. The approach was to pre-process the data before comparison. For the satellite, those of good quality and from the MODIS NDVI were selected. For the field data, good quality images were obtained during the field survey. Each image was computed for ExG (Excessive Green). Then, the linear interpolation was used to obtain phenological graphs. The results showed that there is a significant correlation between MODIS and field data. MODIS can provide the necessary information to monitor rice fields.

In the future, we can use this strategy for the whole province. The results will be more useful in terms of planning (demands and supplies), planting (crop calendar), estimating the yield and the environment (a campaign to reduce rice stubble burning) (Fig. 5 and Table 3).

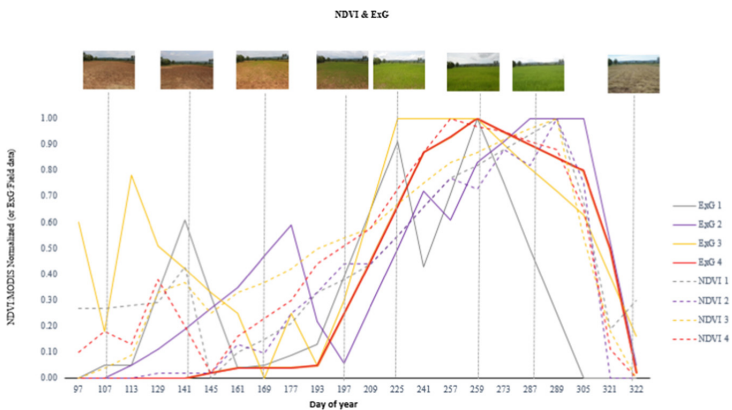
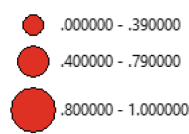
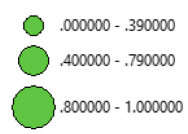










Fig. 5. Graphs of four rice fields

Table 3. NDVI MODIS data and ExG filed data from four rice fields.

NDVI	ExG
<p data-bbox="294 282 458 308">INDEX NDVI</p> 	<p data-bbox="717 282 882 308">INDEX ExG</p> 
	
	
	
	

References

1. Industrial Estate Authority of Thailand, 3 December 1995. <http://www.dit.go.th/region/SA%20KAE0/Content?id=1712>. Accessed 5 Jan 2016
2. Toshihiro, S., Masayuki, Y., et al.: A crop phenology detection method using time-series MODIS data. *Remote Sens. Environ.* **96**(3), 366–374 (2005). sciencedirect

3. Bethany, A.B., Robert, W.J., et al.: A curve fitting procedure to derive inter-annual phenologies from time series of noisy satellite NDVI data. *Remote Sens. Environ.* **106**(2), 137–145 (2007). Science Direct
4. Brian, D.W., Stephen, L.E., Jude, H.K.: Analysis of time-series MODIS 250 m vegetation index data for crop classification in the U.S. Central Great Plains. *Remote Sens. Environ.* **108** (3), 290–310 (2007)
5. Gistda (2016). <http://www.gistda.or.th/main/th/node/948>. Accessed 5 Jan 2016
6. USGS Earth Resources and Observation Science. <https://dx.doi.org/10.3133/fs20143052>. Accessed 5 Jan 2016
7. Narut, S., Panu, S., Preesan, R.: Rice growing stage monitoring in small-scale region using ExG vegetation index. In: 2014 11th International Conference on Electrical Engineering/Electronics, Computer, Telecommunications and Information Technology (ECTI-CON), Nakhon Ratchasima, Thailand. IEEE (2014)
8. Huete, A., Justice, C., van Leeuwen, W.: MODIS Vegetation Index (MOD13) Algorithm Theoretical Basis Document, Version 3. University of Arizona, Tucson, University of Virginia Department of Environmental Sciences, Charlottesville (1999)



Application of Geographic Information System to Predict Land Use Change for Maximum Flow Rate Calculation

Yutthana Chaona¹(✉), Teerawate Limkomonvilas²,
and Sathaporn Monprapussorn²

¹ Department of Highways, Bureau of Location and Design, Bangkok, Thailand
yutthana.2519@hotmail.com

² Department of Geography, Faculty of Social Sciences, Srinakharinwirot
University, Bangkok, Thailand

Abstract. Floods causes enormous loss of human life and damage to human properties. The main causes of floods are heavy rainfall, deforestation, river bank disturbance. The purpose of this study is to apply Geographic Information System and CA-Markov to predict of land-use changes and enlarge of the catchment area in Sattahip, Chonburi, Thailand. Geographical factors were analyzed to calculate a maximum flow rate by Rational Method. It found that four land use types including urban area, forest, agriculture, and miscellaneous area increase maximum flow rate continuously (193.41, 194.68, 200.19, 195.95 and 204.01 cubic meters per second). Moreover, it can help to design a drainage system to support and prevent flood in the future.

Keywords: Geographic Information System · Land use change · CA-Markov · Rational Method · Catchment area · Maximum flow rate

1 Introduction

The problems of flood and drainage system have significant impact on life and property. The cause of this problem comes from many factors such as heavy rainfall, deforestation and invasion of river or canal by human. Proper design of the roadway should consider maximum flow rate (MFR) which consisted of amount of water, period of time and land use change. Therefore, improper design of the roadway might be one of the main reasons behind flooding, leading to damage to life and property [1]. Nowadays, climate and land use are rapidly changed by human activities. The land use is one of the crucial factors to derive MFR value. The accurate classification and prediction of future land use are very important to estimate water quantity in order to properly design reliable drainage system that prevents flooding in a future. Geo-Informatics technology can be used to predict land use trend. Land use change could be projected by finding the suitable land use proportion and allocation [2]. The remote sensing is the effective tool for classifying land use because of its handling capacity of multi-temporal data. User can classify and predict land use change with various models integrated into Geographic Information System (GIS) [3, 4]. CA-Markov model is one

of the land use modelling methods which appeared in previous researches [5, 6]. GIS can accurately define catchment area, including capable of integrating other factors to calculate MFR using Rational method (catchment area less than 25 km²).

Sattahip, Chonburi province, Thailand is raised as a case study. Socioeconomic status for Sattahip area is rapidly growth in term of population, tourist and industrial increase.

As a result, the increase in tourists and labors would be evidence [7]. It is characterized by a proportion of land use change in the last few decades. Drainage problem and flooding are often occurred in this area, and the size of catchment area is less than 25 km². Therefore, this area is very suitable to apply MFR method using Rational method in this study.

The study objectives are to predict future land use change calculate the maximum flow rate and to compare the maximum flow rate in which land uses were obtained by satellite image classification and CA-Markov model. Geographic Information System (GIS) and Remote Sensing (RS) technology will also be used to interpreted and classified satellite imagery data [8, 9]. Land use was classified by supervised classification method and Maximum likelihood classifier decision rule [10, 11]. Accuracy of data was validated by Error matrix [2, 12]. Hence, GIS-RS integrated with the CA-Markov model can capable of projecting trend of land use changes [13, 14]. Geographic Information System was used to prepare spatial data and to analyze catchment areas with other related factors such as slope, soil group, rainfall, altitude, length of river to find out the Runoff coefficient (C), Rainfall intensity (I). The Rational Method was applied to calculate the maximum flow rate in the case of catchment area less than 25 km² [15, 16].

2 Method

2.1 Area Study

The study area locate at Sattahip, Chonburi, Thailand. From topographic map, the L7018 is 5134 II. The upper left corner is 705000 mE, 140500 mN and the lower right corner is 709000 mE, 1401000 mN., shows area 9.84 km². The north area side is parallel with Khao Klet Chalam and Ban Soi Methro. South and west area side parallel to Highway No. 3. East area side parallel with Khao Mon and Khao Sattahip as shown in Fig. 1. Chonburi is under the influence of the monsoon. Two types of seasonal storms come from the northeast monsoon. In the winter, October to February. From above, province are cool and moderate wind wave with the southwest monsoon that prevails in the rainy season from May to October. The average annual temperature of Chonburi is 28.50 °C. The highest temperature is 33.30 °C. The lowest is 24.80 °C [17].

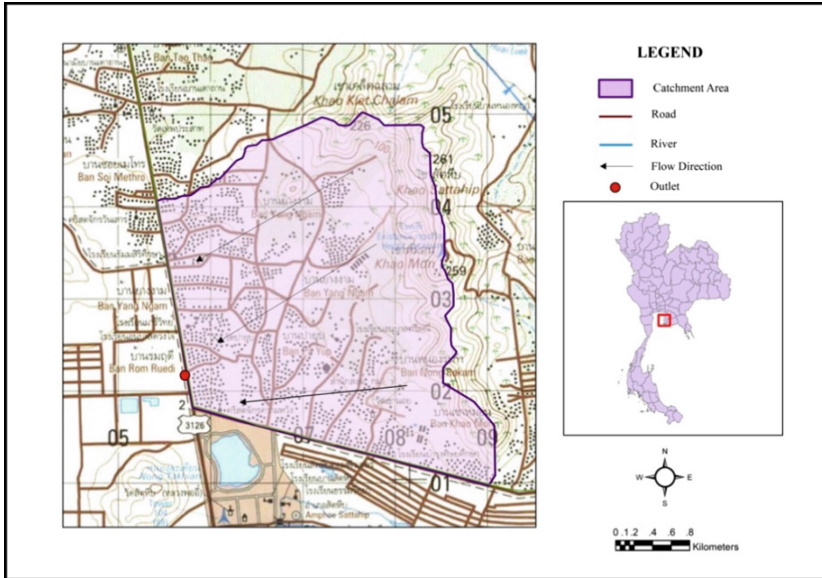


Fig. 1. Study area

2.2 Data Collection and Analysis Method

Data was collected from many government agencies. The details of the data were primary data which included actual data from field surveys such as the location of the rain gauge station. Several secondary data were compiled by textbooks, research papers, topographic map, satellite imagery during the same period of time in 2006, 2011 and 2016. Other data include Digital Elevation Model, average rainfall, soil group, road, river and Runoff coefficient (C) data.

2.2.1 Remote Sensing

Remote Sensing technique has been used to interpret and classify satellite imagery data. It used to manage three satellite images. Satellite imagery of LANDSAT 5 TM and LANDSAT8 OLI observation time with clear cloud will be used to obtain a color image suitable for land use classification. Geometric correction has been adjusted by preprocessing to get a correct position based on topographic map and then has been classified by unsupervised method. Ground check method has also been conducted by field survey to ensure image interpretation correctness.

2.2.2 Geographic Information System

Geographic Information System (GIS) has been used to analyze land use change and projection. Satellite imagery data was transformed into vector data and was assigned attribute data such as the type of land use. Land use change is categorized into three periods; 2006–2011, 2011–2016 and 2006–2016. The land use was analyzed and compared to find out the relationship between each land use type.

2.2.3 CA-Markov Model

CA-Markov is a combined of Cellular Automata and Markov Change landcover prediction procedure that adds an element of spatial contiguity as well as knowledge of spatial distribution of transitions to Markov change analysis [4]. The pattern of changes in each cell and the transition areas were analyzed by Markov process with CA filter of contiguous environment. The CA-Markov data analysis process utilizes the opportunity data of the Markov Chain and CA filter to determine the probability of the cover type at the time of study [18], The result from analysis by CA-Markov model is map of the land cover unchanged areas and areas which land cover changes. Next, Predict trend of land use change with CA-Markov model in Sattahip, Chonburi by determine the probability matrix and the proportion of land use change. By two land use data analysis (2006 and 2011), It can be found the proportion of land use change can construct model for predict land use change (2016) and use data in 2006 and 2016 to predict land use change in 2026, so we can forecast each area and analyze land use change.

2.2.4 Validation of the CA-Markov Model

Accuracy of data from satellite image interpretation is validated by using error matrix to compare with field survey data, deriving user and overall accuracy [19]. Projected land use map in 2016 from CA-Markov model was then overlay with 2016 land use map derived from the classification of satellite data to compare the accuracy of the model by using the error matrix as shown in Table 1 and Eq. 1 [20]. Land use in 2006, 2011, 2016 and 2026 will be analyzed and compared to show the distribution of land use and change processes.

$$Overall\ Accuracy = \frac{\sum_{i=1}^k n_{ii}}{n} \tag{1}$$

When i is row, j is the column, n_{ij} is the row at column i at i, n_{jj} is the row at column j at j, n is the sum total.

Table 1. Comparison two land use by Error Matrix (Congalton and Green, 1999)

Classified data (i = Rows)	Reference data (j = Columns)			
	1	2	k	Row total (n ₁₊)
1	n ₁₁	n ₁₂	n _{1k}	n ₁₊
2	n ₂₁	n ₂₂	n _{2k}	n ₂₊
K	n _{k1}	n _{k2}	n _{kk}	n _{k+}
Column total (n ₁₊)	n ₊₁	n ₊₂	n _{+k}	N

2.2.5 Maximum Flow Rate by Rational Method

The Rational Method is widely used in many literatures. Many agencies/departments/divisions in Thailand, applied this method in their routine works, especially for catchment

area less than 25 km². The calculation of maximum flow rate by rational method is shown in Eq. 2.

$$Q = 0.278CIA \tag{2}$$

When Q is the maximum flow rate of water at the required point in m³/s., C is Runoff Coefficient., I is Rainfall Intensity in mm./h and A is catchment area in km².

Digital Elevation Model (DEM) are created to define boundary and size of the catchment area by using GIS. Runoff coefficient (C) is derived from the land use and soil group. Details of soil group is shown as the following;

Soil group A: high permeability, well drainage, sand and gravel.

Soil group B: moderate permeability, medium to well drainage, fine to medium sand.

Soil group C: low permeability, poor drainage, clayey sand to fine sand.

Soil group D: very slow permeability when wet, very poor drainage, clay.

The slope is set to 0–2%, 2–6% and more than 6% as shown in Table 2.

Table 2. Runoff coefficient value (Ward and Elliot, 1995)

Land use	Soil group and Slope (%)											
	A			B			C			D		
	0–2	2–6	>6	0–2	2–6	>6	0–2	2–6	>6	0–2	2–6	>6
U ^a	0.58	0.60	0.61	0.59	0.61	0.64	0.60	0.62	0.66	0.62	0.64	0.69
Ag	0.14	0.18	0.22	0.16	0.21	0.28	0.20	0.25	0.34	0.24	0.29	0.41
F&M	0.11	0.16	0.20	0.14	0.19	0.26	0.18	0.23	0.32	0.22	0.27	0.39

^aU is Urban area, Ag is Agriculture area, F&M are Forest and Miscellaneous area

Runoff coefficient (C) values in each catchment are different, depending on proportion of land use types and soil characteristics. Catchment area is divided into several sub-catchments and total runoff coefficient value of catchment has derived from the average runoff coefficient value of the sub-area as shown in Eq. 3

$$C = \frac{\sum_{i=1}^n C_i A_i}{A_{Total}} \tag{3}$$

When C_i is the Runoff coefficient for each sub-catchment, A_i is area of each sub-catchment, T_{Total} is total area of all sub-catchment, n is number of sub-catchment.

Rainfall intensity (I) (millimeters/hour) of study area is calculated by using the time of concentration (T_c) or the time of water flow (hours) derived from rainfall intensity graph as shown in Fig. 2. The graph shows relationship between rainfall intensity and time of concentration, which generated by the analysis of rainfall frequency. Time of Concentration (T_c) is calculated from Eq. 4 as shown below.

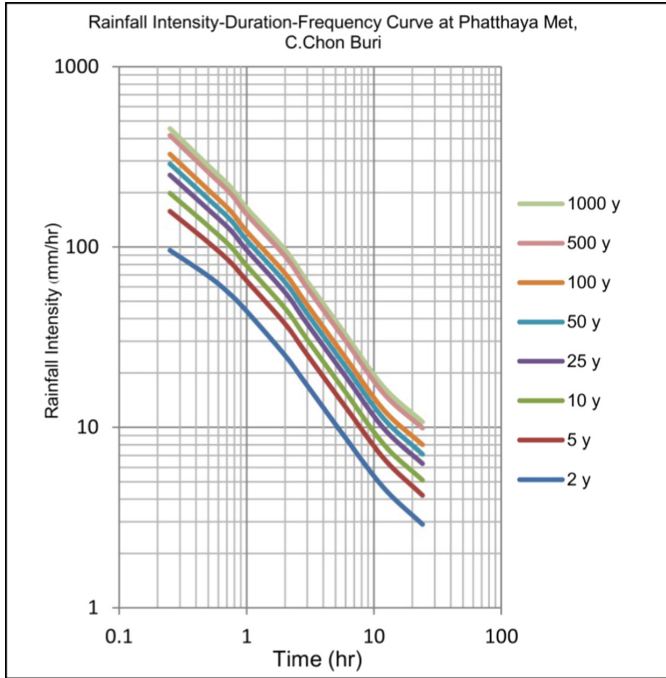


Fig. 2. Rainfall Intensity-duration-frequency curve

$$T_c = \left[\frac{0.87L^3}{H} \right]^{0.385} \quad (4)$$

When T_c is time of concentration in hours, L is length (kilometers) along the main river from the farthest point on the watershed to point of interest in building drainage infrastructure, H is the different between the ground level.

3 Result

This study aims to apply Geographic Information System (GIS) in combination with Remote Sensing (RS) and CA-Markov model to analyze and predict land use change in order to calculate maximum flow rate by using Rational Method for estimating peak flow.

3.1 Study Area

Area of study is located in Sattahip, Chonburi province. It covers an area of 9.84 km², with a maximum height of 261 m and a minimum height of 2 m.

3.2 Land Use

The classification of LANDSAT 5, TM and LANDSAT 8 satellite imagery in 2006, 2011, and 2016 were classified to four types of land use; urban, agriculture, forest and miscellaneous land. The largest proportion of land use from 2006–2011 is urban, forest, agriculture and miscellaneous respectively as shown in Table 3 and Fig. 3.

Table 3. Proportion of land use between 2006–2016

Land use	2006	%	2011	%	2016	%
	(km ²)		(km ²)		(km ²)	
Urban land	5.856	59.49	5.938	60.33	6.243	63.43
Forest	2.354	23.92	2.272	23.08	2.534	25.74
Agriculture	1.335	13.56	1.065	10.82	0.557	5.66
Miscellaneous area	0.298	3.03	0.568	5.77	5.170	5.17
Total	9.843	100.00	9.843	100.00	9.843	100.00

3.3 Land Use Changes

In regard to land use changes during 2006–2011, the urban land has increased by 0.082 km² (1.40%). A rapid expansion was located in the northern of the study area. Forest land has decreased by 0.082 km² (3.48%) which forest land in the north have been transformed into urban land. Agricultural area has decreased by 0.27 km² (20.22%) and miscellaneous area has increased by 0.27 km² (90.60%). Miscellaneous land tends to be changed from agriculture land in the northern and middle parts of study area.

For land use changes between 2011–2016, the urban land area has increased by 0.305 km² (5.136%), especially in the north and middle parts of Sattahip. Forest area has increased by 0.262 km² (11.532%), especially in the southern part of the Sattahip. Agricultural area has reduced by 0.508 km² (47.699%), notably in the middle part of Sattahip. Miscellaneous area has reduced by 0.059 km² (10.387%) which most land in the middle part have been transformed to urban area.

For land use changes between 2006–2016, urban land has increased by 0.387 km² (6.608%) which can be observed at the upper and middle parts of study area. Forest area has increased by 0.180 km² (7.646%), especially in southern part of study area. Agricultural area has reduced by 0.778 km² (58.277%) which is notably in the middle part, mostly transforming into urban and miscellaneous land. Miscellaneous area has increased by 0.211 km² (70.805%). Miscellaneous land tends to be changed from agriculture land in the northern and middle parts of study area.

Comparison of land area from CA-Markov model and satellite image interpretation in 2016 for 4 types of land use: urban, forest, agriculture and miscellaneous land were 3.860%, 12.075%, 79.892% and 20.0395% difference respectively as shown in Table 4.

Table 4. Comparison of area from CA-Markov model and image interpretation in 2016

Land use	Area of Land use (km ²)		Different (km ²)	%
	Image	Model		
Urban	6.234	6.002	0.241	3.860
Forest	2.534	2.228	0.306	12.075
Agriculture	0.557	1.002	0.445	79.892
Miscellaneous	0.509	0.611	0.102	20.039

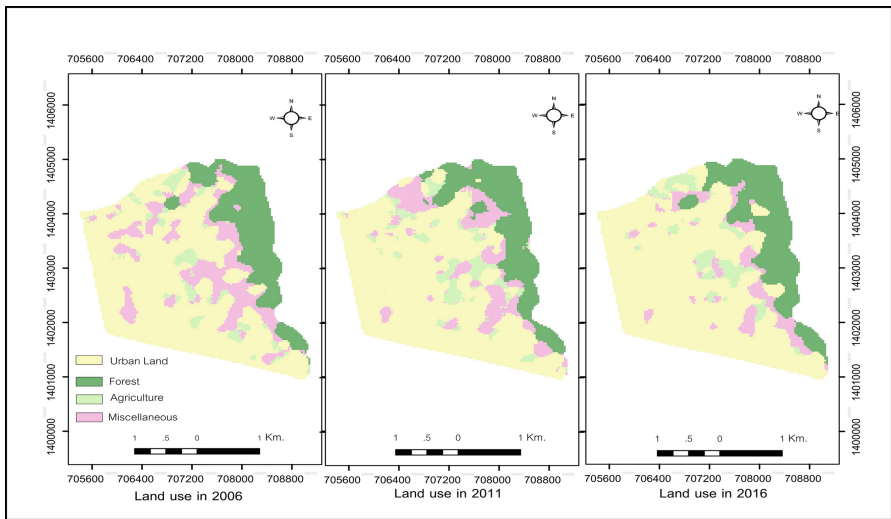


Fig. 3. A comparison of land use in 2006, 2011 and 2016

3.4 Model Validation

Validation of the land use between the data obtained from the image interpretation of 2016 and CA-Markov model is done through error matrix. Overall accuracy value is 79.37% as shown in Table 5.

Table 5. Result of 2016 land use validation

Land use	Forest	Miscellaneous area	Agriculture	Urban land	Total
Forest	0.2107	0.0036	0.0018	0.0106	0.2268
Miscellaneous area	0.0023	0.0098	0.0056	0.0461	0.0638
Agriculture	0.0303	0.0119	0.0292	0.0309	0.1022
Urban land	0.0134	0.0286	0.0212	0.5440	0.6072
Total	0.2567	0.0539	0.0578	0.6316	1.0000

Overall Accuracy = $((0.2107 + 0.0098 + 0.0292 + 0.5440) \div 1.0000) \times 100 = 79.37\%$.

3.5 Land Use Prediction in 2026

CA-Markov model can be used to predict land use in 2026. Result shown that urban land shared the largest land of 6.46 km² (65.58%), followed by forest area by 2.55 km² (25.85%), miscellaneous area by 0.44 km² (4.46%), and agricultural area by 0.41 km² (4.11%) respectively as shown in Fig. 4.

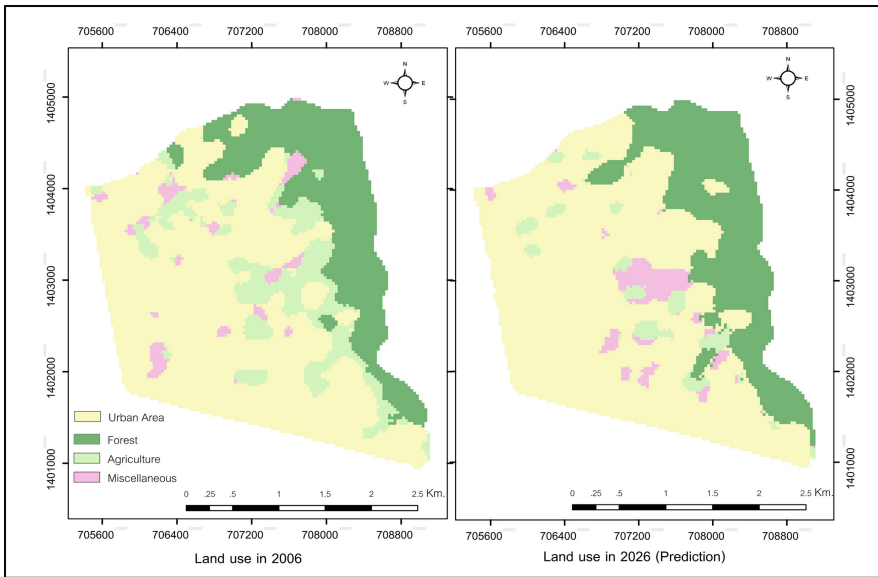


Fig. 4. Comparison land use between 2006 and 2026

3.6 Maximum Flow Rate Analysis

3.6.1 Runoff Coefficient

Deriving runoff coefficient requires several geographical factors such as land use data, slope, and soil data. Land use has been categorized into 4 types; urban, forest, miscellaneous, and agriculture. Slope data can be derived from digital elevation model (DEM). There are 3 levels of slope: slope < 2%, slope 2–6% and slope > 6%. Soil data is classified by loam and sandy loam.

3.6.2 Rainfall Intensity

Digital Elevation Model (DEM) were used to find out the highest and lowest elevation of study area. The highest area is 261 m and the lowest area is 2 m above mean sea level. The difference height is 259 m and the longest river length is 4 km. Total time of water flow (Tc) is 0.55 h, derived by graph of the meteorological stations nearby the study area. Rainfall intensity (I) for 25-year return period is 155 mm per hour.

3.7 Maximum Flow Rate

The maximum flow rate values calculated by using Rational Method in 2006, 2011 and 2016 is 193.405 m³/s, 194.677 m³/s and 200.191 m³/s respectively. While maximum flow rate values regarding to land use modeled by CA Markov in 2016 and 2026 are 195.950 m³/s and 204.008 m³/s respectively. Table 6 and Fig. 5 shows the result of projected maximum flow rate. In 2026, the maximum flow rate is 204.008 m³/s in comparison to 2006, it has increased by 5.197%. While maximum flow rate in 2016 compared to 2006 has increased by 3.389% (6.786 m³/s) and maximum flow rate in 2016 derived by CA Markov model compared with 2006 has increased by 1.298% (2.545 m³/s).

Table 6. Results of maximum flow rate

Year	Coefficient of runoff (C)	Rainfall intensity (I)	Area (km ²)	Maximum flow rate (m ³ /s)
2006	0.456	155	9.843	193.405
2011	0.459	155	9.843	194.677
2016	0.472	155	9.843	200.191
2016 (Model)	0.462	155	9.843	195.950
2026 (Model)	0.481	155	9.843	204.008

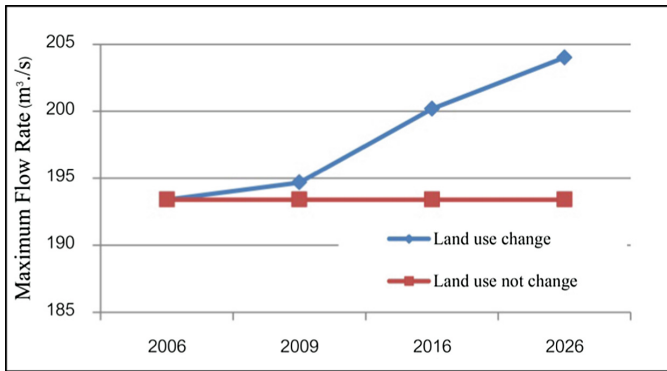


Fig. 5. Comparison maximum flow rate between 2006–2026

4 Discussion

Land use change in Sattahip between 2006–2016 has showed the increasing trend in urban, forests, and miscellaneous land by 0.387, 0.180 and 0.211 km² respectively. While agricultural area has decreased by 0.778 km². The major reason behind shrinking of agriculture land is population growth. Agricultural land tends to be transformed into urban and miscellaneous land. Government agencies attempted to promote reforestation campaign which led to the increase of forest area in the past

decades. When considering land use in 2026 in comparison with that of 2006, urban area has expanded by 0.541 km², followed by forest area by 0.267 km². However, agricultural and miscellaneous land has decreased by 0.675 km² and 0.133 km² respectively. A pattern shows the increase in urban area and decrease in agricultural land. In this study, land use change analysis considered only physical factor while other factors such as socio-economic did not include in a study.

Analysis of maximum flow rate by using digital elevation model, the boundary of catchment area is very useful in term of increasing accuracy and shortening time. Runoff Coefficient (C) could also be useful in defining maximum flow rate. Nonetheless, runoff coefficient (C) can be more accurate if can access to perfect information of land use, slope and soil. Rainfall Intensity (I) Graphs could also be used to determine the rainfall intensity by obtaining data from meteorological stations nearby area of study. The runoff coefficients (C) for 2006, 2011, 2016, 2016 (projected by CA Markov) and 2026 were 0.456, 0.459, 0.472, 0.462 and 0.481 respectively. The rainfall intensity (I) in the 25th recurrence cycle was 155 mm per hour. The maximum flow rate for 2006, 2011, 2016, 2016 (projected by CA Markov) and 2026, were 193.41, 194.68, 200.19, 195.95 and 204.01 cubic meters per second, respectively. The results of the highest flow gradient analysis and the predicted flow rate of water can be used as a basis data to design suitable drainage system. It helps to reduce the damage to life and property of people in that area and help to achieve cost effective road construction.

5 Conclusion

This study aims to study land use change trends in Sattahip catchment area by integrated Geographic Information Systems with Remote Sensing to interpret and analyze satellite imagery data from LANDSAT 5 TM and LANDSAT8 OLI. The land use during 2006–2016 have been classified by supervised classification and maximum likelihood method, following by Error matrix validation. Land use in 2026 is projected by using CA Markov method in order to gain land use change from 2006. Results revealed that during 2006 to 2011, urban and miscellaneous area tended to be increased while forest and agriculture have decreased, The land use changes during 2011 to 2016, urban and forest area tended to be increased while miscellaneous and agriculture area have decreased. For 2006-2016 land use, urban, forest and miscellaneous area have increased but agriculture land tends to be decreased. When considering land use in 2026 in comparison with 2006, trend of land use change is quite similar to that of 2006-2016. Geographic Information System can be effectively used to analyze catchment and other geographic factors such as slope, soil group, rainfall, altitude, length of river. To find out the Runoff coefficient (C) and Rainfall intensity (I), Rational Method has been applied to get maximum flow rate value when catchment area is less than 25 km². The result reveals that maximum flow rates have gradually increased between 2006–2026. Therefore, integrated GIS with Rsand CA Markov model can be used to explore land use change and project future land use change with more accuracy of maximum flow rate estimation. It could be used in proper road drainage system designing in order to

increase cost-effective construction and reduce impact of flooding on physical and socioeconomic aspects.

References

1. Department of Highways. Design Guide for Drainage and Erosion Protection in Highways. Bureau of Location and Design, Bangkok, Thailand (2010)
2. Orwattana, W.: Prediction of land use change in changwat Phuket. Master's thesis. Graduate school Srinakharinwirot University, Bangkok (2012)
3. Geo-Informatics and Space Technology Development Agency (Public Organization). Space Technology and Geo-Informatics. Amarin Printing & Publishing, Bangkok (2009)
4. Jirakajohnkool, S.: Learn Geographic Information System with ArcGIS Desktop 10.1. Nontaburi: S.R. Printing Massproducts (2013)
5. Verburg, P.H., Soepboer, W., Veldkamp, A., Limpiada, R., Espaldon, M.V., Sharifah, S.A. M.: Modeling the spatial dynamics of regional land use: the CLUE-S model. *Environ. Manage.* **30**(3), 391–405 (2002)
6. Eastman, J.R.: IDRISI Andes Guide to GIS and Image Processing. Clark Labs, Clark University, USA (2006)
7. Chonburi statistical office. Census Statistics/Survey (2016). http://chonburi.old.nso.go.th/nso/project/search/result_by_department.jsp. Accessed 10 Apr 2016
8. Tharapan, S., Anongponyoskun, M., Choochit, L., Doydee, P.: Application of remote sensing and geographic information system on studying of coastal land use some areas in Prachuap Khiri Khan province. Bangkok, The Thailand Research Fund. In: Proceedings of 49th Kasetsart University Annual Conference: Fisheries. pp. 472–477 (2011)
9. Phakularbdang, A.: Prediction Model for Land Use Changes of Krabi Province. Master's thesis. Graduate school Mahidol University, Bangkok (2005)
10. Wongwiset, T.: Prediction Model for Coastal Land Use Change in Ban Lam District, Phetchaburi Province. Master's thesis, Graduate school Kasetsart University, Bangkok (2008)
11. Phamornchantaramast, S., Karnchanasutham, S., Nualchawee, K., Pleerux, N.: Application of Geo information technology to forecast electricity demand: A case study of Chon Buri province. *J. KMUTNB.* **26**(1), 113–120 (2015). (in Thai) (2016). <https://doi.org/10.14416/j.kmutnb.2015.07.005>
12. Limgomonvilas, T.: Predicting the use of Lam Ta Khong River Basin in 2024 with the CA-Markov model. *J. Soc. Sci. Srinakharinwirot University* **17**, pp. 94–113, January–December 2014. <http://ejournalsswu.ac.th/index.php/JOS/article/view/4763/4575>. Accessed 24 Apr 2016
13. Subedi, P., Subedi, K., Thapa, B.: Application of hybrid Cellular Automaton – Markov (CA-Markov) model in land-use change prediction: a case study of saddle creek drainage Basin, Florida. *Appl. Ecol. Environ. Sci.* **1**(6), 126–132 (2013)
14. Syphard, D., Clarke, C., Franklim, J.: Using a cellular automaton model to forecast the effects of urban growth on habitat in southern California. *Ecol. Complex.* **2**, 185–203 (2005)
15. Moskong, H., Jothityangkoon, C.: Analysis of drainage capacity and flood risk areas for integrated urban planning of Sam Khok District, Pathumthani Province. *J. Archit. Planning Res. Stud.* **13**(2), 41–56 (2016)
16. Para, A.: Application of Geoinformatics to Study the Peak Flow Discharge in Watershed Area by Rational Method. Master's thesis, Graduate school Srinakharinwirot University, Bangkok (2014)

17. Meteorological Department. Climate of Chonburi Province (2016). <http://climate.tmd.go.th/data/province/%E0%B8%95%E0%B8%B0%E0%B8%A7%E0%B8%B1%E0%B8%99%E0%B8%AD%E0%B8%AD%E0%B8%81/%E0%B8%A0%E0%B8%B9%E0%B8%A1%E0%B8%B4%E0%B8%AD%E0%B8%B2%E0%B8%81%E0%B8%B2%E0%B8%A8%E0%B8%8A%E0%B8%A5%E0%B8%9A%E0%B8%B8%E0%B8%A3%E0%B8%B5.pdf>. Accessed 10 Apr 2016
18. Sang, L., Zhang, C., Yang, J., Zhu, D., Yun, W.: Simulation of land use spatial pattern of towns and villages based on CA-Markov model. *Math. Comput. Modell.* **54**, 938–943 (2011)
19. Congalton, R.G., Green, K.: A practical look at the sources of confusion in error matrix generation. *Photogram. Eng. Remote Sens.* **59**, 641–644 (1993)
20. Congalton, R.G., Green, K.: *Assessing the Accuracy of Remotely Sensed Data: Principles and Practices*. CRC Press, Boca Raton (1999)
21. Ward, A.D., Elliot, W.J.: *Environmental Hydrology*. CRC Press, Inc., Florida (1995)



A Study of Köppen-Geiger Climate Classification Change in Thailand from 1987–2017

Nutthakarn Phumkokrux^(✉)

Department of Geography, Faculty of Education, Ramkhamhaeng University,
Bangkok, Thailand

ph.nutthakarn@hotmail.com, ph.nutthakarn@ru.ac.th

Abstract. This study aims to update the map of climate classification of Thailand. Although many researches created world climate classification maps by using the Köppen-Geiger's theory, the previous global map cannot provide a lot of detail for each area. The up-to-date Thailand's climate maps are presented and can be used to support the future works. The study was executed by gathering the average monthly temperature data and monthly rainfall data of 99 meteorological stations, which were collected by Thai Meteorological Department and Weather Division of Royal Thai Air Force. Then, the Köppen-Geiger Climate Classification maps of Thailand were created in order to analyse the changes of Thailand's climate over 31 years passed. The maps of this work are quite different from the previous climate classification map by Köppen-Geiger's theory. The result shows that Thailand has climate types of the Equatorial Climates (A). Although the Tropical rainforest climate (Af) was found in some year of this study, the overall of this study can be classified that Thailand has only 2 climate classes which are the Tropical wet and dry or savanna climate (Aw) and the Tropical monsoon climate (Am). These climate classes are occurred because of southwest monsoon and northeast monsoon.

Keywords: Climate change · Köppen climate classification · Thailand

1 Introduction

Climate is essential for life species including human. Moreover, it can determine any soil types and plants which appropriate for specific areas thus, provided that the climate is varied from the past, it can affect to all activities such as agriculture, land use, forest area and ecosystem. Therefore, the study of climate system is greatly necessary. Köppen climate classification was the first quantitative of world climate classification, which was invented in 1884 by the Russian-German geographer Wladimir Köppen (1846–1940). In 1918 and 1936. Then, Rudolf Oskar Robert Williams Geiger (1894–1981), a German meteorologist and climatologist collaborated with Köppen to develop this method to the classification system called the Köppen–Geiger climate classification system, which is widely used [1–4]. This climate formula considers two main points which are monthly temperature and annual precipitation. Classification method is presented in form of two letters. The first letter is written in a capital letter and

demonstrates the main climate. The second letter is labeled in a small letter and defines the subsequent precipitation [5, 6] as shown in Table 1.

Köppen-Geiger climate system of Thailand is considered as Equatorial Climates (A). Moreover, these situations affected to all plants grow up fruitfully thus, this climate system sometime called Tree climate [7]. In the past, the rainfall of Thailand had uneven distribution, therefore the Köppen-Geiger climate system was classified in three types: tropical rainforest climate (Af), tropical monsoon climate (Am) and tropical wet and dry or savanna climate (Aw). The frequently used Köppen climate data of Thailand was proposed by Köppen and Geiger long ago and was out of date. Furthermore, the Köppen method requires the data of monthly temperature and annual precipitation [8]. Although various researchers published update Köppen classifications for the whole world, the published Köppen climate data could not intensively describe the climate of Thailand because of the large scale of maps. In addition, the climate change phenomenon also affect the climate of Thailand. In order to clarify the Köppen climate classification change of Thailand, the climate map needs to be updated.

This work aims to update the Köppen-Geiger climate classification of Thailand. The analyzed data was collected by Thai Meteorological Department and Weather Division of Royal Thai Air Force (RTAF) Thailand from 1987 to 2017. The updated climate maps are illustrated and can be used to support the future works.

2 Köppen-Geiger Climate System of Thailand

Thailand is located at 5°37'N–20°28'N and 97°21'E–105°37'E [9] which has the monthly average temperature higher than 18 °C (64.4 °F) all year and the annual total rainfall is higher than 1,500 mm [10]. The main Köppen-Geiger climate of Thailand is Equatorial Climates (A) [11]. From the previous data as presented in the Fig. 1(A) [12, 13] the Köppen-Geiger climate system of Thailand was classified in 3 types: (1) Tropical rainforest climate (Af) has the monthly rainfall higher than 62 mm. (2.4") for every month (2,000 mm per year). It could be found in some part of east coast of the southern region of Thailand, especially the areas where are located in front of the large mountains such as Nakhon Si Thammarat mountain range and Sankala Khiri mountain range. These areas are affected by southwest monsoon, northeast monsoon and trade wind. (2) Tropical monsoon climate (Am) has annual rainfall higher than Af (1,300–3,750 mm per year) but it has monthly rainfall of the driest month lower than 62 mm. It could be found in some part of west coast of the southern region next to Andaman Sea and some coastal areas of eastern region next to the Gulf of Thailand where are located in front of the mountain range such as Chanthaburi mountain range and Banthat (Cardamom) mountain range. Both of these areas are affected by southwest monsoon. And (3) Tropical wet and dry or savanna climate (Aw) was found in the most area of Thailand such as Northern part, Central part and Northeastern part of

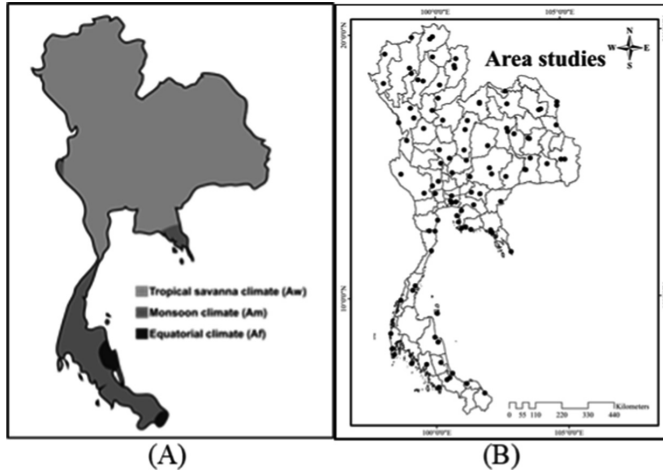


Fig. 1. (A) Previous Thailand climate classification and (B) Area studies of this work

Thailand. It has dry season affected by southern monsoon alternate with dry season affected by northeast monsoon. This climate also has monthly rainfall of the driest month lower than 62 mm (1,011–1,524 mm per year) [6, 7].

3 Materials and Methods

This study used two main types of data which are monthly rainfall data and average monthly temperature data, which were collected by Thai Meteorological Department and compared with the data from Weather Division of Royal Thai Air Force (RTAF) since 1987 to 2017 of 99 meteorological stations all Thailand as shown in the Fig. 1 (B). For the next step, the climate type is classified by consideration of the first and second letters of Köppen-Geiger method. The first letter focuses on the temperature criterion which considers about the average monthly temperature data of the coldest month of each year as demonstrated in the Table 1. The first letter of climate type of Thailand is “A” or Equatorial Climates.

Classification of the second letter of Köppen-Geiger method considers these following steps. Step 1: If the monthly rainfall data of the driest month of each year is higher than 6 cm, the second letter of climate type by Köppen-Geiger method is “f” (Tropical rainforest climate: “Af”). Step 2: If the monthly rainfall data of the driest month of each year is lower than 6 cm, the analyse of climate type by Köppen-Geiger theory can be use Eq. (1) [6]. The result of Eq. (1) can be used to classify that the second letter is “m” (Tropical monsoon climate: “Am”) or “w” (Tropical wet and dry or

savanna climate: “Aw”). If “a” from the equation result is higher than the monthly rainfall of the driest month, the second letter is “w” (Aw). However, if “a” is equal or lower than the monthly rainfall of the driest month, the second letter is “m” (Am) as shown in the Table 1.

$$a = 10 - \left(\frac{r}{25}\right) \tag{1}$$

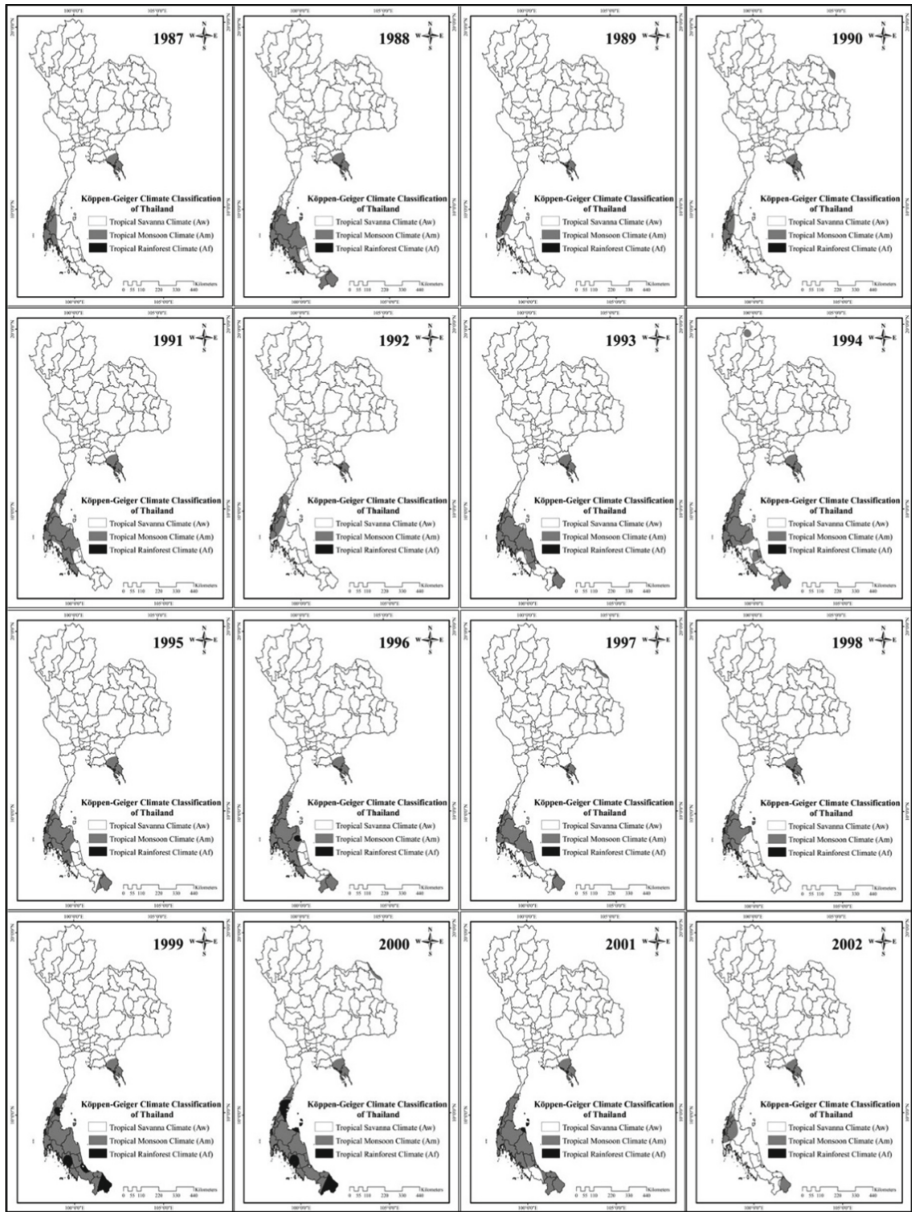
Where “a” is classification criterion between “Am” and “Aw”, and “r” is the total rainfall of each year.

Table 1. Key to classify type of Thailand climate by Köppen method.

Type	Description	Criterion
A	Equatorial climates	Temperature > + 18 °C
Af	Tropical rainforest climate	Monthly rainfall data of the driest month > 6 cm.
Am	Tropical monsoon climate	Monthly rainfall data of the driest month ≥ a
Aw	Tropical wet and dry or savanna climate	Monthly rainfall data of the driest month < a

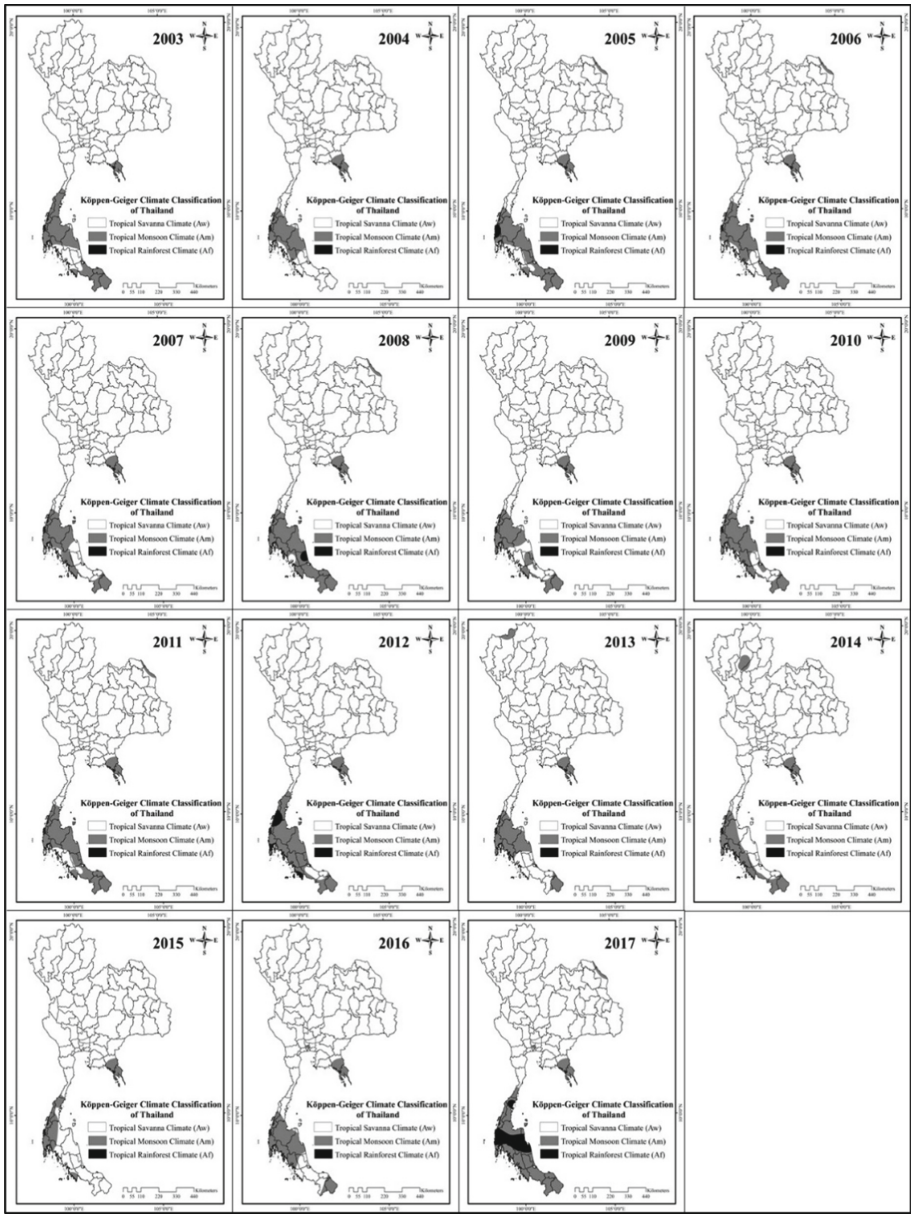
4 Results

Updated Köppen-Geiger Climate Classification of Thailand maps were created by using the average monthly temperature data and monthly rainfall data, which were collected by 99 meteorological stations of Thai Meteorological Department and Weather Division RTAF Thailand from 1987 to 2017. After classifying the data with two letters following the criterion in the Table 1, the results are shown in the Figs. 2(A) and 2(B). There are three climate classes illustrated with different gray tone colors, which are “Af” (■), “Am” (▒) and “Aw” (□). The climate of most area of Thailand was “Aw” while “Am” occurred in the large area of southern region and the small area of eastern region which located in front of mountain range (Chanthaburi mountain range and Banthat mountain range) near Gulf of Thailand for all study’s year. “Am” also occurred in the small area of northeastern region in 1990, 1997, 2000, 2005, 2006, 2008 and 2011. Moreover, it occurred in few area of north region in 1994, 2013 and 2014. Furthermore, this climate type also presented in 2016 and 2017 in central region. “Af” demonstrated only 8 years, which are 1996, 1999, 2000, 2001, 2005, 2008, 2012 and 2017 in the small area of southern region.



(A)

Fig. 2. (A). Köppen-Geiger climate classification maps of Thailand in each year from 1987 to 2002



(B)

Fig. 2. (B). Köppen-Geiger climate classification maps of Thailand in each year from 2003 to 2017

5 Discussion

The results were then compared with the old-Köppen-Geiger Climate Classification map of Thailand [12, 13] which was using the theory of Köppen and Geiger as shown in the Fig. 1(A). The maps of this work are rather different from the previous climate map because the data of this work were collected from more number of meteorological stations in Thailand than the previous map. Therefore, the updated maps can give more details than the previous map. Although the climate classifications which occurred in Thailand were totally illustrated in three classes of the main climate group A, “Af” climate is seldom found in over 31 years past. The reason of this climate change situation might cause by drought, changing of world temperature, changing of sea level, El Nino and La Nina phenomena, the deforestation and human activities [10]. Therefore, the climate system of Thailand can only be summarized as two classes from the overall of 31 study’s year, which are “Am” and “Aw” as shown in the Fig. 3.

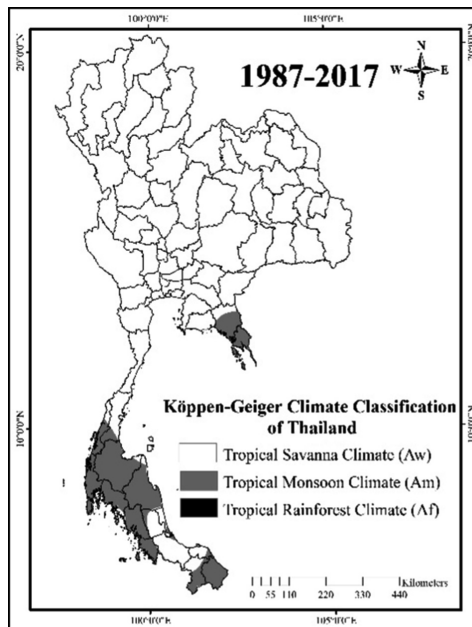


Fig. 3. The overall of Köppen-Geiger climate classification map of Thailand over 31 years past. (1987–2017)

6 Conclusions

The Köppen-Geiger climate classification of Thailand is classified in Equatorial climates (A) group which categorize into 3 classes: Tropical wet and dry or savanna climate (Aw), Tropical monsoon climate (Am) and Tropical rainforest climate (Af). “Aw” is located in the most area of Thailand. “Am” is located in the large area of

southern region next to Andaman Sea and the small area of eastern region of Thailand next to the Gulf of Thailand. “Af” occurs only 8 from 31 years in the small area of southern region of Thailand and does not exist in the 31-year overall map. From the result, it is rather changed from the previous climate classification map by the theory of Köppen-Geiger.

The summary of this work can replies the question asked by Sanderson [14]: “*Is it not time for modern atmospheric scientists to develop a “new” classification of world climate?*”. The result indicated that climate is changed day by day due to the effect of various activities which happened on the earth. The climate classification is certainly changed therefore the updated climate classification map is necessary to develop for being aware of the future.

Acknowledgments. Author would like to say thank you to Thai Meteorological Department and Weather Division RTAF Thailand for supporting all data which necessary in this study.

References

1. Köppen, W.: Die Wärmezonen der Erde, nach der Dauer der heissen, gemässigten und kalten Zeit und nach der Wirkung der Wärme auf die organische Welt betrachtet (The thermal zones of the earth according to the duration of hot, moderate and cold periods and to the impact of heat on the organic world). *Meteorol. Z.* **1**, 12 (1884)
2. Köppen, W.: Das geographische system der Klimate. In: *Handbuch der Klimatologie*, vol. 1. Borntraeger, Berlin (1936)
3. Geiger, R.: Klassifikation der Klimate nach W. Köppen. In: *Landolt-Börnstein – Zahlenwerte und Funktionen aus Physik, Chemie, Astronomie, Geophysik und Technik*, alte Serie, vol. 3. pp 603–607. Springer, Heidelberg (1954)
4. Rubel, F., Kottek, M.: Comments on “The thermal zones of the Earth” by Wladimir Köppen (1884). *Meteorol. Z.* **20**(3), 361–365 (2011). <https://doi.org/10.1127/0941-2948/2011/0258>
5. Kottek, M., Grieser, J., Beck, C., Rudolf, B., Rubel, F.: World map of the Köppen-Geiger climate classification updated. *Meteorol. Z.* **15**(3), 259–263 (2006). <https://doi.org/10.1127/0941-2948/2006/0130>
6. Weather Division RTAF Thailand: *Climatology, Air mass, Climate of Thailand and Climate change*. RTAF, Bangkok (2013)
7. Dasri, P.: *Climatology*. Silapakorn University, Nakhon Pathom, Thailand (1977)
8. Attavanich, P.: *Climatology*. Ramkhamhaeng University Press, Bangkok, Thailand (1989)
9. Tourism Authority of Thailand: *The ‘Personality’ of Thailand*. Darnsitha Press Co., Ltd. (1996)
10. Thai Meteorological Department: *Climate of Thailand* (2015). https://www.tmd.go.th/info/climate_of_thailand-2524-2553.pdf. Accessed 29 Oct 2017
11. Learning center for Earth Science and Astronomy: *World Climate Zone*. <http://www.lesa.biz/earth/atmosphere/earthzones>. Accessed 11 Dec 2013
12. Peel, M.C., Finlayson, B.L., McMahon, T.A.: Updated world map of the Köppen-Geiger climate classification. *Hydrol. Earth Syst. Sci.* **11**(5), 1633–1644 (2007). <https://doi.org/10.5194/hess-11-1633-2007>

13. Wikimedia Commons: Thailand map of Köppen climate classification.svg. Wikimedia Commons, the free media repository. https://commons.wikimedia.org/w/index.php?title=File:Thailand_map_of_K%C3%B6ppen_climate_classification.svg&oldid=241329123. Accessed 19 Apr 2017
14. Sanderson, M.: The classification of climates from Pythagoras to Koeppen. *Bull. Am. Meteor. Soc.* **80**(4), 669–674 (1999). [https://doi.org/10.1175/1520-0477\(1999\)080%3c0669:tcocfp%3e2.0.co;2](https://doi.org/10.1175/1520-0477(1999)080%3c0669:tcocfp%3e2.0.co;2)



Analysis Forest Fire Cause and Different Land Use Within Buffer Zones in Kanchanaburi Province, Thailand

Walaiporn Phonphan^(✉)

Environmental Science, Faculty of Science and Technology, Suan Sunandha Rajabhat University, Bangkok, Thailand
walaiporn.ph@ssru.ac.th

Abstract. The most important causes of forest fire are due to human's activities both intentionally and unknowingly. These are the human behaviors in land use at the edge to forest or buffer area. Due to this reason, land use within the buffer area, which caused forest fire in Kanchanaburi, is being studied using Geo-informatics in order to explore and analyze the way of utilizing the buffer area, which caused forest fire. Satellite imagery is used to classify the land use. By creating buffer at the edge of forest can classify the ways of land use, which possibly cause forest fire. Moreover, the study of previous statistics and caused of forest fire is to find which land use are possible to cause forest fire. From the study, the highest cause forest fire is searching of forest products and the lowest cause forest fire is hunting. Over 82% of the forest fire caused by searching of forest product and unknown caused. There is a likelihood of forest fire, which caused by forest product searching to be increased during 2015–2017. Moreover, the study of the way of utilizing land around buffer area within 1 km from the edge of forest found that more than 60% of forest fire found in the area of deciduous forest, while 20% found in agricultural area. This research can show the relationship between land use and causes of forest fire.

Keywords: Forest fire · Land use · Cause of forest fire · Geo-information · Buffer

1 Introduction

There is a gradual change of forest area due to forest invasion for shelter and work and reclaiming for agriculture [1]. Moreover, the cause of decreasing in forest area is due to forest fire, which caused in nature and by human actions. Forest fire rapidly causes the decreasing of forest fire and affects the balance of an ecosystem. Moreover, forest fire also causes air pollution and draught. The frequency of forest fire in Kanchanaburi is quite high and caused the biggest damage in the Central region. The reason might be that most of Kanchanaburi area is consisting of forest – both tropical rain forest and sparse forest, which gives Kanchanaburi Province a higher chance for forest fire than any other provinces.

The studies on forest fire using Geo-information technology [2], it can following and monitoring forest fire areas. For example, Forest Protection and Fire Control Office

have applied a remote sensing in order to study fire area for 10 years continuously by using hotspot as an investigation point. However, this project was conducted only in the area of Department of National Parks, Wildlife and Plants Conservation, which found that the possibility of fire is constant. Additionally, satellite imagery from SPOT was interpreted in order to study and classify land use and search for the remaining forest area, as well as conducts a vector map in Geo-information technology [3] Moreover, there were the study on the changes of land use during 2006–2013 by using the information on land use from Land Development Department in 2006 and satellite imagery of 2013. LANDSAT 8 satellite imagery shows there are a lot of changes on forest area the most. An area of 0.0157 km^2 has been converted to an agricultural area. Most of the forest area has been converted to agricultural area. This dues to people in the area invaded forest area to convert in to agricultural area such as forest invasion for rubber or pineapple plantation [4] Moreover, Geo-information technology was applied in order to search for a fire area by using information on range of heat wave. The suggestion on managing forest fire in the studied area is done by using LANDSAT-5 TM and LANDSAT-8 satellite imagery. The result from LANDSAT satellite imagery can be used in analyzing temperature value. From this study, it shows that LANDSAT satellite imagery can be used in the study of forest fire in Thailand, as LANDSAT is a satellite with $30 \times 30 \text{ m}$ resolution. This can show the target area and help in analyzing forest fire area, which makes it more convenient in planning for managing and controlling the fire, as well as planning to reach the area better [5]. This leads to a question in the study as follow: Whether or not the different land use in buffer areas can be cause forest fire. Therefore, in this study, the main objective is to study land use, which risks for forest fire in buffer area at the edge of forest in Kanchanaburi Province by using Geo-information technology. The result of this research can help governmental organization to work better on watching closely on the areas at risk in order to prevent fire.

2 Study Areas

Kanchanaburi Province, Thailand has a total area of 0.02 million km^2 . Most of its topography is sparse forest and tropical rain forest. Kanchanaburi is divided into 13 districts. It has borders with Tak, Uthaithani, Ratchaburi, Supanburi, Nakhon Phathom, and Myanmar. The scope of this research is within the area the edge to the forest in Kanchanaburi's national parks (Fig. 1). The distance from the edge of forest is one kilometer. The study of land use in the area of forest fire and nearby is done by using satellite imagery.

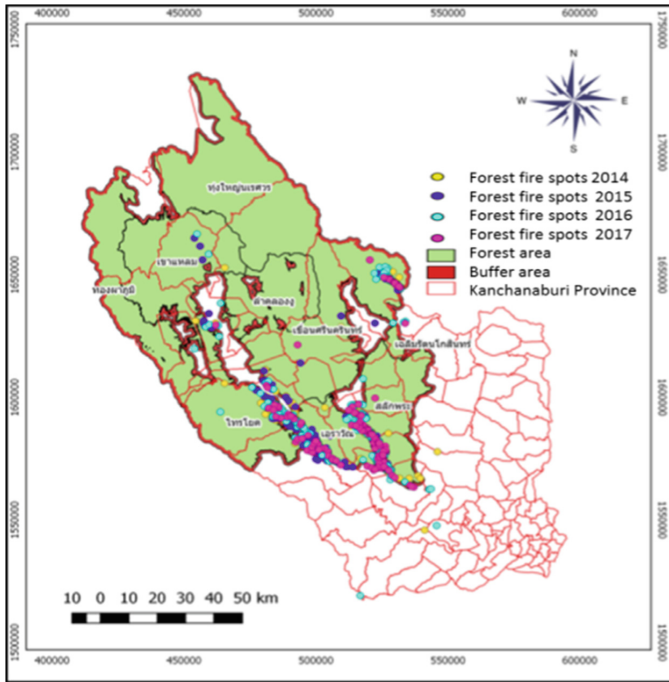


Fig. 1. The study areas is within the area the edge to the forest (red zone) in Kancharaburi’s national parks

3 Methodology

3.1 Collect the Data by Survey and Recording Data in the Studied Area

Investigate on land use, topography characteristics, location where fire existed. Record coordinates of the location, which fire existed and the nearby area. Prepare statistical information on previous fire from related organizations and information on factors influencing forest fire in the form of Geographic information system (GIS) in order to use in the analytical process with GIS.

3.2 Study on Land Use from Landsat8 Satellite Imagery

Image Classification with supervised classification method and classification accuracy assessment was used in this research. To begin, prepare information for further analyze by checking area of different ways of land use using 100 GPS coordinates in order to create training site for supervised image classification. Moreover, field data collection were collected another 100 coordinates in order to assure the accuracy of information gathered

from satellite imagery. In preparation of satellite imagery data collection, Atmospheric correction, image error correction, and satellite imagery data emphasis were made in order for a better resolution when comparing to the original data. This can help in distinguishing target objects and its surrounding area. Color composition technique was used in order to study on the condition of land use. Bring the prepared photos from satellite imagery to the process of supervised classification and compare with those areas which fire existed. They were classified by shape, pattern, color, site, and association.

4 Result

4.1 The Study of Causes and the Land Use Which Forest Fire Existed

From data collection, National Park, Wildlife and Plant Conservation Department analyzed causes of forest fire during 2012–2017. From the data, the causes of fire for each year can be concluded (Table 1), which shows that there is likelihood that numbers of forest fire will increase since 2012 until 2016. The year 2016 marked with the highest number of forest fire in total 222 times. However, in the later year, the number of forest fire decreased. When considering on the causes of fire, these behaviors or activities; searching for forest product, unknown causes, burning crop residual, and hunting rank high in possibility to cause fire respectively. When considering on causes or behaviors that caused fire in Kanchanaburi Province, searching for forest products and unknown causes accounted for 82% of all causes. You can see that the number of the unknown causes is quite high. This might cause an error when creating a relationship between the causes and forest fire emerging. The study also found that the tendency of forest fire caused by forest product searching is likely to increase since 2012–2016, while the tendency of forest fire caused by unknown caused is likely to decrease when examining the data during 6 years since 2012 until 2017. The unknown caused is decreasing might due to the reason that officers were able to identify the causes better. 61.47% of forest fire found in the area of conserved forest, wildlife conservation area, and national parks. There were more forest fire in the area of Khuen Srinagarindra National Park, Sai Yok National Park, Erawan National Park, and Salakpra Wildlife Sanctuary – especially at the edge area between the national parks and villages (Fig. 2). Moreover, the survey found that forest fire often occurs at the edge between Sai Yok National Park, Erawan National Park, and Salakpra Wildlife Sanctuary, as there are communities and villages around. Most of forest fire in national parks often occurs in deciduous forest and agricultural area. The main causes are forest product searching, unknown cause, and burning of crop residual. When considering the time for forest fire, it is spread in all period of time. In terms of physical and topographical factors, the study found that forest fire often occurs in areas at 200–600 m above sea level.

Table 1. The forest fire cause in Kanchanaburi Province, Thailand (2012–2017)

Cause	2012	2013	2014	2015	2016	2017	Total
Burning crop	2	3	15	26	11	8	65
Searching for forest product	21	28	31	108	111	87	386
Hunting	3	3	13	22	9	5	55
Animal domestication	2	1	1	1	0	2	7
Tourists	0	0	1	1	0	2	4
Burning of crop residual	0	0	0	1	0	0	1
woodworking	2	5	1	0	0	0	8
Cigarette	0	0	0	0	1	0	1
Dissimuler	0	0	0	0	0	0	0
Government	2	0	1	4	0	0	7
Unknown cause	33	70	86	21	90	25	325
Total	65	110	149	184	222	129	859

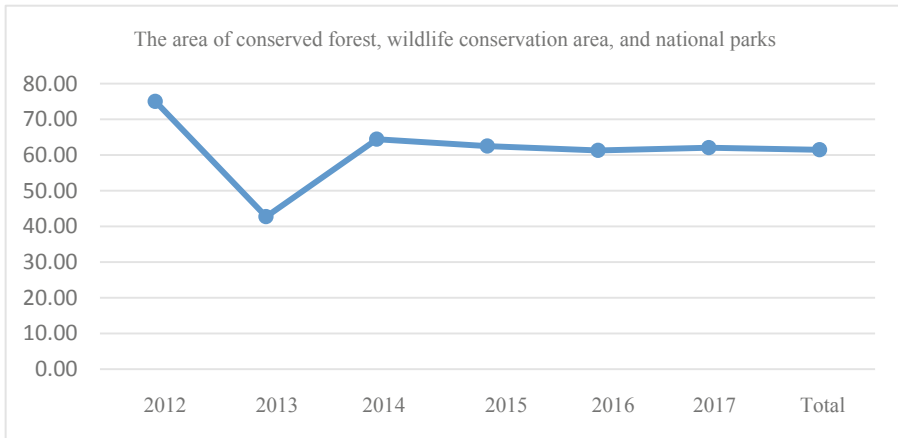


Fig. 2. Percent of forest fire found in the area of conserved forest, wildlife conservation area, and national parks.

4.2 Study on Land Use from Landsat8 Satellite Imagery

When classifying data using supervised classification method, the study found that land use (Fig. 3) is classified into 4 types, which are forest area, agricultural area, water body, and city area. Forest area is accounted for 52.11% of all area. 40% of all area is an agricultural area, while city area and water body are accounted for 4.9 and 2.82% respectively.

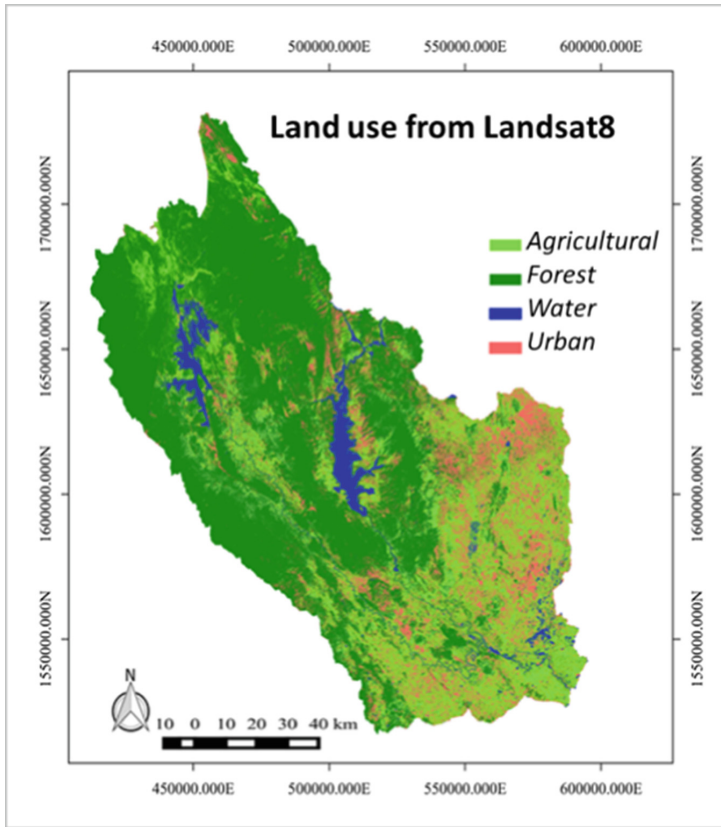


Fig. 3. Land use from Landsat8 through supervised classification method

To test the accuracy of data from satellite imagery by using supervised classification method. Take the data which classified by supervised classification method to overlay with those coordinates, which recorded during the survey. In order to test the accuracy, the following formula will be used:

$$\text{Percentage of accuracy (\%)} = \frac{\text{Number of correct coordinates}}{\text{Number of all coordinates}} \times 100$$

The study found that data from Landsat8 satellite imagery gave 82% accuracy, which is acceptable for remote sensing. This data can be used for a survey in forest and area at the edge of forest for further planning of studying on factors, which cause forest fire. To do so, take spots where fire occurred to overlay with data of land use from satellite imagery. Then, select sample spots for field surveys and analyze the data on ways of land use with forest fire spots.

Accuracy test of each area classification found that satellite imagery gives the highest accuracy on water body and is able to classify agricultural area, forest area, and city area accurately by 77, 91, and 92% respectively (Table 2).

Table 2. Accuracy test of each area classification

Land use	Percentage of accuracy (%)
Agricultural	77
Forest	91
Urban	92
Water	100

4.3 Examination and Analysis of Lands Utilization Characteristics in Buffer Areas, Which Caused Forest Fire

The data used in this study were data collected from field survey in the edge area to the forest and statistical data of forest fire occurring and damage area during 2012–2017. The results of the study on land use by using satellite imagery are used to overlay with data of forest fire spots and a survey was conducted on buffer area within one kilometer (Fig. 1).

Analyzing on land use that give possibility for forest fire that found the following land use on fire spot cause high chance of fire: (1) utilization of forest like deciduous forest, planted forest, evergreen forest, deciduous forest waiting for restoration, and grassland, (2) utilization of agricultural area to plant rubber trees, tamarind, corn, banana, fruits, sugar cane, and perennial plants, (3) utilization of land as a city to build roads, recreation areas, houses (Table 3). From data analysis, it shows that the type of land use that causes fire the most is in deciduous forest, which is accounted for 61%. The latter is agricultural area with 20% and planted forest with 8%.

Table 3. Land use on fire spot cause high chance of fire

Land use		Fire spot (%)	Land use		Fire spot (%)
Forest	Deciduous forest	61	Planted forest	8	
	Deciduous forest waiting for restoration	5.3	Evergreen forest	1.6	
	Grassland	2.4			
Agricultural	Rubber trees	4.8	Tamarind	0.7	
	Fruits	0.2	Corn	7.2	
	Sugar cane	6.3	Banana	0.3	
	Perennial plants	0.5			
Urban	Recreation areas	0.5	Village	1	
	Road	0.2			

Data collection from field survey in buffer areas, which is risky for forest fire and data analysis results can give a conclusion of number of times forest fire occur and area of fire damage in Kanchanaburi during the past 5 years (Table 4). The highest time of fire occurring and biggest damage was in 2016.

Table 4. Number of times forest fire occur and area of fire damage in 2012–2017

Year	2012	2013	2014	2015	2016	2017
Number of times forest fire occur	65	110	149	184	222	129
Area of fire damage (km ²)	0.77	1.37	1,388	2.22	3.59	2.27

The data for analysis in terms of area such as size of damage in fire area, date and time which fire occurred, place, and causes of fire were prepared. A map marking spots where fire occurred by using Geo-information technology was also made in order to use in the analytical process in terms of area by using Geo-information.

The results from the analysis found that the causes of forest fire can be classified as follow: burning of crop residual, searching of forest products, hunting, animal rising, tourists, conflicts on reforestation, accidents, carelessness, and unknown.

5 Discussion and Conclusion

5.1 Examination and Analysis of Land Use in Buffer Areas Which Cause Forest Fire

There are two parts of data using in the analysis, which are statistical data on the occurrence and causes of fire and data on land use, which interpreted from satellite imagery. Examination and analysis of land use in buffer areas, which cause forest fire, used the data from National Park, Wildlife, and Plants Conservation. The data is related to number of times forest fire occur and area of damage in Kanchanaburi during the past 5 years. In order to study as a primary data, which will lead to finding factors to build a relationship between land use and forest fire occurrence, the causes of fire can be concluded as follow: burning of crop residual, forest product searching, hunting, animal domestication, tourists, conflicts on reforestation, accident, carelessness, and unknown. It can also be concluded that the causes of fire from the highest to the lowest risk are forest product searching, unknown, burning of crop residual, and hunting. When considering on causes of forest fire in Kanchanburi, forest product searching and unknown causes in total is accounted for 82% of all causes. Moreover, the tendency of fire causing by forest product searching is likely to increase during 2015–2017, while the tendency of fire causing by unknown cause is likely to decrease during the same period. The reason why it is decreasing might be due to data gathering from the past statistics by governmental agencies. Therefore, the unknown causes can be defined and the number decreased in 2017. From this study, it shows that there were many fire occurred during dry season in forest area of sanctuary, national parks, non-hunting area, and wildlife conservatory area. It can be concluded that 61.47% of forest fire occurred in sanctuary, wildlife conservatory area, and national parks. Unknown causes of fire ranks in the second largest data as secondary data gathered from organizations. This causes the analysis in this research to create a relationship according to data during 2012–2017. In the future, if the data in terms of number of years of forest fire

occurrence becomes larger and the unknown causes will decrease, this will probably affect the analysis results.

5.2 Studying on the Relationship of Ways of Land Use and Forest Fire Occurrence

The study on land use was done by using photos from Landsat8 satellite imagery with 30-m resolution. The method used was supervised classification method, which classified land use into 4 types: forest area, agricultural area, water body, and city area. When testing the accuracy, the interpretation of Landsat8 satellite imagery is 82% accurate. In order to see the characteristics of land use in buffer area within the distance of one kilometer from the edge of forest, it is used in the survey of forest area and the edge of forest. The analysis of relationship of land use is done by overlaying spots where fire occurred with land use, which interpreted from satellite imagery. Specify spots in buffer areas to be examined for land use in order to classify sub level of land use. The area where fire occurred the most is found to be utilized as deciduous forest accounted for 61%. The latter is utilized as agricultural area accounted for 20%. This result is relevant to the research of [6] which analyzing the relationship of spots where fire occurred and factors on topography, land use and groundcover in Chiang Mai. The study found that March is when fire occur the most. The area with highest fire occurrence is mixed forest (53.9%). The second area is agricultural area (23.8%) and fertile forest (16.2%). From this study, it shows that forest fire can easily occur in deciduous forest during dry season, as it consists of all three factors: combustible, oxygen, and heat. Dried leaves are combustible and the temperature is high during dry season. This causes higher possibility for forest fire [7]. The study found that relative humidity affects the changes in combustible's humidity 54.31% in dry deciduous dipterocarp forest in Chiang Mai. This causes a large number of combustible during dry season in deciduous forest, which causes fire easily. The second area where fire often occurs is agricultural area. The area studied in this research is within 1-kilometer distance from forest area. From the interpretation of satellite imagery and field survey of land use, it shows that most of the agricultural area is small and invading forest area relevant to mobile plantation. Together with the cause of human activities, it shows that land use as mobile plantation is the main cause of forest fire occurring from human activities. However, if the area used in the study is smaller than 900 m², it can cause error in the classification of land use. In the future, the satellite imagery should have higher resolution due to agricultural area in Kanchanaburi is rather small.

This research helped the researcher to be able to analyze today's utilization of land before conducting field survey, as well as be able to make plan in selecting the area. This is an advantage on time saving. Geoinformatic is a tool that is suitable for analyzing problems of big areas, collecting up-to-date information, and rapid examining of area. The application of geoinformatic technology from remote sensing of satellite imagery becomes a device that supports specification of location and land use in forest and area where forest fire occurred. It can quickly show an area with risk of forest fire occurrence and examining land use of the covered area with wider region. Moreover, Landsat satellite imagery can be downloaded for free, which is cost saving. It can show targeted area, With this reasons, planning in order to monitoring and

preventing forest fire can be done in timely manner or it can help reducing the damages from forest fire more effectively [8]. For further study, the intense of damages from forest fire related to ways of land use can be included for the benefit of forest fire prevention plan.

References

1. Forest Land Management Homepage. <https://www.forest.go.th>. Accessed 24 Mar 2017
2. De Santis, A., Asner, G.P., Vaughan, P.J., Knapp, D.E.: Mapping burn severity and burning efficiency in California using simulation models and Landsat imagery. *Remote Sens. Environ.* **114**, 1535–1545 (2010)
3. Griffiths, P., Kuemmerle, T., Baumann, M., Radeloff, V.C., Abrudan, I.V., Lieskovsky, J., Munteanu, C., Ostapowicz, K., Hostert, P.: Forest disturbances, forest recovery, and changes in forest types across the Carpathian ecoregion from 1985 to 2010 based on Landsat image composites. *Remote Sens. Environ.* **151**, 72–88 (2014)
4. Ketsri, S., Triphomma, A.: Application Remote sensing for study land use change in 1990–2013. Master's thesis, Naresuan University (2014)
5. Suksabai, K., Nakaphakorn, K.: Application the geo-information technologies to identify the areas of forest fire using thermal band Thai journal citation index Centre, vol. 22, Issue 4 October 2014
6. Suwanwaree, P.: Impacts of forest fire on the forest fertility and air quality in Chiang Mai Province. Suranaree University (2015)
7. Aukaauk, S.: The study fire forest in Dipterocarp forest Changmai province. Report of office of fire protection, Thailand (1992)
8. Clark, J., McKinley, R.: Remote sensing and geospatial support to Burned Area Emergency Response Teams. *Fire Manag. Today* **71**, 15–18 (2011)



Spatiotemporal Analysis of Urban Agglomeration: A Case Study of Hyderabad City, Telangana State, India

Ashok Kumar Lonavath^(✉), Karunakar Virugu, V. Sathish Kumar, B. Ravi Naik, and Krishna Naik

Department of Geography, Osmania University, Hyderabad 500 007, India
ashokouprof@gmail.com

Abstract. An Urban Agglomeration is a continuous urban spread consisting of a defined town with neighboring outgrowths of the city. The concept was first introduced in India in 1971. The outgrowth is an adjacent town with minimum 20000 population and does not qualify as an independent town. Hyderabad city is 425 years old and it is the capital city of newly formed Telangana state in India. The rapid growth and uneven pattern of development rooted from the 1970's. Hyderabad city is located between 17°22' N latitude and 78°28' E longitude with the elevation of 600 m. The area has increased from 172 Km² to 650 Km² from 1971 to 2011 and the population increased from 1, 58, 162 to 67, 31,790 during the same period. This research paper explains the spatiotemporal study of urban growth.

Keywords: Urban agglomeration · Land use patterns · Urbanisation

1 Introduction

The world population will reach 9.1 billion by 2050 and it is also estimated that more than 70% world population will live in urban areas [1]. The urban facilities attract the people from rural areas to urban units. The shift of population from village to city and the process of transformation of villages into cities is called urbanization. Urban, according to Indian census, is defined as the town with a minimum of 5000 population, a density of 4000 Persons per Km² and 75% of male population engaged in non-agricultural activities. In Telangana state there are 160 urban centers which is divided into six classes based on population.

Urban population explosion has occurred in every country, leading to the formation of fibroblast and sarcoma settlement [2]. It is difficult to characterize urban expansion without a comprehensive understanding of urbanization processes [3]. The unplanned and uncontrolled rapid growth results in serious concerns on the urban dwellers and their environment [4]. Urbanization is a dynamic socio-economic process which leads to spatial and temporal variations. In case the process is viewed with a definite regional background, urbanization influences the adjoining rural-urban fringe; it could also be looked as rural-urban linkages [5]. Urbanization is a socioeconomic phenomenon taking place at an unprecedented scale and rate all over the world [6]. The level of

urbanization means the proportion of urban population to the total population [7]. Urban sprawl is an uneven urban development often linked to sparse building density over rural areas [8]. Urban Growth has two dimensions, physical and demographic [9]. The Phenomenal increase of urban population of cities has taken place mostly in case of cities and larger towns [10]. The growing tendency towards a greater concentration of population in larger towns and a co-incidental decrease in smaller towns. Hierarchy of urban centers depends upon level of economic activity of urban centers [11].

Prominent studies on urbanization in India were done by Ashish Bose, Rao, V.L.S. P., Roy, B.K., Sinha, A.K., Alam, R.R.etc., in Telangana were done by Pothna (1979), Simhadri (1981), Kalpana Markandey (1980)], and Ashok Kumar Lonavath (2014).

1.1 Study Area

Hyderabad, the capital city of Telangana state and is known as ‘Hitech city’ in India. It was built by the Nizam’s kings 425 years ago; later it also served as the British residency from 1700 AD to 1947 AD. It is located on the bank of the river Musi. Hyderabad city is ranked 1st among in “Best of the World places you should see” by National Geographic, San Francisco (2015) and “Must Visit cities in the world” by New York Times. Hyderabad stands 2nd in India as ‘Hottest IT destinations’ by Rediff Business and also stands 2nd for “Easy of Doing Business in India” by The World Bank (2018).

The city, expansion started in the 1970’s mainly due to internal migration, people started floating to the city for search of employment, education and health facilities. Subsequently, the globalization policies that was initiated in India during the 1990’s has focused on the tertiary activities such as trade, commerce, transportation and construction industries. Establishment of industries, such as manufacturing, chemical, pharma, information technology and setup of international education institutions, hospitals, science and research centers, banking and housing have created a market hub in India. Hence basic services such as international airports, rail connectivity, road network, power (electricity), sewerage and drainage, street lighting, drinking water, recreation hubs, green spaces (lung spaces) have become priority services. Rapid growth in software technology has transformed Hyderabad into a smart city.

1.2 Objective of the Paper

To examine urban growth spatially and temporally, identifying factors responsible for the rapid growth and mapping of growth pattern of urban agglomeration.

1.3 Methodology

Census data of India for 1971, 1981, 1991, 2001 and 2011, Arc Map 9.3 and ERDAS Imagine 8.4, Landsat imageries [*] from USGS Earth Explorer have been used for processing the data.

[*] LAND SAT-5 (bands 1 to 7, Jan 27, 1991, SCENE_CENTER_TIME = “04:30:13.3580310Z (1991); Mar 03, 2001, SCENE_CENTER_TIME = “04:57:58.0880817 Z” (2001); LAND SAT-7 TME, bands 1–8, Jan 18, 2011, SCENE_CENTER_TIME = 04:59:36.4440630Z” (2011)).

2 Hyderabad Urban Growth Study

Hyderabad’s urban growth has been examined demographically and physically. Physical growth is horizontal in Hyderabad. The population of Hyderabad city was 12, 48, 969 and growth rate was 44.72% in 1961. Population in 1971 was 18, 07, 485. The highest growth rate of population was found during 1981–1991, i.e. 66.72%. The lowest growth rate is recorded as 18.6% during 2001 to 2011 (Table 1) .

Table 1. Hyderabad city population and growth rate-1961–2011.

Year	Population	Growth rate
1961	12,48,969	–
1971	18,07,485	44.72
1981	25,96,598	43.66
1991	43,29,071	66.72
2001	57,42,036	32.64
2011	68,09,970	18.60

(Source: Census of India, 2011)

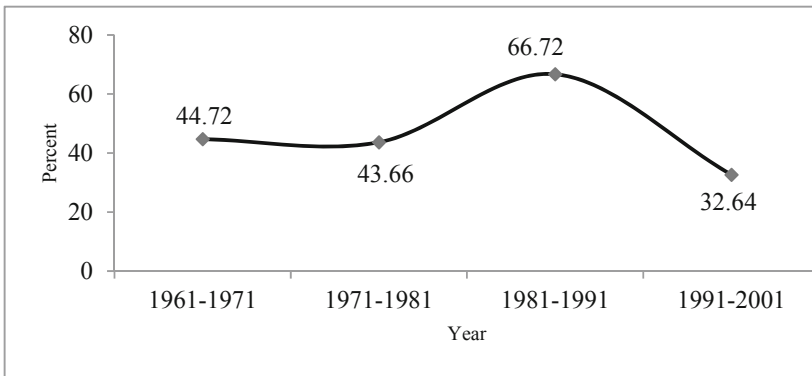


Fig. 1. Hyderabad population growth rate, 1961–2011

Table 2. Internal migrants to Hyderabad city - 1991 and 2001.

No	Type of internal migration	Internal migration in 1991	Internal migration in 2001	%Migrations to total migrants in 1991	%Migrations to total migrants in 2001	Growth rate of in-migrants (%) 1991–2001
1	Born elsewhere in the district of enumeration	3,61,781	5,55,873	41.89	47.33	53.6
2	Born in other districts of the state	3,61,781	4,78,152	41.89	40.71	32.2
3	States in India beyond the state of enumeration	1,40,052	1,40,396	16.22	11.95	0.25
Total		8,63,614	11,74,421	100	100	35.9

(Source: Census of India, 2011).

Migration is another important factor for city growth. The number of internal migrants in 1991 was 8, 63, 614, and it increased to 11, 74, 421 in 2001. Growth rate within the district is maximum of 53.6%, the migrants from other district were 32.2% and migrants from other state's were 0.25% (Table 2) (Fig. 1).

2.1 Hyderabad Urban Agglomerations

Seven adjoining towns which were agglomerated into Hyderabad in 1971. 4 towns were agglomerated in 1981 by leaving behind one outgrowth. 21 towns were agglomerated in 1991 by leaving behind 13 outgrowths. 5 towns were agglomerated in 2001 by leaving behind 3 outgrowths. The highest of 31 towns were agglomerated into Hyderabad city in 2011 by leaving behind 24 outgrowths (Table 3).

During 1991–2001, the independent towns as mentioned in the Table 4 emerged as municipalities in the process of agglomeration. The urban municipalities which observed high growth rate in a preceding decade subsequently noticed low growth rate in succeeding decade and vice versa during 2001 and 2011. This is because of stagnation of area in 1–8 municipalities. It is observed that uniform growth in urban municipalities 9–13 as their location is comparatively far from the city. Area of the urban municipalities as mentioned in the Table 5 indicates that the area has been increased from 1991 to 2011 along with a rise in density. Increased density is the indicator of urban sprawl (Fig. 6).

Table 3. Number of Census Town and Out Growth 1971-2011.

Sl. No	Year	Total census towns	Out growths
1	1971	7	0
2	1981	5	1
3	1991	21	13
4	2001	5	3
5	2011	39	24
	Total	77	41

(Source: Census of India, 2011)

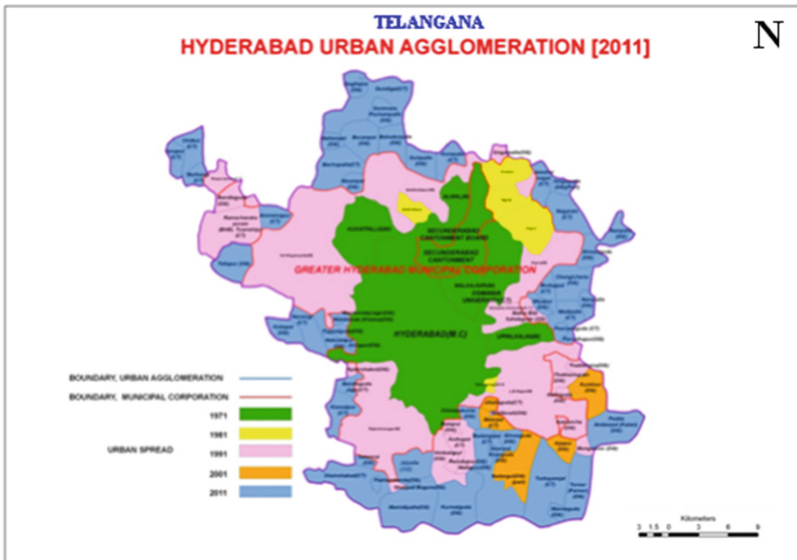


Fig. 2. Hyderabad urban agglomeration-2011.

Table 4. Population Growth rate in Urban Agglomerations of Hyderabad city.

Sl. No	Urban municipalities	Decadal population			Population growth rate	
		1991	2001	2011	2001	2011
1	Alwal	66,471	93,206	1,05,736	40.22	13.44
2	Ramachandrapuram	46,129	52,363	1,17,217	13.51	123.85
3	Cantonment	1,71,148	2,06,102	2,17,910	16.95	5.79
4	Kukatpally	1,86,963	2,92,289	3,41,709	56.33	16.9
5	Malkajgiri	1,27,178	1,93,863	4,13,571	52.43	113.3
6	Gaddiannaram	35,187	52,835	53,622	50.15	1.48

(continued)

Table 4. (continued)

Sl. No	Urban municipalities	Decadal population			Population growth rate	
		1991	2001	2011	2001	2011
7	Kapra	87,747	1,59,002	1,98,349	81.2	24.7
8	Patancheru	26,862	40,273	1,14,559	49.92	184.45
9	Qutbullapur	1,06,591	2,31,108	4,95,683	116.8	114.48
10	Rajendranagar	84,520	1,43,240	2,29,823	69.47	60.44
11	L.B Nagar	1,55,514	2,87,781	NA	NA	NA
12	Serilingamapally	72,320	1,53,364	3,09,320	112.0	101.69
13	Uppal	75,660	1,18,085	3,84,835	56.07	69.3

(Source: Census of India, 2011)

Table 5. Area and density in urban Agglomerations of Hyderabad city.

Urban municipalities	Area in Sq. Km			Density		
	1991	2001	2011	1991	2001	2011
Alwal	NA	NA	NA	–	–	–
Ramachandrapuram	25.87	25.8	42.84	1783.108	2024.082	2736.158
Cantonment	40.7	40.7	NA	4205.111	5063.931	–
Kukatpally	43.69	72	NA	4279.309	4059.569	–
Malkajgiri	17.3	18	NA	7351.329	10770.17	–
Gaddiannaram	NA	NA	NA	–	–	–
Kapra	43.9	65	NA	1998.793	2446.185	–
Patancheru	11.65	14	55.29	2305.751	2876.643	2071.966
Qutbullapur	46.87	46.9	92.12	2274.184	4930.83	5380.84
Rajendranagar	52.25	52.8	NA	1617.608	2715.45	–
L.B Nagar	70	102	165.3	2221.629	2821.382	–
Serilingamapally	108.2	98	NA	668.7009	1564.939	–
Uppal	19.16	19.7	NA	3948.852	6006.358	–

(Source: Census of India)

2.2 Land Use Patterns of Hyderabad City

The land-use pattern is critically examined by using Landsat imageries of 1991, 2001 and 2011. Thematic maps are created with the help of unsupervised classification techniques in order to identify land-use patterns. For the purpose of the study land use classification is categorized as Built-Up area, Water-bodies, Vegetation and Other Lands. The uneven distribution of settlements due to overcrowded population is identified by thematic maps and it clearly shows that urban sprawl activity in Hyderabad

city. The sprawl indicates the physical expansion of the Built Up area beyond the city limits is due to over migration. 2011 Hyderabad base map is used to identify the variations in land-use patterns of a defined period. In 1991 the Other Lands share is the highest as 67% followed by built-up area (16%), Vegetation (14.7%) and Water bodies (1.3%) (Figs. 2 and 3).

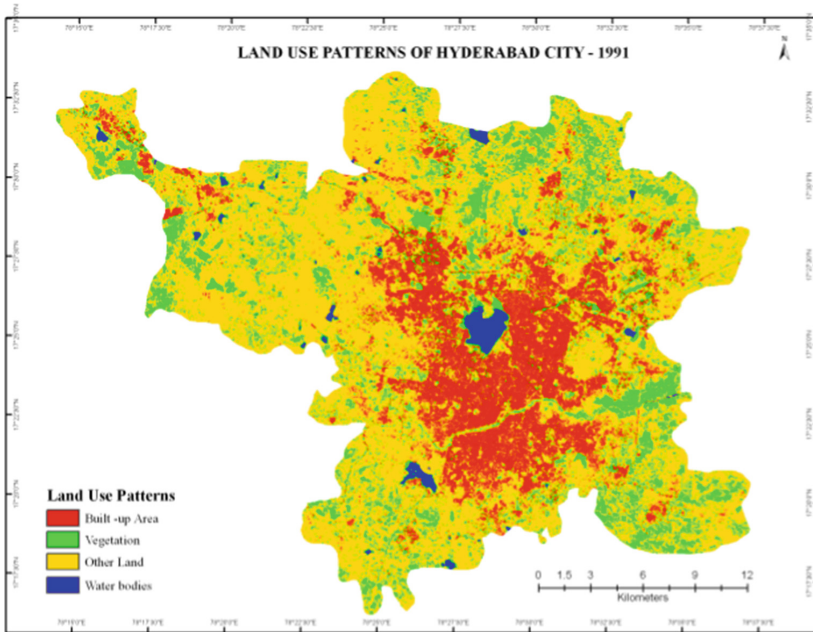


Fig. 3. Land-use pattern of Hyderabad city, 1991

In 2001 the Built-Up area covers 45.9% of growth followed by Other Lands i.e. 31.67% and Vegetation as 21.19%, only 1.23% of land area covered by water bodies. In 2011 the Built-Up area covers 56.35%, followed by Other Lands (34%), Vegetation (8.41%) and Water body (1.32%) (Table 6).

The land-use pattern of Hyderabad city during 1991 to 2011 shows that, the Built Up area increased drastically from 1991 onwards. The Built-up area was extended to 193 Sq. Km from 1991 to 2001 and 69 Sq. Km from 2001 to 2011. Subsequently the Other Lands area is decreased from 1991 to 2011 due to its conversion into built-up areas. There is no change in the area occupied by water bodies from 1991 to 2011 (Figs. 4 and 5).

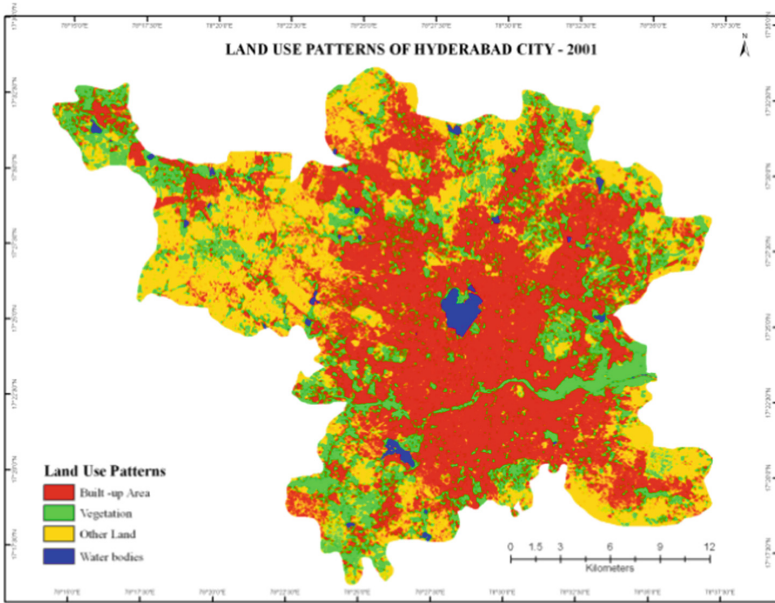


Fig. 4. Land-use pattern of Hyderabad city, 2001

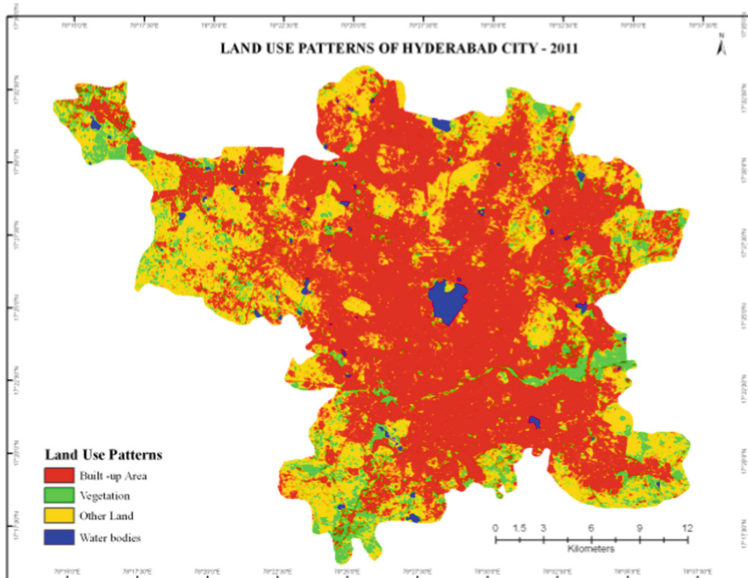


Fig. 5. Land-use pattern of Hyderabad city, 2011

Table 6. The land-use patterns of Hyderabad city -1991, 2001 and 2011

Class	Area in Sq. Km			Percentage land use		
	1991	2001	2011	1991	2001	2011
Built-up area	110.43	303.42	372.31	16.71	45.92	56.35
Water bodies	8.62	8.10	8.73	1.30	1.23	1.32
Vegetation	97.26	139.99	55.54	14.72	21.19	8.41
Other land	444.43	209.23	224.17	67.26	31.67	33.93
Total	660.75	660.75	660.75	100	100	100

(Source: Formulated by authors by using Land sat Imageries in ERDAS Imagine).

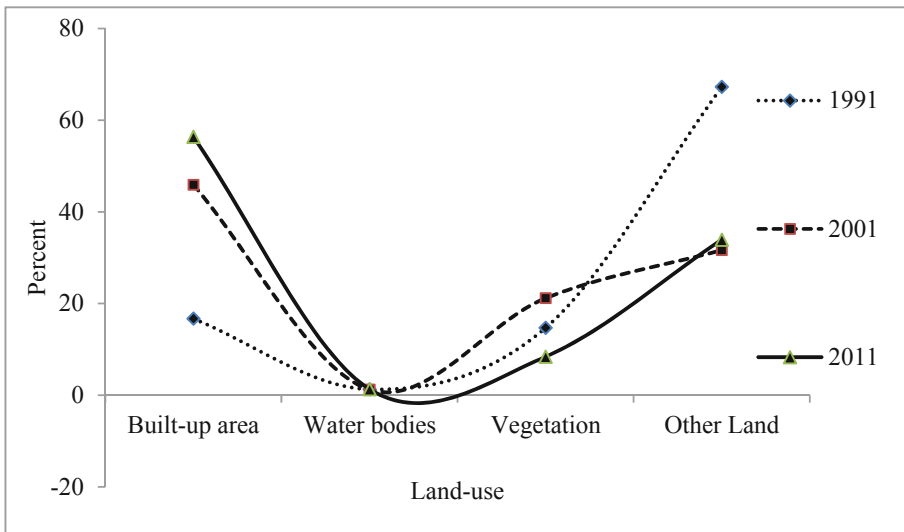


Fig. 6. Percent variation in land-use patterns of Hyderabad city-1991–2011.

3 Results and Conclusions

The population rate in Hyderabad city was recorded of maximum in 1971. It is due to inter district migration occurring from the other two regions of the state such as Andhra and Rayalaseema to Hyderabad city causing to urban sprawl. New out growths were coming up on the outskirts' due to the onset of Liberalization, Privatization, and Globalization (LPG) Policies, implemented in India after 1991. The inflow of foreign direct investment has entered in all the sectors and giving wider scope for the further expansion of urban settlements especially in industrial areas. As the city has the potential to generate jobs and has sufficient space for residence, this is likely to attract migrants on a massive base from the rural area. GHMC (Greater Hyderabad Municipal Corporation) Geographical Contours has been changing very frequently cater ever increasing population of the city to administer the growing population and ever

increasing investments in the city effectively. During 2001 to 2011, Population of Hyderabad has increased by 87%, the city has added over 3.1 million people to its ever growing population in the last 10 years. A majority of the increased figure belongs to migrants from other parts of India. Today these migratory population stands at 24% of overall city population. Hyderabad is generating wealth, employment and driving the human process, and these three key factors are not only defining the city's characteristics but also preparing it to join the club of megacities those with population above 1 crore by 2025. The Hyderabad city population has increased from 3,637,483 in the 2001 census to 6,809,970 in the 2011 census.

References

1. Peters, G.L.: Third world urbanization: towards the year 2000. In: Mandal, R.B., Peters, G.L. (eds.) *Urbanization and Regional Development*, pp. 22–39. Concept Publishing Co., New Delhi (1982)
2. Xinliang, X., Min, X.: Quantifying spatiotemporal patterns of urban expansion in China using remote sensing data. *Cities* **35**, 104–113 (2013)
3. Chadchan, J., Shankar, R.: An analysis of urban growth trends in the post-economic reforms period in India. *Int. J. Sustain. Built Environ.* **1**, 36–49 (2012)
4. Mandal, B.R.: *Urban Geography*. Concept Publishing Company, New Delhi (2000)
5. Sun, C., Zhi-feng, W., Lv, Z.-q., Yao, N., Wei, J.-b.: Quantifying different types of urban growth and the change dynamic in Guangzhou using multi-temporal remote sensing data. *Int. J. Appl. Earth Obs. Geoinf.* **21**, 409–417 (2013)
6. Trewartha, G.: *The Geography of Population-World Pattern*. Wiley Publishing Co., New York (1969)
7. Altieri, L., Cocchi, D., Pezzi, G., Scott, E.M., Ventrucci, M.: Urban sprawl scatterplots for urban morphological zones data. *Ecol. Ind.* **36**, 315–323 (2014)
8. Kuffer, M., Barrosb, J.: Urban morphology of unplanned settlements: the use of spatial metrics in VHR remotely sensed images. *Procedia Environ. Sci.* **7**, 152–157 (2011)
9. Rao, R. M., Simhadri, S.: Growth trends of cities and large towns of Andhra Pradesh: a temporal study (1901–1981). *Land Scape Systems*, December 1981
10. Kalpana, M.: *Spatial and Temporal Pattern of Urban Growth in Rayalaseema (1901–1971)*. Osmania University, Hyderabad (1981)
11. Lonavath, A.K.: *Urbanization and Regional Disparities in Andhra Pradesh (2014, unpublished thesis)*



Modelling of Potential Sites for Residential Development at South East Peri-Urban of Kolkata

Rukhsana^(✉) and Md. Hasnine

Department of Geography, Aliah University, Kolkata, India
rukhsanasarkar33@gmail.com

Abstract. During last few decades' unprecedented growth of population and migration from various districts and countries, causes traffic congestion, unplanned and disperse development at Peri-urban regions. To prevent this type of urban extension, researcher and planner are introduced various model such as Cellular Automata, SLUETH etc. for predicting future growth. That's why south east peri-urban area of Kolkata has been selected for detail study due to its fast expansion of area in to rural region. Due to rapid growth of urban development, multi criteria analysis, analytic hierarchy process (AHP), weighted linear combination (WLC), overlay weight age analysis (OWA) and remote sensing GIS tool has been used to find out the most and least suitable location for the systematically residential development in the selected study area. For finding out the suitable of planned residential area six factors including central proximity, network proximity, existing build-up, small industry, waterlogged/wetland, horticulture has been taken under the multi criteria analysis (MCA) with the weight age of 0.46, 0.24, 0.15, 0.09, 0.04, and 0.03 respectively. Present study result reported that very high class suitable area covers 8.81973 sq.km (13.94%) and high class suitable area contributes 15.55106 sq.km. (24.58%) while 12.75603 sq.km. (20.16%) accounted for moderate class suitable area. Low and very suitability area has been recorded as 15.32807 sq.km. (24.23%) and 10.80379 sq. km. (17.08%) areas respectively, which shows the unsuitability zone for next residential development in the sample study area.

Keywords: Geographical Information System · Analytic hierarchy process · Multi criteria analysis · Weighted linear combination · Site suitability · Spatial analysis

1 Introduction

At the earlier stage of urban development, migration occurred inward to the city but after a certain period of time in different phase of urban development usually people move outward from the city or from central business district to avoid traffic congestion, overcrowding, increasing land value [4]. Hence, both inner and outer migration of people leads urban expansion at the surrounding area of the city. It is expected from the United Nation's Population Division report, 1975 that 23% population may increase (from 38% to 61%) in living in urban areas within 50 years (i.e. 1975–2025). So this

unprecedented growth of population and transformation of urban economy [11] leads huge pressure on urban core resulting demand of extra land required for the establishment of residence which is fulfilled by peri-urban land utilization. Peri-urban areas are characterized by both urban and rural landscape and it's carried out diversified habitat, different types of land uses, heterogeneous economic activity and also has mixture of social structure. Gradually these characteristics will be converted to urban system [18]. Hence, unplanned conversion of peri-urban area into urban system is known as urban sprawl which will hamper the sustainability of peri-urban areas [2]. This process also encroach the prime agricultural land which has a negative effect on local food system and land productivity [8]. But to accomplishing the desire of peri-urban land for new urban development, appropriate physical planning [20] must require.

At present urbanization or urban development is great concern for researcher, academician, and planners. Many researchers have done a lot of study on urban expansion for the development or to develop a city in a planning way. Now days in this challenging or technological world in the fast growing cities a planning through a most recent technique or tools that is remote sensing and GIS is very necessary to apply or use for finding out suitable area for urban development. The said technique has been used by many authors and applied on the study of the urban expansion and other aspect. Population density which is a main factor to increase of urbanization is occupying the large number of area of a region for their survival that's why for the purpose a planning of residential development is very necessary which can be find out through site suitability analysis to use the remote sensing and GIS. Shifting of population from rural to urban and urban development is a global concern, it has been noticed that most of the small and isolated population centres are rapidly transforming and moving towards metropolitan cities. In urban areas to identification the potential sites for residential development is one of the significant issues of planning, before taking the decision for residential development, except basic chosen basic criteria for residential development, sites must be in areas that would make new developments successful. This means that potential sites must be located in residentially zoned areas and in areas that are available for new growth. Site suitability is the process of understanding existing site qualities and factors based on certain such as distance from existing transmission lines, distance from potentially hazardous sites and distance from existing groundwater supplies etc. The analysis may also determine how those factors will fit into the design process to evaluate site suitability [9]. Proper data is necessary for any suitability analysis including topographic maps, satellite data, thematic maps and field data. The different land qualities, which can be considered for suitability modelling are, present land-use/land-cover, slope, proximity of transportation network, flood hazard, groundwater condition etc. Rajesh et al. [18] integrated AHP and GIS technique to find out best suitable location for agriculture in peri-urban area in Hanoi province, Vietnam. This work provides cost effective and rapid land evaluation model which will help to other researcher studying in different study area. Shahadat et al. [10] tried to examine the suitable site for urban aquaculture development in Chittagong, Bangladesh. In this research ASTER imagery, topographic map at 1:10000 (survey of Bangladesh) were used along with ENVI and GIS capabilities to find out the appropriate urban water bodies (UWBs) for crop farming. In this study 362 hectore area identified UWBs as appropriate area for crop farming in which 77% is the most suitable site. Nirmalya [6]

used the multi criteria decision analysis (MCDA) process of find out the suitable site for small industry in part of Barasat II, Deganga, Rajarhat block of North 24 Pargana district, West Bengal. Various determine factors like settlement, road network, vegetation, water bodies, agriculture and land use were used to achieve the objective (Fig. 1).

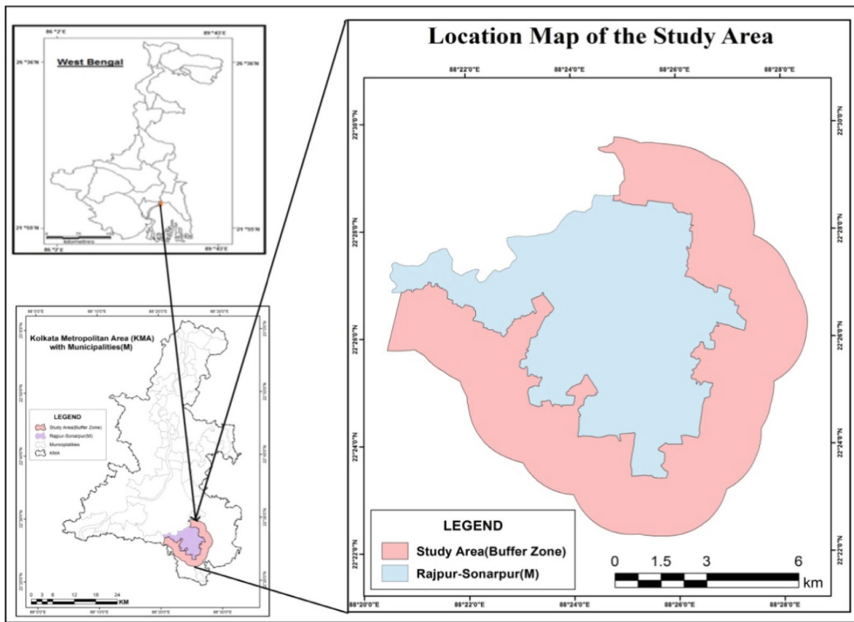


Fig. 1. Shows the location map of selected study area.

The peri-urban area of the Rajpur-Sonarpur Municipality has been chosen for the details study which lies at the south east part of Kolkata Municipal Corporation between 22° 22'00'' to 22°30'00'' north latitude and 88° 20'00'' to 88° 28'00'' east longitudes. The study area is selected of 2 km buffer area which is a part of Sonarpur CD block of South 24 Parganas district. The delineated peri-urban fringe of Sonarpur CD block is surrounded by the other CD block including Bhangar-I, Bhangar-II and Canning in the east, Bishnupur and Mahestala municipalities in the west and Garia neighbourhood of Kolkata as found in the north. As per census 2011 the total population is recorded 219863 in Sonarpur CD block which increased from 2001 (167368).

The main objectives are as follows: First to determine and analyze new residential locations, and second design an implementation plan and discuss the constraints for development to develop a model of site suitability for future residential development at peri-urban areas.

2 Methods

The study is based on both secondary and primary data as site visit for field work. Qualitative and quantitative technique completed to the research work. For the secondary data census of India, published work and as books, article etc. assisted to the paper for completing the work. The Survey of India (SOI) Topographical map no. 79B/7 and satellite data were registered using polyconic projection system. Satellite images (OIL Sensor Data, 30 m resolution date: 16 March, 2017) was digitally enhanced in order to extract maximum information. For suitability analysis, different parameters such as land use, roads, ground water availability and water bodies are considered and categorized with various attribute layers by using spatial analyst tools in ArcGIS Software. Methodology is shown as flow diagram.

This exemplifies the fact that selecting suitable sites for residential development is a complex process involving technical, physical, economic, social, environmental and political requirements that may result in conflicting objectives. These complexities are what necessitate the simultaneous use of several decision support tools such as Geographical Information System (GIS) and Multi Criteria Evaluation (MCE) technique using Analytical Hierarchy Process (AHP) [3, 12].

For this purpose, six criteria, those are urban centre proximity, existing land use, network proximity, industry, water logging area, horticulture. The generated thematic maps of these criteria were standardized using a pairwise comparison matrix generated from the Analytical Hierarchy Process (AHP). A weight for each criterion was computed by the developed AHP computation program by comparing them with each other according to their importance and with the help of these weights and criteria, final suitability map was prepared. Integration of GIS and MCE added some valuable insight to a strong analysis platform. This is due to the fact that the analysis results depended not only on the geographical distribution of attributes, but also on the value judgments involved in the decision making process.

Six factors including Central proximity of Rajpur-Sonarapur municipality, Network proximity, Existing build-up, Industries, water logging area and horticulture has been taken into consideration to developing a model for the said purpose. Following parameters have been considered for the suitability analysis which includes Urban centre Proximity ((Rajpur-Sonarapur municipality), Existing land use, Road proximity, Industry, Water logging area and Horticulture.

Analytical Hierarchy Process (AHP): Analytical Hierarchy process is a tool which used in decision making process with multi-criteria that is introduced by Saaty [16]. Six factors including network proximity, educational institution, industry, wetland, horticulture has been taken under the criteria analysis. A pair wise comparison between multi factors will execute to make a scaled set of preferences. It will show the relation between each factor with other every factor [14]. A Weight for each factor has been given (Table 1). After the weight distribution to all sub factors, consistency of weight will be checked by consistency ration (CR) also known as ration of consistency index (CI), CR is define as

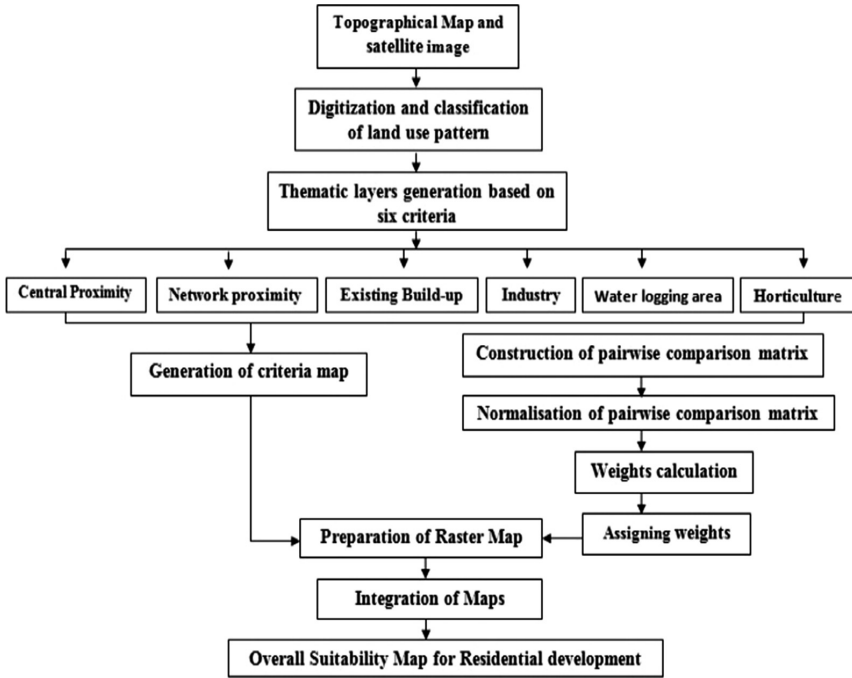


Fig. 2. Flow chart for site suitability analysis for residential development.

$$CR = CI/RI \tag{i}$$

$$CI = (\lambda - n)/(n - 1) \tag{ii}$$

Where, CI will be calculated from the matrix through the equation: Where λ is the largest Eigen value of the matrix and N is the number of matrix. RI (random index) is the consistency index of a randomly created pair-wise comparison matrix of order 1–10 obtained by approximating random indices using a sample size of 500 [13]. After all calculation CR value should be 0.10 or less will considered a reasonable level of consistency. Here the CR is 0.08 which is acceptable.

Weight Linear Combination (WLC): Integration of GIS with weight linear combination method is best for the multi-criteria decision making purpose [5, 19–22]. Here, all determined factors are aggregated by using a weight to each, which pursued by a total of the result to make a map of suitability [7].

$$S = \sum (W_i \times X_i) \tag{iii}$$

Where, S = suitability index for residential development, W_i = weight values of the i factor, X_i = is the potential rating of factor i. After completion of all reclassified map and computation of all weight (Table 2) value from the principal eigenvector were

multiplied. The site suitability map was created as the sum of these weighted factor maps applying map algebra equation (iii). In this way the final site suitability map was prepared.

Table 1. Pair wise comparison matrix

	UC	NP	LU	Industry	AFW	AFH
UC	1.00	3.00	5.00	7.00	9.00	9.00
NP	0.33	1.00	3.00	3.00	9.00	7.00
LU	0.20	0.33	1.00	3.00	7.00	5.00
Industry	0.14	0.33	0.33	1.00	3.00	5.00
Wetland	0.11	0.11	0.14	0.33	1.00	3.00
Horticulture	0.11	0.14	0.20	0.20	0.33	1.00
Total	1.90	4.92	9.68	14.53	29.33	30.00

Consistency Ration = 8.4% or 0.08(Consistency is Acceptable)

Table 2. Normalized matrix for pair wise comparison

	UC	NP	LU	Industry	AFW	AFH		Weight (W)
UC	0.53	0.61	0.52	0.48	0.31	0.30	2.74	0.46
NP	0.18	0.20	0.31	0.21	0.31	0.23	1.44	0.24
LU	0.11	0.07	0.10	0.21	0.24	0.17	0.89	0.15
Industry	0.08	0.07	0.03	0.07	0.10	0.17	0.52	0.09
AFW	0.06	0.02	0.01	0.02	0.03	0.10	0.25	0.04
AFH	0.06	0.03	0.02	0.01	0.01	0.03	0.17	0.03
Total	1.00	1.00	1.00	1.00	1.00	1.00	6.00	1.00

Note: AHP Scale: 1=Equal Importance, 3=Moderate importance, 5=Strong importance, 7=Very strong importance (2,4,6,8 values in-between).

UC = urban centre, NP = Network Proximity, LU = Land Use, AFW = away form Wetland, AFH = away from Horticulture

Weights and Consistency Ration: Selection of desirable criteria and influence weight calculation is the most important part of the analysing suitability. To assign the weight or score of importance to each factors, saaty’s scale [15] which was developed in 1980s, has been used in this study. Here, the method of pair-wise comparison, introduced by Thomas Saaty (1970s and 1980s), expresses an approach to calculating weights for relative importance of the criteria [1, 17]. Therefore, applying the 1–9 scale value for generating the influence weight of each criterion followed by the Saaty’s [16] pair-wise comparison matrix Table 1.

3 Result and Discussion

With rapidly increasing urbanization and high technologies is encroaching agriculture land in haphazard manner, for keeping the importance of recent burning issues land use change effect on fertile land due to augmenting population, study is focused on how to develop a model for residential suitability through Remote Sensing and GIS for sustainable residential development plan.

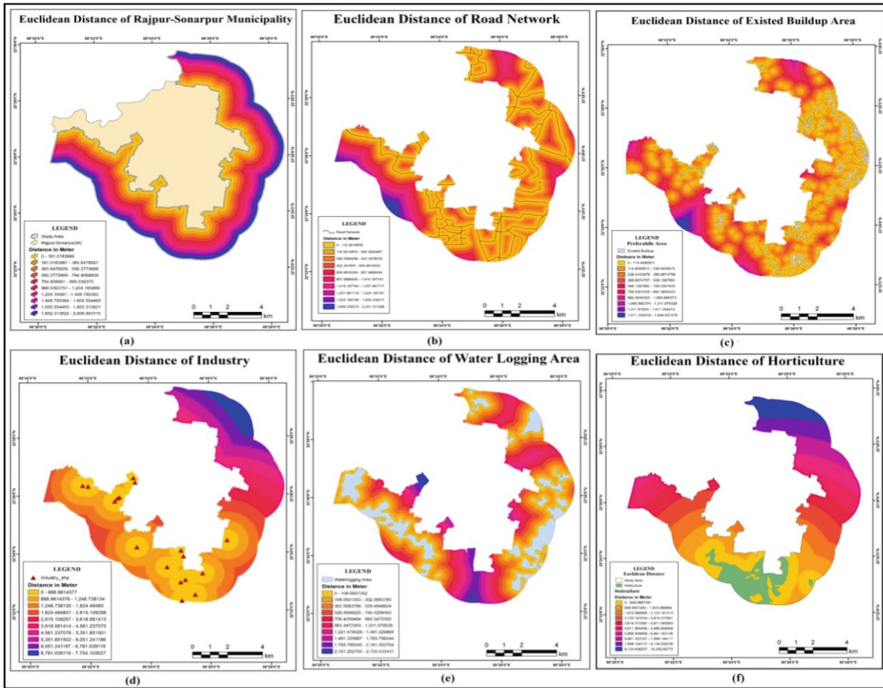


Fig. 3. Exhibits the preferable areas for residential development expressed by various Euclidean distances and demonstrate the distribution of all selected variables which has been grouped into ten classifications based on 0–181 m from the outer boundary of the selected respective variables.

Assessment of Selected Parameter for Residential Suitability: Urban centre Proximity ((Rajpur-Sonarpur municipality): According to Christaller’s Central Place theory, the place which provide amenities, facilities and services its own and surrounding areas is known as central place. Here, Rajpur-Sonarpur municipality is considered as central place because its provide various to the surrounding peri-urban areas. On the basis of this municipality five buffer zones [Fig. 3(a)] were created to show the five types of preferable zones for residential housing development in the study area.

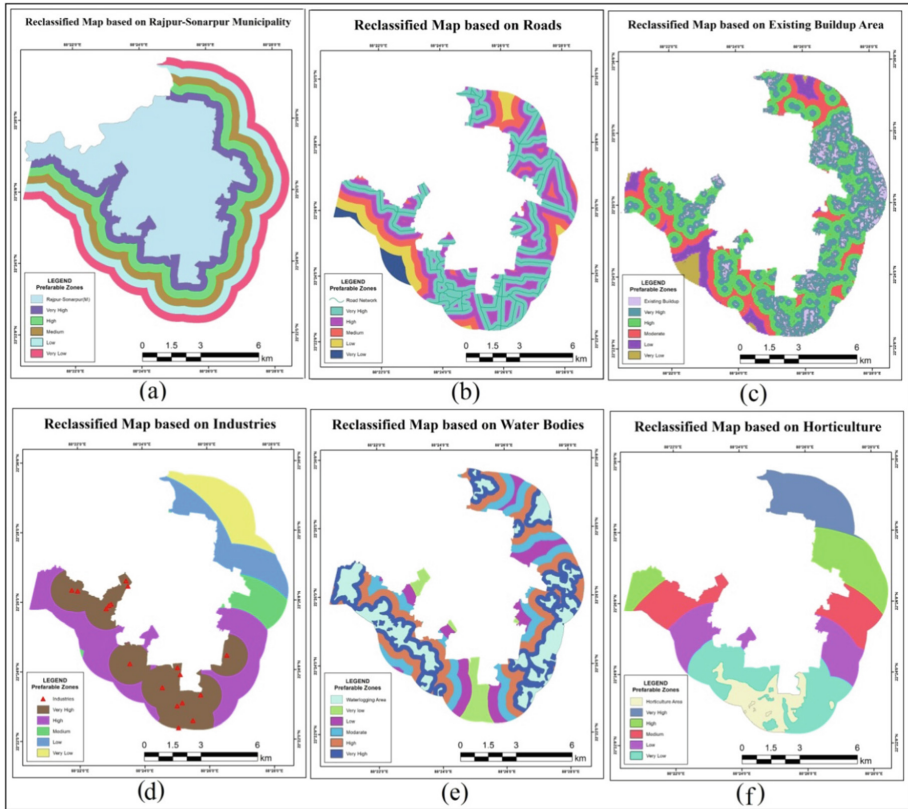


Fig. 4. Elucidates the reclassification of delineated preferable five zones based on different variable. For standardization of the study this figure has been reclassified into five ones for finding out preferable area at the selected study area.

Existing land use: First of all the plan for acquiring new land to make housing residents will be conducted on the basis of vacant land availability. Therefore, at the beginning time existing build up area was extracted and eliminated from the whole study area. Various buffer areas have been delineated through Euclidean distance and after that it also reclassify in into five zones [Fig. 3(b)]. Most nearest zone is considered as the very high suitable zone and most far zone is least suitable area for residential development.

Road proximity: All the railways line, major and minor roads have been digitized to trace out the accessibility region from the Topographical map. In the same ways as previously done, various buffer zones have created according to the Euclidean distance default given by computer and after that, buffer zones have been reclassified into five accessibility regions i.e. very high suitable, high suitable, moderate suitable, low suitable and least suitable zones considered from the closest to most far respectively [Fig. 3(c)].

Industry: Some industries have been pointed out through the triangle shape symbol. On the basis of those marks Euclidean distance buffer zones demarcated and reclassified in to five zones. These small industries provide job opportunities to the local peoples. So, it's have some influence area which is categories in to five preferable zones [Fig. 3(d)].

Water logging area: Water logged areas as well as wetland areas have been delineated by supervised classification from the satellite image. This criterion is a measure to validate site suitability of residential development area. Higher the distance from water logged/wetland area for residential development is more suitable and vice versa [Fig. 3(e)].

Horticulture: Horticulture is being selected for one of the criteria which has been digitised from LULC map of Sonarpur Block. Many research scholars revealed that rapid growth of urbanization leads encroachment of prime farmlands in peri-urban areas. But here efforts have been made to analyse suitable location for residents which should be set up away from the Horticultural lands. Here, distant most land from the Horticultural land will be best suitable site for residents [Fig. 3(f)] and eventually it can be beneficial for sustainable development.

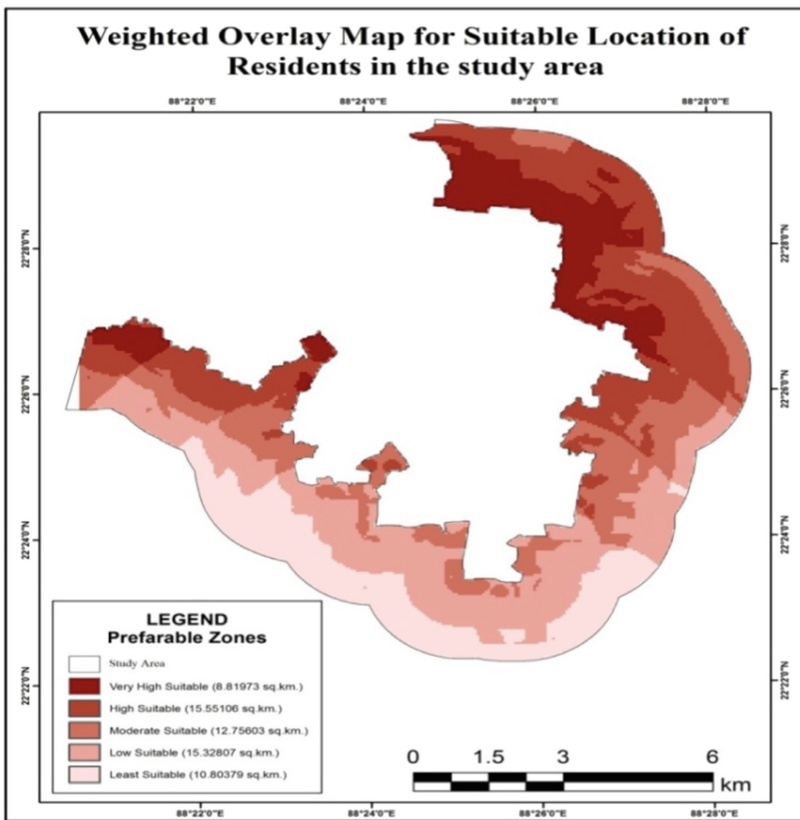


Fig. 5. Weighted overlay map for suitable location of residential area has been develop based on Figs. 2 and 3 which already mapped out or classified based on selected factors or criteria. (Site Suitability Map = \sum [weight * Criteria Map] Site Suitability Map = \sum [(0.46*re-classed urban centre) + (0.24 * re-classed network proximity) + (0.15 * re-classed land use) + (0.09 * re-classed industry) + (0.04 * re-classed away from wetland) + (0.03 * re-classed away from Horticulture)])

Suitability Assessment for Residential Development: Figure 5 shows the suitable location for residential development at the peri-urban area of Rajpur-Sonarpur municipality. North east and western portion of the selected study is reported for very high, high and moderate suitability zone for residential development. But southern portion has been noticed low and very low suitability for residential development. A suitability residential model has been developed with the help of weighted linear combination (1 to 5 scale) and AHP through spatial analyst tools to find out the suitable site for residential development at peri-urban area of Rajpur-Sonarpur Municipality.

Table 3. Residential suitability index and area coverage

Sl. no.	Suitable index	Area (Sq. Km.)	Area in percentage
1	Very high suitable	8.81973	13.94
2	High suitable	15.55106	24.58
3	Moderate suitable	12.75603	20.16
4	Low suitable	15.32807	24.23
5	Very low suitable	10.80379	17.08
Total		63.25869	100.00

Source: computed by author based on Fig. 4.

Table 3 shows the five different preferable areas for residential development in the southeast peri-urban site of Kolkata. The perusal Table 3 indicate that 13.94% (8.81973 sq.km.) area comes under very high class suitable zone and on the another hand 24.58% (15.55106 sq.km.) covered high class suitable zone followed by 20.16% (12.75603 sq.km.) moderate class suitable zone of residential development in peri-urban area of south east Kolkata. These zones are reported for housing development or suitable residential development in the north-east and west side of Rajpur-Sonarpur Municipality. The reported suitable zones for residential development in Rajpur-Sonarpur municipality have positive relation with the central proximity, road proximity, existing build-up area and industry. While on the other hand, these zones have negative association with water logged/wet land and Horticulture area. From the same table it is also find out that unsuitable zone comes under the low or very classification which is recorded as 23.24% under low categories while 17.08% area lies under the very low categories. These unsuitable zones are lies in the southern portion of the study area which are not suitable for the residential development as per analysis and selected criteria based.

4 Conclusion

From the above analysis and after thoroughly study regarding suitability or modelling of residential development plan, it has been concluded that integration of remote sensing, GIS and AHP technique developing very useful tools to develop the said model for residential housing development in new emerging urban area of any region. In this study the peri-urban area of south east part of Kolkata which has been choosing

for same study to develop model of suitable site for residential development in the peri-urban area. Through the various technique (AHP&GIS), it is find out that 13.94% area comes under the very high suitable zone while 24.58% covered by high suitable zone which followed by 20.16% under moderate suitable zone. The analysis also reveals that a large amount of area occupies by waterlogged/wetland and Horticulture (mainly Goava cultivation). According to Neuppenau ([13] and Thapa [18] 'Peri-urban agriculture shall provide a solution to ecologically unhealthy development of large urban agglomerations. Hence, in this study, the maximum distance was maintained from the Horticulture and Wetland to demarcate the suitable location for housing. In this ways, uncontrolled urban sprawl and hazard will be identified and predicted respectively through this approach in the concern area. Overall, this technique can provide a picture of which areas have the potential for residential development, provided the data for current available land is accurate and data layers are chosen that illustrate prerequisites for successful development. The result of this analysis could be used as a guide for land use planning. And also this information may help the planners and decision makers to identify the problematic residential areas, to understand the course and effects of the problems and locate the suitable areas for future development to overcome the existing land use conflicts.

It is recommended that the information provided in this research could be used as a framework for preliminary investigations in planning and development of a land for residential purposes, further on site detailed investigations are recommended before the implementation of development work. And it is also recommended that the results of limitation analyses could used to predict on range of problems such as construction difficulties, which can be encountered in the construction of housing and local roads. The limitation analysis could be used in proposed urban areas for identifying special design which is necessary to address the specific problems related to housing and local roads construction and to minimize the initial cost of land development.

Acknowledgement. We would like acknowledged to Aliah University, Kolkata for finishing entire digital work and completing the paper to use lab and facilities. Further "Indian Council of Social Science Research (Ministry of Human Resource Development, New Delhi, 110067, India, Website: www.icggs.org) is being duly acknowledged for proving me financial assistance to attend the conference in Thailand Bangkok (ICGGS 2018) which helped me a lot to enriched in my research to interacted with expertise from different countries in the conference and I came to know about so many new things, I am really thankful to them.

References

1. Abdullahi, S., Mahmud, A.R., Pradhan, B.: Spatial modelling of site suitability assesment for hospital using gephographical information system-based multicriteria approach at Qazvin city. *Iran. Geocarto Int.* **29**(2), 164–184 (2014)
2. Allen, A.: Environmental planning and managment of the peri-urban interface: perspectives on an emeing field. *Environ. Plann. Ang Manag.* **15**(1), 135–148 (2003)
3. Aydi, A., Zairi, M., Dhia, B.H.: Minimization of environment risk of landfill site using fuzzy logic, analytical hierarchy process, and weight linear combination methodolgy in a geographic information system environment. *Environ. Earth Sci.* **68**, 1375–1389 (2013)

4. Basu, R., Dhar, S.B.: In-migration, commutation and urban sprawl: a case study Kolkata metropolitan area. *Spaces Flows Int. J. Urban Extra Urban Stud.* **3**, 59–77 (2013)
5. Charabi, Y., Gastli, A.: PV site suitability analysis using GIS-based spatial fuzzy multi-criteria evaluation. *Renewable Energy* **36**(9), 2554–2561 (2011)
6. Das, N.: Suitable site selection for small scale industries through GIS analysis: a case study conering part of Barasat-II, Deganga, Rajarhat Block of North 24 Pargana district, West Bengal. *Int. J. Sci. Res.* **5**(3), 329–331 (2016)
7. Eastman, J.R., Jin, W., Kyem, P.A., Toledano, J.: Raster procedures for multi-criteria/multi-objective decisions. *Photogram. Eng. Remote Sens.* **61**(5), 539–547 (1995)
8. Fazal, S.: Urban expansion and loss of agricultural land - a GIS based study of Saharanpur City, India. *Environ. Urbanization* **12**(2), 133–149 (2000)
9. Hofstee, P., Brussel, M.: Analysis of suitability for urban expansion in Villavicencio. International Institution for Geo-Information and Earth Observation (1995)
10. Hossain, M.S., Chowdhury, S.R., Das, N.G., Sharifuzzaman, S.M., Sultana, A.: Integration of GIS and multicriteria decision analysis for urban aquaculture development in Bangladesh. *Landscape Urban Plan.* **90**, 119–133 (2009)
11. Jain, K., Subbaiah, V.Y.: Site suitability analysis for urban development using GIS. *J. Appl. Sci.* **7**(18), 2576–2583 (2007)
12. Kumar, S., Kumar, R.: Site suitability analysis for urban development of a hill town using GIS based multicriteria evaluation technique: a case study of Nahan Town, Himachal Pradesh, India. *Int. J. Adv. Remote Sens. GIS* **3**(1), 516–524 (2014)
13. Neuppenau, E.A.: Agro-ecologically oriented land use and the creation of viable rural urban interfaces. In: *Peri-Urban Development in South East Asia*, 2nd Newsletter (2002)
14. Saaty, T.L.: Decision-making with the AHP: why is the principal eigenvector necessary. *Eur. J. Oper. Res.* **145**(1), 85–91 (2003)
15. Saaty, T.L.: *Fundamentals of Decision Making and Priority Theory With the Analytic Hierarchy Process*. RWS Publications, Pittsburg (2000)
16. Saaty, T.L.: How to make a decision: the analytic hierarchy process. *Eur. J. Oper. Res.* **48**(1), 9–26 (1970)
17. Saaty, T.L.: How to make a decision: the analytic hierarchy process. *Interfaces* **24**(6), 19–43 (1994)
18. Thapa, R.B., Murayama, Y.: Land evaluation for peri-urban agriculture using analytical hierarchical process and geographic information system techniques: a case study of Hanoi. *Land Use Policy* **25**, 225–239 (2008)
19. Voogd, J.H.: *Multicriteria evaluation for urban and regional planning*, p. 367. Pion, London (1983)
20. Weldu, W.G., Deribew, I.A.: Identification of potential sites for housing development using GIS based multi-criteria evaluation in Dire Dawa City, Ethiopia. *Int. J. Sci. Basic Appl. Res.* **28**(3), 34–49 (2016)
21. Youssef, A.M., Pradhan, B., Tarabees, E.: Integration evaluation of urban development suitability based on remote sensing and GIS technique: contribution from the analytic hierarchy process. *Arab. J. Geosci.* **4**, 463–473 (2011)
22. Zhang, R., Zhang, X., Yang, J., Yuan, H.: Wetland ecosystem stability evaluation by using analytical hierarchy process (AHP) approach in Yinchuan Plain, China. *Mathematical Comput. Model.* **57**, 366–374 (2013)

Author Index

A

Arunplod, Chomchanok, 12

C

Chaithong, Thapthai, 75

Chaona, Yutthana, 96

Chatewutthiprapa, Chuti, 21

Chavanavesskul, Sutatip, 85

Chotpantararat, Srilert, 21

H

Hasnine, Md., 138

I

Intacharoen, Prasarn, 68

Ito, Michio, 1

J

Jangkorn, Siriprapha, 68

K

Kulpanich, Nayot, 46

L

Limkomonvilas, Teerawate, 96

Lonavath, Ashok Kumar, 128

Losiri, Chudech, 32

M

Monprapussorn, Sathaporn, 96

N

Nagai, Masahiko, 1, 32

Naik, Krishna, 128

Na-U-Dom, Tawatchai, 68

Niemmanee, Talisa, 59

P

Phonphan, Walaiporn, 59, 118

Phumkokrux, Nutthakarn, 109

R

Ravi Naik, B., 128

Rukhsana, 138

S

Sae-ngow, Pornperm, 46

Sathish Kumar, V., 128

Sirirattanapol, Chairath, 1

Soontranon, Narut, 85

Srichupieam, Wannaphorn, 85

T

Tamkuan, Noppawan, 1

Thodsan, Thippawan, 68

V

Virugu, Karunakar, 128

W

Waiyasusri, Katawut, 46

Worachairungreung, Morakot, 46

Y

Yumuang, Sombat, 21